

The role of cFLIP in regulatory T cell homeostasis

Dissertation

zur Erlangung des akademischen Grades

doctor rerum naturalium

(Dr. rer. nat.)

genehmigt durch die Fakultät für Naturwissenschaften

der Otto-von-Guericke-Universität Magdeburg

von

M. Sc. Carlos Plaza Sirvent

geb. am 31.10.1982 in Elche (Alicante), Spanien

Gutachter: Prof. Dr. Ingo Schmitz

Prof. Dr. Andreas Krueger

eingereicht am 23. Juni 2015

verteidigt am 23. September 2015

Table of contents

1. Abstract	1
2. Introduction	2
2.1. Cell death	2
2.2. Apoptosis	5
2.2.1. Morphological features	5
2.2.2. Caspases	6
2.2.3. BCL-2 family	8
2.2.4. Death receptors.....	8
2.2.5. Signaling pathways of apoptosis	9
2.2.5.1. The intrinsic pathway	9
2.2.5.2. The extrinsic pathway.....	10
2.2.5.3. The crosstalk between the pathways	12
2.2.5.4. The granzyme B pathway	12
2.2.6. The FLICE-inhibitory proteins	14
2.2.7. The role of the FLICE-inhibitory proteins (cFLIP) in the immune system ..	16
2.3. Apoptosis and immune homeostasis.....	17
2.3.1. Function of immune system	19
2.3.2. Lymphocyte development.....	19
2.3.3. Treg development.....	20
2.3.4. Treg function	22
2.3.5. Treg homeostasis.....	23
2.4 Aims of the thesis	25
3. Materials.....	26
3.1. Chemicals.....	26
3.2. Cell culture material and devices.....	26
3.2.1. Cell culture media and supplements.....	27
3.2.2. Medium for cell culture.....	27
3.2.3. Reagents, antibodies and cytokines used for cell stimulation.....	28
3.3. Materials, devices and reagents for flow cytometry	28
3.3.1. Devices	28
3.3.2. Fluorescent dyes	29
3.3.3. Flow cytometry antibodies	29

3.4. Reagents and materials used for Western blotting.....	30
3.4.1. Primary antibodies.....	30
3.4.2. Horseradish peroxidase-conjugated secondary antibodies.....	30
3.5. Reagents and devices for confocal microscopy	31
3.5.1. Reagents for microscopy	31
3.5.1.1. Fluorescent dyes	31
3.5.1.2. Fluorochrome-labeled antibodies	31
3.6. Reagents for <i>in vivo</i> treatments.....	31
3.7. Frequently used buffers	32
3.8. Oligonucleotides	33
3.8.1. Oligonucleotides for quantitative RT-PCR.....	33
3.8.2. Oligonucleotides for mouse genotyping	33
3.9. Mouse strains	34
4. Experimental procedures.....	34
4.1. Molecular biology methods	34
4.1.1. RNA isolation.....	34
4.1.2. Photometric determination of DNA/RNA concentration.....	34
4.1.3. Reverse transcription.....	35
4.1.4. Polymerase chain reaction (PCR)	35
4.1.5. Analytic agarose gels	36
4.1.6. Quantitative real-time polymerase chain reaction (qRT-PCR).....	36
4.2. Protein biochemical methods.....	37
4.2.1. Cell lysis.....	37
4.2.2. Determination of protein concentration	37
4.2.3. SDS-Polyacrylamide gel electrophoresis (SDS-PAGE)	37
4.2.4. Western blotting	37
4.3. Mouse surgery and cellular methods	38
4.3.1. Isolation of organs from mice	38
4.3.2. Flow cytometry analysis.....	38
4.3.3. Cell isolation by flow cytometry	39
4.3.4. Viability studies in Tcon and Treg cells.....	39
4.3.5. Active caspase 3 detection by Western blot.....	39
4.3.6. <i>In vitro</i> stimulation with death ligands.....	39

4.3.7. Active caspase 3/7 determination by confocal microscopy	40
4.3.8. Histology and immunohistochemistry	40
4.3.9. Determination of cytokines in serum	40
4.3.10. Autoantibodies determination	41
4.3.11. <i>In vivo</i> treatments	41
4.4. Statistical Analysis.....	41
5. Results.....	42
5.1 Regulatory T cells manifest a higher apoptosis rate than conventional T cells....	42
5.2 Pan-caspase inhibitor and IL-2 improves Treg viability.....	45
5.3 cFLIP deficiency in Treg cells caused autoimmune disease in mice.....	51
5.4 Treg cells are sensitive to CD95-, but not DR5- or TNFR1-induced cell death...	66
5.5 Tcon and Treg cells show identical death receptor profile expression.....	68
5.6 Neither anti-CD95L nor QVD could protect the Treg cells of <i>Cflar</i> ^{ΔFoxp3} mice <i>in vivo</i>	69
5.7 cFLIP _L protects Treg cells from CD95-mediated cell death <i>in vitro</i>	71
6. Discussion	74
6.1. Treg cells show an elevated apoptosis rate under steady-state conditions	74
6.2. Treg cells behave like TCR-activated Tcon cells	76
6.3. X chromosome inactivation produces Treg chimeras in females	77
6.4. Lack of cFLIP in murine Treg cells results in the disappearance of the Treg cells in the periphery but not in the thymus	79
6.5. Absence of Treg cells in <i>Cflar</i> ^{ΔFoxp3} mice originates an autoimmune disorder comparable to <i>scurfy</i> phenotype	79
6.6. Blocking CD95L or pan-caspase inhibitor treatment is not sufficient to rescue the <i>scurfy</i> -like phenotype on <i>Cflar</i> ^{ΔFoxp3}	80
6.7. cFLIP-deficient Treg cells manifest higher susceptibility to CD95L <i>in vitro</i> stimulation	81
6.8. Concluding remarks	82
7. Abbreviations.....	83
8. References.....	87
9. Acknowledgements	104
10. Declaration of originality	105
11. Curriculum vitae	106

1. Abstract

Regulatory T (Treg) cells are essential for immune homeostasis, maintaining peripheral tolerance and preventing autoimmune diseases. Moreover, cancer cells and pathogens may take advantage of the suppressive capacity to escape from the immune response. Thus, the regulation of Treg cells represents an essential mechanism to build an adequate response against threats and to keep immunological self-tolerance. This thesis showed that the Treg cells manifest high dynamics in steady-state conditions, having a high cell death rate to control the size of the population. Furthermore, in contrast to naïve T cells, it was demonstrated that apoptosis contributes considerably to the Treg cell death. Together with the expression of certain markers, this fact supports the concept of Treg cells having an activated status.

cFLIP proteins inhibit death receptor-mediated apoptosis and their role in the regulation of cell populations of the immune system has been proved. A deletion of *Cflar*, the gene encoding all cFLIP isoforms, was performed specifically in Treg cells of mice in order to investigate their role in Treg homeostasis. As a consequence, Treg cells disappeared in the peripheral lymphoid organs and the mice developed a fatal autoimmune disease. Analysis of the gene expression of the cFLIP proteins revealed significant differences in the expression of the long isoform cFLIP_L. This might explain the increased sensitivity to CD95-mediated apoptosis found in Treg cells compared to conventional T cells, despite the fact that both populations have identical expression of the CD95 receptor. Furthermore, Treg cells from the thymus of *Cflar*^{ΔFoxp3} mice have increased sensitivity to CD95L stimulation, suggesting that cFLIP is important to protect Treg cells from CD95-mediated apoptosis.

The study on the role of cFLIP in Treg homeostasis improved the knowledge about the regulation of the Treg cell population in order to understand better the behavior of the immune system. This would be beneficial for the development of immunomodulatory treatments to regulate the immune system in pathogenic scenarios such as autoimmune diseases or cancer.

2. Introduction

2.1. Cell death

Death of an organism can be defined as an irreversible event that implicates the impossibility to maintain homeostasis. Paradoxically, cell death is necessary for the life of multicellular organisms. Cell death can occur in a controlled manner, i.e. that a genetic program mediates cell death, hence programmed cell death. Complex organisms use cell death during development to build parts of the body, creating cavities, separating structures and eliminating useless components¹. Immune cells are constantly generated and the organism needs to eliminate surplus cells in order to control the population size and to remove potential dangerous cells that might harm own structures²⁻⁴. Programmed cell death is also an effective method to erase infected cells and preserve the integrity of the neighboring healthy cells⁵. Programmed cell death contributes remarkably to the elevated replacement rate occurring in certain tissues like the skin and the gut, where thousands of cells are substituted by new cells every day^{6,7}.

The point-of-no-return within the cell death program is not clearly defined by a biochemical event. Nevertheless, the loss of the plasma membrane integrity and the cell fragmentation, including the nucleus, have been considered as morphological and molecular criteria to define the cell death⁸. Morphological appearance, enzymological activity, functional aspects and immunogenicity can be used as criteria to classify the different types of cell death. Necrosis is a type of cell death characterized by the loss of plasma membrane integrity and the cell collapse⁹. It is produced by physiochemical stress such as osmotic shock, mechanical stress, freeze and heat¹⁰. The release of the cytoplasmic content, due to the loss of the plasma membrane integrity, results in the induction of inflammatory responses caused by the detection of damage-associated molecular patterns (DAMP) by immune cells¹¹.

Apoptosis, a term coined in 1972¹², is another type of cell death characterized by reduction of cellular volume (pyknosis), chromatin condensation, nuclear fragmentation (karyorrhexis), cell membrane blebbing and the formation of apoptotic bodies⁸. During the course of apoptosis, the plasma membrane maintains its integrity until the final stages and therefore the intracellular content remains inside the cell. This fact promotes the low immunogenicity of the process^{8,13}. Moreover, apoptotic cells display “eat me” signals and release attractant substances in order to promote the localization and the

engulfment of the apoptotic bodies by phagocytes¹⁴⁻¹⁶. During this late phase, the elimination of cell debris occurs in a controlled environment of low immunogenicity to avoid inflammatory processes. The maintenance of the apoptotic cell cytoplasm within the plasma membrane, the release of anti-inflammatory mediators and the inhibition of pro-inflammatory cytokine production by the phagocytes avoid the activation of inflammatory response and tissue damage^{17,18}.

Autophagy is defined as the sequestration and degradation of cytoplasmic material within autophagosomes¹⁹. This regulated process is involved in the recycling of cell structures and organelles within the normal cell cycle program of the cell, promoting the cell survival¹⁹. Autophagy is important to degrade unwanted and damaged cell organelles and to re-use the subunits to build new structures as well as during cell starvation¹⁹. Autophagosomes are double-layered membrane vesicles containing degenerating organelles. The fusion of the vesicle with lysosomes causes the digestion of the inner content¹⁹. The regulation of autophagy is a very complex process involving the Atg proteins, phosphatidylinositol 3-kinase-I (PI3K-I), GTPases and the mammalian target of rapamycin (mTOR) pathway²⁰. The autophagic machinery can be used also by the cell to capture and eliminate intracellular pathogens, which is also called xenophagy²¹. However, autophagy has a close relationship with cell death as well²². Nowadays there is not a consensus about if autophagy is a type of cell death or whether it is a process related with some stages of cell death. Some studies support the idea that autophagy participates in cell destruction by means of a massive autophagic vacuolization^{23,24}. Others denominate “autophagic cell death” when the cell show similar features along with absence of chromatin condensation and the possibility of recovering upon withdrawal of the death-inducing stimulus²⁵⁻²⁸. Besides this controversy, the cross-talk between autophagy and apoptotic signaling has been clearly demonstrated. Autophagy can be induced by several pro-apoptotic signals, like some components of the extrinsic apoptosis pathway²⁹⁻³². Conversely, autophagy can be suppressed by anti-apoptotic signals^{33,34}. Thus, autophagy and apoptosis are two processes closely regulated and coordinated.

Another type of cell death is cornification. This term refers to the process of envelope regeneration occurring in the skin epidermis^{35,36}. Like apoptosis, cornification is a programmed cell death, but it presents numerous morphological and biochemical differences. It involves the transformation of corneocytes in keratinocytes containing

lipids and proteins, such as keratin and ceramides, necessary to provide to the skin layer certain attributes, like elasticity, mechanical resistance and water repellence^{35,36}.

Thanks to the scientific progress, it is possible to identify and classify additional types of cell death. Some of them share characteristics with other forms of cell death but have diverse features that allow them to be cataloged differently. That is the case for necroptosis, which is a programmed cell death dependent on the protein kinase RIP-1 and sharing morphologic features with necrosis^{37,38}. In addition to the above mentioned types of cell death, other atypical cell death modalities have been described, such as pyroptosis, pyronecrosis, entosis, paraptosis, mitotic catastrophe, anoikis, excitotoxicity, and wallerian degeneration⁸.

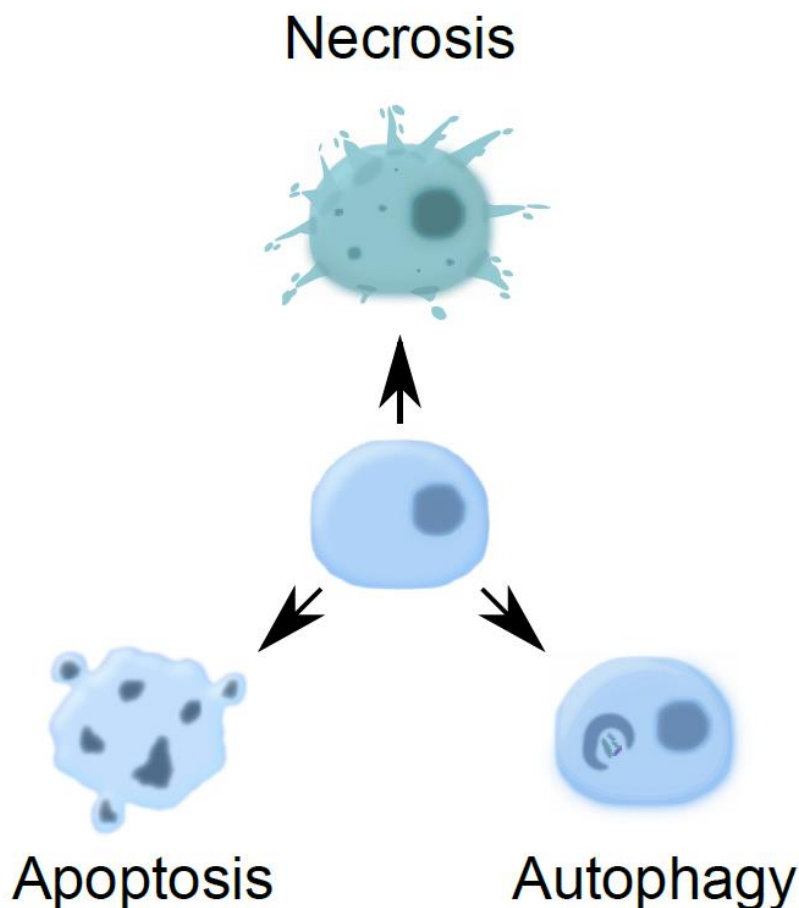


Figure 1. Main types of cell death. Necrosis is characterized by the escape of the intracellular content to the extracellular space due to the loss of membrane integrity. In apoptosis the plasma membrane blebs forming apoptotic bodies that contain fragmented DNA and cell organelles. Autophagy is a mechanism by which the cell organelles are engulfed by a double membrane inside the cells and further degraded.

2.2. Apoptosis

Apoptosis is an evolutionary conserved process regulated by genes³⁹. It is a complex and programmed cell death mechanism characterized by a controlled demolition of the cell architecture. Furthermore, apoptosis promotes cell debris removal under low-immunogenicity conditions in order to avoid an unwanted immune response^{8,13}.

2.2.1. Morphological features

During the course of apoptosis, different changes occur in the cell architecture. In the beginning, the cell becomes rounded up and retracts from surrounding cells followed by plasma membrane blebbing and finally the formation of apoptotic bodies¹³. The condensation and fragmentation of the nucleus is a remarkable hallmark of apoptosis. Caspase activity causes the proteolysis of the nuclear lamina and the collapse of the nuclear envelope⁴⁰. Furthermore, the genomic DNA is fragmented followed by chromatin condensation⁴¹. Many important components of the cytoskeleton are targeted by caspases. Actin microfilament components such as actin and myosin are substrates of the protease activity⁴²⁻⁴⁴. Microtubular proteins, including tubulin, as well as intermediate filament proteins are also degraded by caspases⁴⁵⁻⁴⁸. The demolition of the cytoskeleton enables the rounding and the retraction from the surrounding cells and facilitates the membrane blebbing. Nevertheless, some intact actin filaments are required for the blebbing and the formation of apoptotic bodies⁴⁹. Organelles are also affected by the apoptotic obliteration. Golgi apparatus and mitochondria are fragmented and packed into apoptotic bodies^{50,51}. The pore formation in the outer mitochondrial membrane promotes the fragmentation of these organelles^{52,53}. During late stages of apoptosis, chromatin is enveloped by endoplasmic reticulum (ER) and redistributed into apoptotic bodies⁵⁴. Moreover, apoptosis affects drastically the protein synthesis machinery. Several transcription factors and multiple translation initiator factors and ribosomal proteins are affected by caspase activity⁵⁵. Looking at the outer part of the cell, there are also changes in the plasma membrane during the apoptotic process. The organization of the membrane structure is altered. Molecules usually located in the inner leaflet of the membrane, like phosphatidylserine (PS), are exposed on the cell surface^{15,16}. The molecule externalization enables the identification of apoptotic cells and promotes the engulfment by phagocytes^{15,56,57}. The removal of the cell debris is the terminal phase of apoptosis. The collapse of the cell into apoptotic bodies facilitates the phagocytosis and the elimination of the apoptotic cell. In contrast to pathogen clearance,

apoptosis promotes a low-immunogenic environment, inducing immunosuppressive cytokine production, such as IL-10 and TGF- β , to avoid undesirable immune responses, inflammation and tissue damage^{17,18}.

2.2.2. Caspases

Apoptosis is orchestrated by members of a proteases family known as caspases (cysteine aspartic acid-specific proteases)^{58,59}. Structurally, caspases are comprised of a pro-domain followed by a large and a short subunit and they can be cleaved after particular tetrapeptide motifs, where the last residue is an Asp⁵⁹. This cleavage is necessary to achieve the caspase active form. Regarding their enzymatic activity, caspases have two catalytic conserved regions including the histidine residue in the His-Gly motif and the essential cysteine residue in the Gln-Ala-Cys-X-Gly motif (where X denotes any amino acid)⁶⁰. The caspase family can be divided into apoptotic and inflammatory members, according to their function. Caspases 1, 4, 5, 11, 12 belong to the inflammatory group whereas the apoptotic group can be subdivided into initiator and effector caspases⁶¹. Caspase 2, 8, 9 and 10, which are able to react upon apoptotic stimuli and are able to initiate the proteolytic processing of other caspases, are considered as initiator caspases⁶¹. On the other hand, caspase 3, 6 and 7, which are activated by other caspase proteases and are able to cleave the majority of substrates during apoptosis, belong to the effector caspases⁶¹. In steady-state conditions, caspases are present in the cell in an inactive form (zymogen). Upon apoptotic stimuli, the initiator caspases are cleaved and activated, leading to the initiation of the caspase cascade and the proteolytic activation of the effector caspases⁶². The active caspase conformation consists of a heterotetramer originating from the cleavage of two procaspase molecules resulting in two small and two large subunit arrangement^{59,61}. Initiator caspases are present as monomers whereas effector caspases exist as pre-formed dimers in the cell⁶¹. The prodomain region includes motifs, like the caspase recruitment domain (CARD) or the death effector domain (DED), that facilitates the recruitment of caspase units⁶².

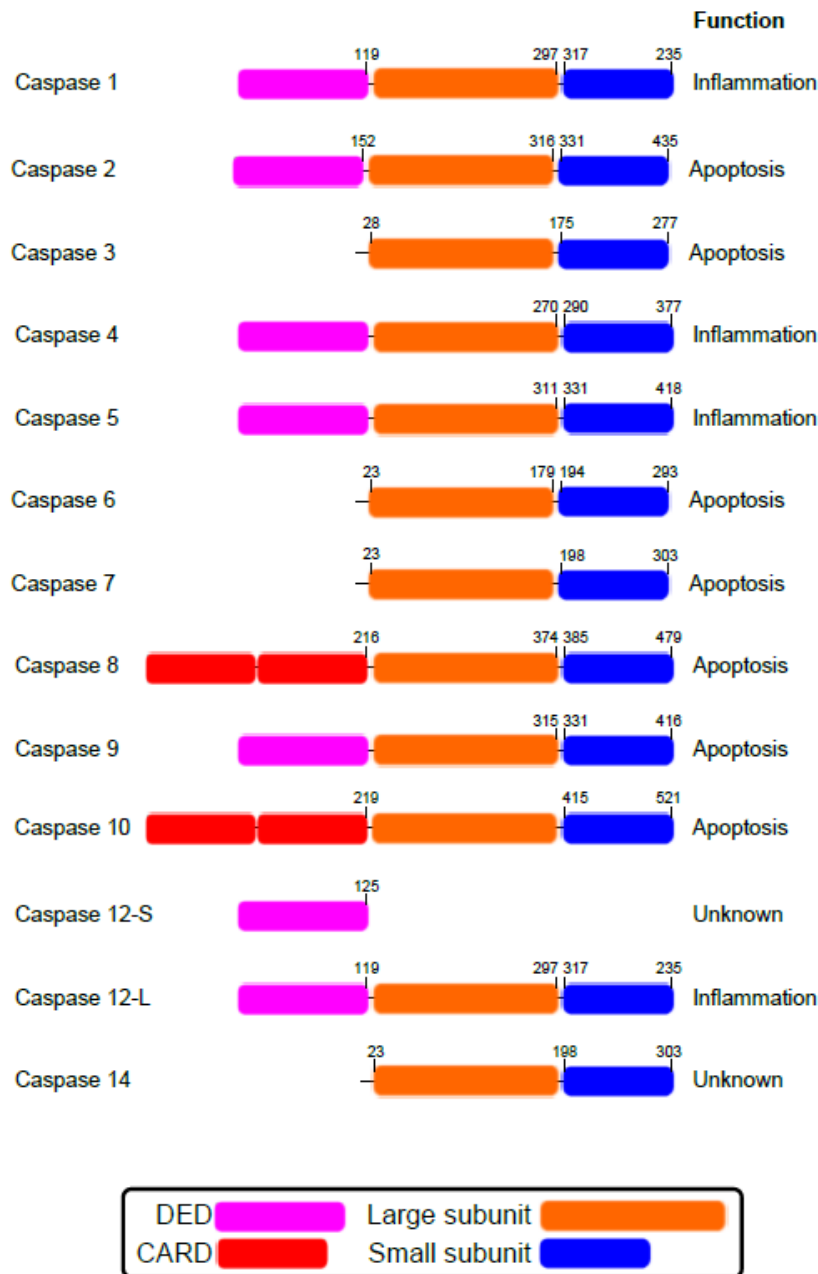


Figure 2. Caspases are a family of proteases that cleave their substrates after specific tetrapeptide motifs (P4-P3-P2-P1) where P1 is an Asp residue. All the caspases have similar structures. They are formed by a pro-domain sequence that participates in the recruitment of initiator caspases. So far, two pro-domains have been identified, the caspase recruitment domain (CARD) and the death effector domain (DED). The caspases can be divided into two functional groups, the initiators, which are able to auto-activate and cleave other caspases, and the effectors, which are activated by other caspases and cleave the majority of substrates. A broad group of caspases participates in apoptosis; however, there is a group involved in inflammatory responses produced by the innate immune system. Caspase 12 does not contain the catalytic region within its sequence. Interestingly, a group of African individuals express the complete form of caspase 12 containing the catalytic site. These individuals show higher susceptibility to inflammatory diseases. Adapted from Taylor et al. 2008¹³

2.2.3. BCL-2 family

Apoptosis can be mediated by the intrinsic pathway, also called B-cell lymphoma-2 (BCL-2)-regulated or mitochondrial pathway. The induction of such mechanism is caused by developmental cues, cytotoxic injury and cellular stress, like DNA damage, viral infection, low ATP levels, pH variations, reactive oxygen species (ROS) massive production or growth-factor deprivation⁶³. BCL-2 family proteins regulate tightly this pathway. The members of this family are classified into three groups. BCL-2-associated X protein (BAX), BCL-2-antagonist/killer-1 (BAK) and BCL-2-related ovarian killer (BOK) are included in the group of effector proteins⁶⁴. BAX and BAK produce the permeabilization of the outer mitochondrial membrane (OMM) causing the release of apoptogenic molecules (such as cytochrome c and DIABLO/SMAC) from the mitochondria, promoting the activation of caspases⁶³. In healthy conditions BAK resides on the OMM, inactivated by the binding with myeloid cell leukaemia 1 (MCL-1) and B-cell lymphoma-extra-large protein (BCL-XL)^{65,66}, whereas BAX and BOK are located at the cytosol^{67,68}. Cytosolic BAX masks its hydrophobic C-terminal membrane anchor in the BH-3 binding pocket⁶⁷. Upon apoptosis induction, BAX proteins translocate to mitochondria and are inserted into the OMM via the C-terminal anchor⁶⁷. In addition to MCL-1 and BCL-XL, the group of anti-apoptotic proteins is completed by BCL-2, BCL-2-like-2 (BCL-W), BCL-B (also called BCL-2L10), and BCL-2-related protein A1A (A1A, also named BCL-2A1)⁶⁴. A third group of the BCL-2 family, consisting in BCL-2 antagonist of cell death (BAD), BH3-interacting domain death agonist (BID), BCL-2-interacting killer (BIK), harakiri (HRK), BCL-2-like-11 (BIM), Bcl-2-modifying factor (BMF), NOXA and PUMA (BCL-2 binding component-3), have a conserved BH-3 domain that can bind to the group of anti-apoptotic members, producing the repression of their interaction with the effector proteins BAX and BAK⁶⁴.

2.2.4. Death receptors

The extrinsic pathway, also named death receptor-mediated apoptosis pathway, is initiated by signals coming from death receptors located on the cell surface. The death receptors belong to the tumor-necrosis factor (TNF) receptor superfamily that includes TNF receptor 1 (TNFR1), CD95 (alternatively called FAS or APO-1), TNF-related apoptosis-inducing ligand receptor 1 (TRAILR1), TRAILR2, death receptor 3 (DR3) and DR6. These receptors have the presence of a death domain (DD) motif in their cytoplasmic tail in common and they can be triggered by their respective ligands,

namely TNF, CD95 ligand (CD95L, also named FASL) and TNF-related apoptosis-inducing ligand (TRAIL)⁶⁹⁻⁷².

2.2.5. Signaling pathways of apoptosis

2.2.5.1. The intrinsic pathway

During intrinsic apoptosis induction, anti-apoptotic proteins are degraded^{65,73} or their interaction with BAX or BAK is disrupted by BH3-only proteins⁶⁶. Once BAX is inserted in the OMM or BAK is free of inhibitory proteins, the pore formation in the OMM is accomplished. This causes the release of apoptogenic molecules from the mitochondria to the cytosol, facilitates the fragmentation of the mitochondria and finally the cellular apoptosis takes place⁶³. Some studies have demonstrated that the presence of either BAX or BAK is sufficient to make the intrinsic pathway functional, whereas the double deletion of these proteins abolishes the apoptotic pathway⁷⁴. Nevertheless, the absence of one of these proteins produces some abnormalities, indicating that the functional redundancy is not complete⁷⁴⁻⁷⁶. Regarding the pro-apoptotic protein BOK, its role is poorly understood so far and recent studies suggest its importance on tumor suppressor⁶⁸ or restrict its apoptotic activity to certain tissues⁷⁴.

One of the consequences of the OMM permeabilization is the escape of cytochrome c to the cytoplasm. Cytochrome c is a component of the electron transport chain and it is essential in the mitochondrial energy production⁷⁷. Besides its role on the cellular metabolism, the release of this molecule to the cytoplasm promotes apoptosome formation. This complex is comprised of apoptotic protease activating factor 1 (APAF-1), cytochrome c and ATP/dATP. Cytosolic cytochrome c binds to APAF-1 molecules, which are usually inactive in the cytoplasm, facilitating the binding of dATP to APAF-1⁷⁸. Simultaneously, procaspase-9 units are recruited to the APAF-1 CARD. Once the apoptosome is assembled, the cleavage of the initiator caspase-9 takes place and the caspase cascade is initiated, triggering apoptosis⁷⁹. This mechanism can be repressed by another group known as inhibitor of apoptosis proteins (IAPs), such as X-linked inhibitor of apoptosis protein (XIAP). They regulate apoptosis downstream of apoptosome assembly, binding to and inhibiting effector caspases⁸⁰. This group of anti-apoptotic proteins can be counterbalanced by another element released from the mitochondria known as DIABLO/SMAC^{81,82}. This protein binds directly to IAPs preventing their binding and inhibition of effector caspases⁸³.

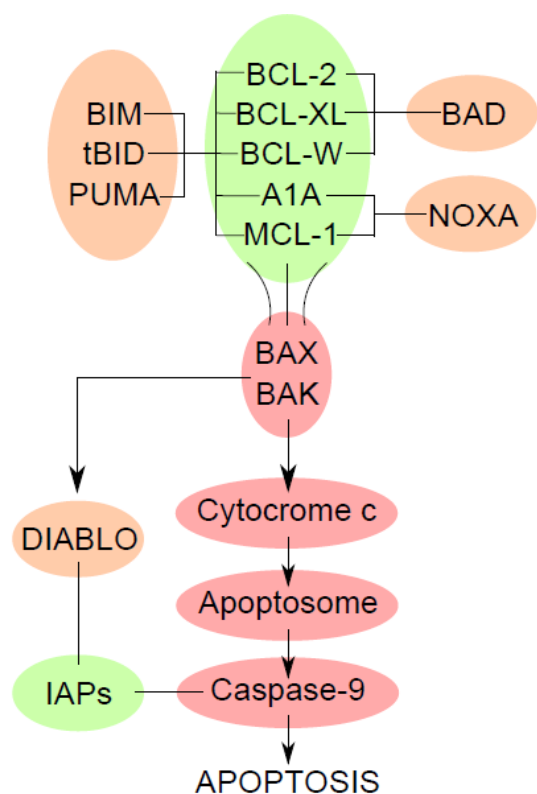


Figure 3. BCL-2 protein family tightly regulates the intrinsic pathway of apoptosis. Within this family, the group of anti-apoptotic proteins (BCL-2, BCL-XL, BCL-W, A1A and MCL-1) inhibits the pore formation on the outer mitochondrial membrane mediated by the pro-apoptotic proteins BAX and BAK. Another group of the BCL-2 family (BID, tBID, PUMA, BAD, and NOXA) represses the anti-apoptotic proteins promoting the mitochondrial permeabilization and facilitating the release of cytochrome c and DIABLO (also known as SMAC). The apoptosome is assembled by the cytoplasmic cytochrome c together with APAF-1 and pro-caspase 9 units. This complex initiates the activation of the caspase cascade and therefore the cell apoptosis. IAPs located in the cytoplasm can repress caspase activity and block apoptosis. The inhibition of IAPs by cytoplasmic DIABLO facilitates the apoptotic process.

2.2.5.2. The extrinsic pathway

The signal transduction from the death receptors initiates the formation of the death-inducing signaling complex (DISC)⁷⁰. The CD95 and TRAILR DISC consist of oligomerized CD95/TRAILR, Fas-Associated Death Domain (FADD) and pro-caspase 8 (also known as FLICE) or pro-caspase 10, which is exclusively present in humans^{70,84}. DISC interactions are based on homotypic contacts. The DD of CD95/TRAILR interacts with the DD of FADD and the DED of FADD interacts with the DED of the pro-caspases⁷⁰. The assembly of the DISC results in the recruitment and auto-proteolytic activation of the initiator caspases, consisting of a double cleavage of the pro-caspases. The resulting activated heterotetramer from pro-caspase 8, consisting of two large subunits (p18) and two small subunits (p10), is released into the cytosol initiating the caspase cascade and finally causing cell death⁷⁰. The activation of apoptosis mediated by the heterotetramer of caspase 10, in absence of caspase 8, is still controversial^{70,85}.

On the other hand, TNFR1 signaling mechanism is different because it results in the formation of 2 complexes. Signaling complex I is formed at the membrane upon

TNFR1 stimulation and consists of TNF, TNFR1, receptor interacting protein (RIP-1), TNFR1-associated death domain protein (TRADD) and TNFR-associated factor (TRAF-1/2). This complex may activate nuclear factor kappa B (NF- κ B) through inhibitor of κ B kinase (IKK) complex recruitment and may activate (c-Jun N-terminal kinases) JNK in a TRAF-2 dependent manner⁸⁶. Complex I can translocate into the cytoplasm and recruit FADD and procaspase 8/10, forming the complex II, also called traddosome⁸⁶. This complex is able to activate the caspase cascade and initiate apoptosis. The efficiency of complex II formation and its interaction with inhibitory proteins allows for the activation of the survival or the death program in the cell⁸⁶.

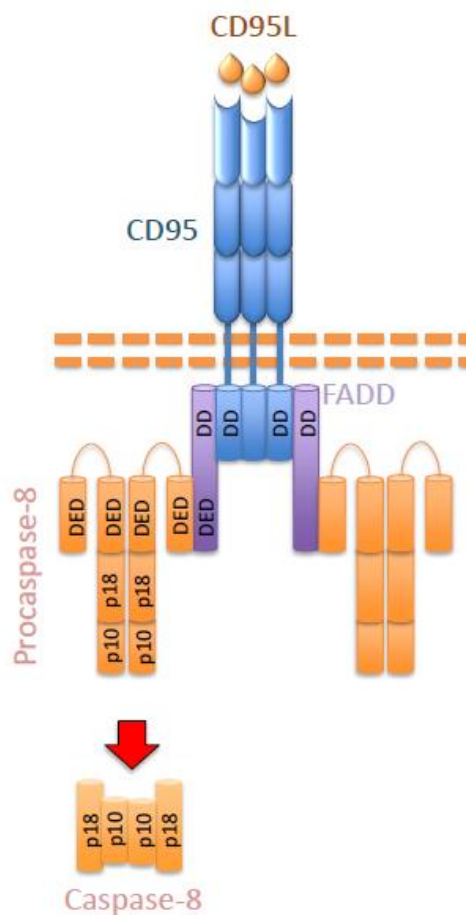


Figure 4. The death-inducing signaling complex (DISC) consists of death receptor oligomerized subunits, adaptor protein FADD and pro-caspase 8/10 recruitment, upon ligand stimulation. The interaction between the death receptor and FADD is mediated by death domain (DD) motifs whereas the interaction between FADD and pro-caspase is due to death effector domain (DED) contacts. The DISC assembly results in the cleavage and activation of the initiator caspases. Adapted from Krammer et al. 2007⁸⁷

2.2.5.3. The crosstalk between the pathways

The extrinsic pathway is able to interact and activate the machinery of the intrinsic apoptosis. High levels of DISC formation promote high amounts of active caspase 8, which further trigger effector caspases. This mechanism is characteristic of type I cells⁸⁷. However, when the amounts of DISC are not able to trigger the activation of effector caspases, the little amounts of caspase 8 need to implement an amplification loop that consists of the cleavage of BID^{87,88}. The truncated form of BID (tBID) produces BAX and BAK aggregation on the OMM, releasing cytochrome c to the cytoplasm and producing the subsequent activation of apoptosis^{88,89}. Type II signaling can be repressed by anti-apoptotic BCL-2 family members, such as BCL-XL and BCL-2, whereas they are dispensable to block type I-mediated apoptosis since this pathway bypasses the mitochondrial mechanism⁸⁸.

2.2.5.4. The granzyme B pathway

Cytotoxic T lymphocytes (CTL) and Natural Killer (NK) cells of the immune system can induce apoptosis in order to remove virus infected cells and tumor cells. To eliminate them, CTLs and NK cells release cytolytic granules containing pore-forming proteins, such as perforin, and serine proteases, known as granzymes⁹⁰. It has been demonstrated that this protein is able to cleave the initiator caspase 8 and the effector caspase 9, causing cell apoptosis^{91,92}. Additionally, granzyme B can cleave BID and promote its translocation to the mitochondria and the subsequent OMM permeabilization by BAX and BAK, inducing the formation of the apoptosome and the consequent caspase cascade activation^{93,94}.

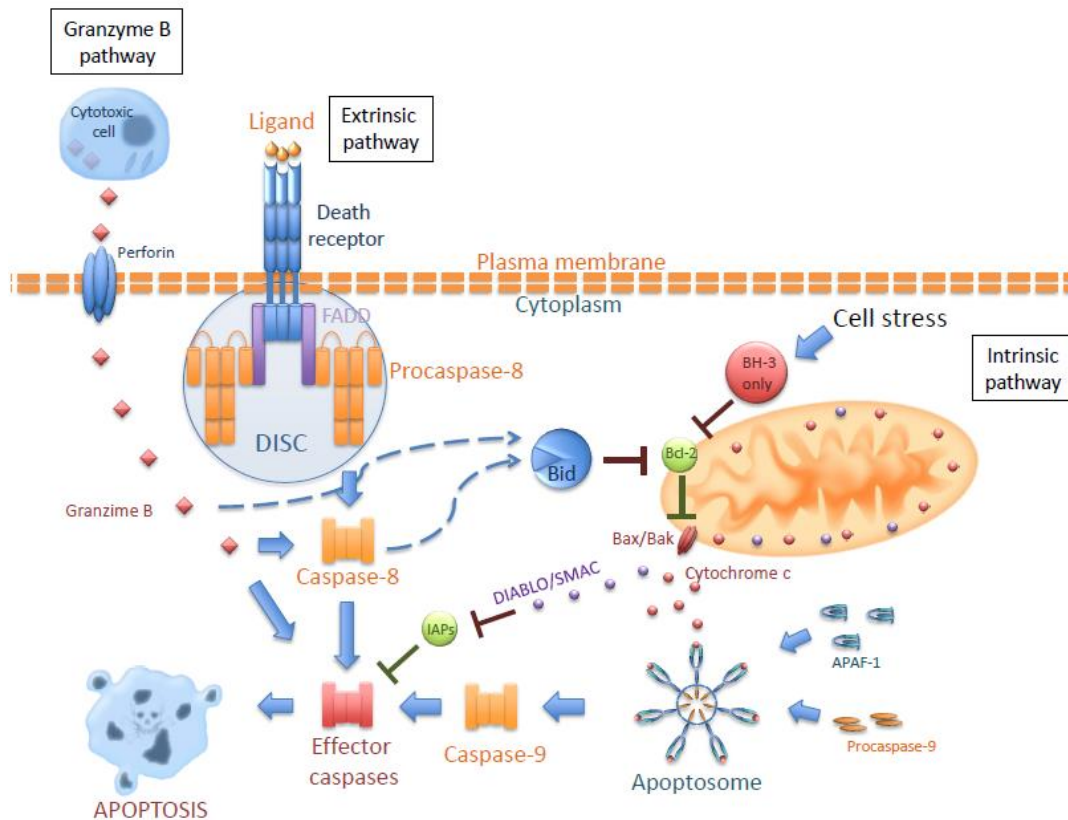


Figure 5. Apoptosis pathways. Cell stress promotes the triggering of the intrinsic pathway. The activation of BH3-only proteins inhibits the anti-apoptotic BCL-2 proteins, facilitating the pore formation in the outer mitochondrial membrane by BAX and BAK. In consequence, cytochrome c is released to the cytoplasm producing the assembly of the apoptosome, consisting of APAF-1 subunits, cytochrome c molecules and pro-caspase 9. The formation of this complex results in the cleavage of caspase 9 and the further activation of effector caspases. The engagement of death receptors causes the recruitment of adaptor proteins, like FADD, which facilitates the recruitment of pro-caspase 8 molecules, leading to the formation of the death-inducing signaling complex (DISC). This recruitment triggers the activation of caspase 8, which is able to activate effector caspases. Low levels of active caspase 8 can crosstalk with the intrinsic pathway through the cleavage of BID. The truncated form of BID (tBID) promotes the pore formation and the further permeabilization of the mitochondria. The entrance of granzyme B through the pore formed on the plasma membrane by perforin, both released by cytotoxic cells, initiates apoptosis by effector caspases cleavage as well as BID proteolysis. Adapted from Krammer et al. 2007⁸⁷

2.2.6. The FLICE-inhibitory proteins

Cellular caspase 8 (FLICE)-like inhibitory protein (cFLIP) is an anti-apoptotic regulator that suppresses death-receptor mediated apoptosis. Originally, FLIP proteins were identified as viral gene products, called vFLIPs, produced by several γ -herpesviruses. These proteins contain DEDs that are able to interact with caspases^{95,96}. After the discovery of these viral proteins, the cellular homologue was identified and named cFLIP (also known as CASH, Casper, CLARP, FLAME, I-FLICE, MRIT and usurpin)⁹⁷⁻¹⁰⁴. So far, the expression of three different splice variants has been identified. The longest isoform of 55 kDa, known as cFLIP_L, contains two DED and a catalytically inactive caspase-like domain^{61,97}. The C-terminus of cFLIP_L resembles the structures of caspase 8 and 10, but lacks a functional caspase domain¹⁰⁵. The lack of catalytic activity is due to the substitution of several amino acids, particularly the cysteine residue in the catalytic domain¹⁰⁵. Heterodimerization of caspase 8 with cFLIP_L produces a partial processing of caspase 8 generating the p10 fragment of caspase 8 and a p12 fragment from cFLIP_L. The product of this combination results in a limited activity of caspase 8¹⁰⁶. Furthermore, cFLIP_L has a caspase 8-cleavage site (Asp-376) independent of death receptor ligation¹⁰⁷. This interaction of cFLIP_L with caspase 8 produces the formation of the fragment variant p43-cFLIP¹⁰⁷. An alternative function of the early caspase 8 cleavage product from cFLIP_L p43 is the activation of the NF- κ B pathway. Concretely, p43 can efficiently interact with RIP-1 and TRAF-2 and initiate the activation of the NF- κ B pathway^{108,109}.

Moreover, two short isoforms have been described, the 26 kDa cFLIP_S form and the 24 kDa cFLIP_R form^{110,111}. cFLIP_S is present in human but not in mice and consists of two DED followed by a ~20 aminoacids sequence, relevant for the ubiquitylation and the further proteasomal degradation^{111,112}. Similarly, cFLIP_R consists of two DED. This isoform, present in human and mouse, was originally identified in the Raji B cell line¹¹⁰. In human, the expression of the short isoforms is decided by a single nucleotide polymorphism (SNP) in a particular splice site¹¹³.

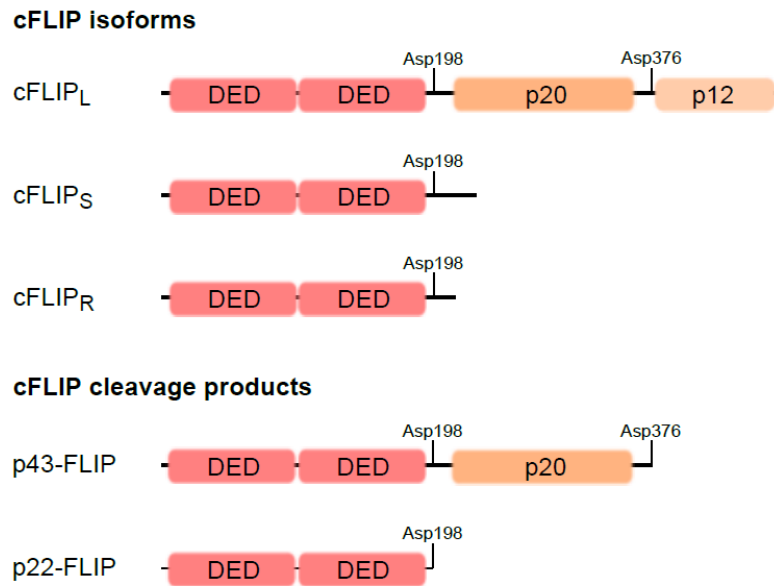


Figure 6. Three isoforms of cellular caspase 8 (FLICE)-inhibitory protein (cFLIP) are known: cFLIP_{long} (cFLIP_L), cFLIP_{short} (cFLIP_S) and cFLIP Raji (cFLIP_R). The death effector domains (DED), the catalytically inactive caspase-like domains p20 and p12 as well as the cleavage sites are shown. cFLIP cleavage products include p43-FLIP and p22-FLIP. Adapted from Krammer et al. 2007⁸⁷

Death receptor-mediated cFLIP inhibition is regulated by the interaction of the DED of these molecules with the adaptor protein FADD and, in consequence, cFLIP proteins compete with pro-caspase 8 recruitment at the DISC level. The short isoforms of cFLIP are considered full inhibitors of caspase 8 recruitment^{97,106}, whereas the function of cFLIP_L is more complex. cFLIP_L can compete with caspase 8 recruitment and therefore repress the initiation of apoptosis¹⁰⁵. However, it can also form a heterodimer with caspase 8 through the interaction of both caspase-like domains, resulting in a limited apoptotic activity¹⁰⁵. Regarding this dual function, it has been reported that low levels of cFLIP_L promote apoptosis by caspase 8 processing, whereas high levels of cFLIP_L repress apoptosis¹⁰⁵. In addition, the processed fragment p43FLIP recruits efficiently RIP-1 and TRAF-2 and, after caspase 8 interaction, can activate the NF- κ B pathway^{114,115}.

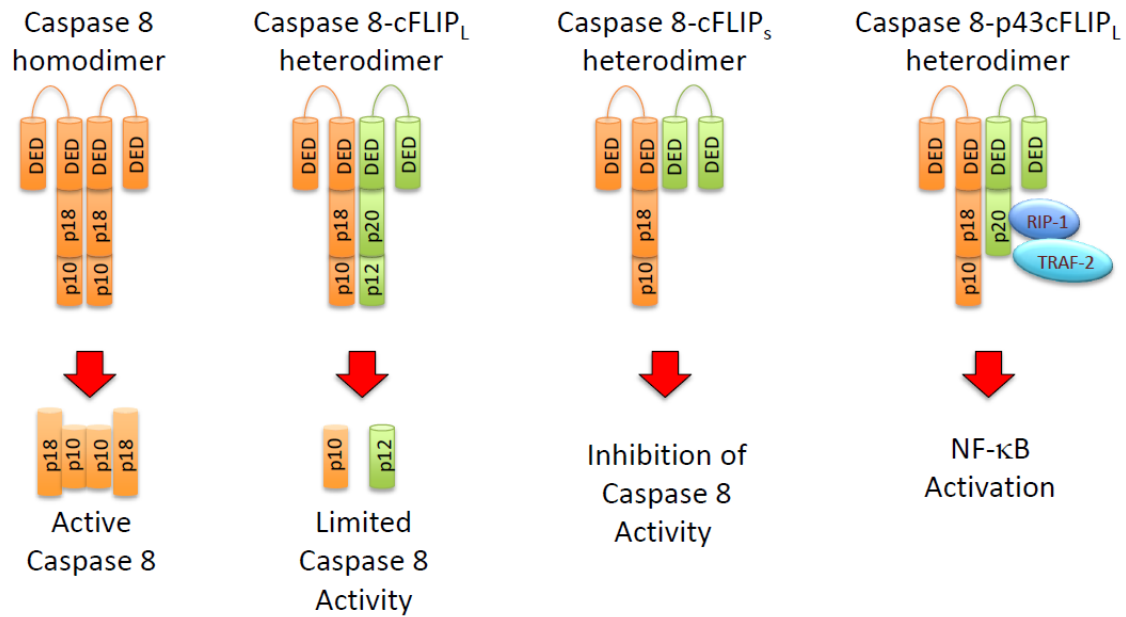


Figure 7. The homodimerization of caspase 8 results in the auto-proteolytic and trans-proteolytic cleavage initiating the activation of this caspase. The caspase 8-cFLIP_L interaction leads to the formation of the p10 and p12 respective fragments and a limited apoptotic activity. On the other hand, the interaction of caspase 8 and cFLIP_S inhibits completely the activation of caspase 8. Finally, the caspase 8-p43FLIP interaction results in the activation of the NF-κB pathway, supported by the recruitment of RIP-1 and TRAF-2. Adapted from Budd et al. 2006¹²³

2.2.7. The role of the FLICE-inhibitory proteins (cFLIP) in the immune system

cFLIP is expressed in a wide variety of cells, such as myocytes, keratinocytes, neurons, endothelial cells, as well as in cells of the immune system, including hematopoietic stem cells, dendritic cells (DCs), macrophages, B cells and T cells^{116–123}. These molecules are very important not only in cell survival but also in the activation of certain functions and developmental stages of cells in the immune system. For instance, low cFLIP levels have been reported in monocytes, whereas macrophages and immature DCs show high levels^{122,124}. Since CD95L stimulation upregulates the production of several cytokines in these cells, they need to be protected against CD95L-mediated apoptosis^{121,122,125}. Furthermore, cFLIP seems to be important in the activation of different pathways, like NF-κB, through CD95L stimulation¹²⁶. cFLIP has also an important role in B and T cell development and function. In the case of the B cells, CD40 and antigen-receptor stimulation upregulates cFLIP and protects these cells from CD95-mediated cell death^{127,128}. The function of cFLIP seems to be important in the

germinal centers, where B cells initiate the caspase machinery and, upon CD40 stimulation and DC contact, achieve the apoptosis inhibition¹²⁹. Similarly, T cells elevate cFLIP expression upon T cell receptor (TCR) stimulation¹³⁰. This fact is linked to the T cell activation. It has been demonstrated that Jurkat T cells overexpressing cFLIP_L show an elevated NF-κB pathway activation upon TCR stimulation. As a consequence, these cells produce more interleukin 2 (IL-2) than wild-type Jurkat cells¹²⁶. Furthermore, cytokines, such as IL-2, IL-4, and IL-12, can also modulate the gene expression of cFLIP^{131,132}. Interestingly, it has been shown that IL-4 negatively regulates cFLIP in T cells¹³¹. This cytokine promotes T helper 2 (Th2) differentiation from naïve T cells, and consistent with the cFLIP expression, the differentiated cells have higher caspase activity¹³³.

An indirect way to decipher the impact of the cFLIP function in the cells is to study the effects of its deletion *in vivo*. Since the deficiency of cFLIP is embryonically lethal in mice¹³⁴, cFLIP has been deleted specifically in T cells. The result of this deletion revealed a reduction of the αβ-T cell compartment due to a proliferation and survival defect^{135,136}. cFLIP-deficient thymocytes and cFLIP-deficient mature T cells, both manifest an impaired viability compared to the respective wild-type cells. Additionally, the requirement of cFLIP for normal proliferation in response to TCR stimulation was proved¹³⁵. Looking more in detail into the specific role of the different isoforms, all cFLIP variants can repress death receptor-mediated apoptosis by preventing caspase 8 cleavage^{95,105,106}. In addition, cFLIP_L has the capacity to form p43-FLIP-caspase 8 complexes, which are able to activate the NF-κB pathway and, in consequence, improve the T cell survival and activation competence^{114,115}.

2.3. Apoptosis and immune homeostasis

One of the main functions of the immune system is to defend the organism against harmful pathogens as well as to clear unwanted and dangerous cells. Apoptosis is an important mechanism to develop these functions. On one hand, several cells of the immune system induce apoptosis to eliminate infected or cancer cells. There are particular cell types specialized in this task, like CTL and NK cells^{137,138}. They can induce apoptosis by means of the granzyme B pathway, activating death receptors located on the surface of the undesired cell, or induce cell death by cytokine-mediated cytotoxicity^{137,138}. Another scenario where apoptosis has a significant relevance is the

regulation of the immune homeostasis by controlling the cell number of the different populations. Normally, under steady-state conditions, the immune system remains in a surveillance mode. Only when there is a threat, the cells of the immune system are activated and begin to proliferate to act against the threat. Following the resolution, the system needs to return to the previous situation to avoid damage to its own tissues and a waste of energy. To do this, many cells involved in eliminating the threat must disappear and therefore apoptosis becomes important to recover towards homeostasis again. For instance, activation-induced cell death (AICD) is crucial to reduce the population of T cells after clonal expansion. Resting T cells are resistant to CD95-mediated apoptosis due to low receptor expression¹³⁹. Upon antigen encounter, these cells proliferate, get activated and upregulate CD95¹³⁹. Despite this fact, T cells remain resistant to death receptor-mediated apoptosis favored by the presence of the anti-apoptotic protein cFLIP_s^{140,141}. After antigen disappearance, cFLIP_s is downregulated and the T cells become sensitive to CD95-mediated apoptosis¹⁴¹. Only few cells that result from clonal expansion maintain high levels of the anti-apoptotic protein, promoting the survival of memory cells¹⁴². Thus, death receptor-mediated apoptosis has been demonstrated effective to regulate the clonal expansion and deletion of T cells. In addition, the intrinsic pathway also plays a role in the shut-down of the immune response. The BH3-only proteins mediate the activation of the intrinsic machinery of apoptosis upon cytokine withdrawal¹⁴³. That represents an additional mechanism that ensures the reduction of the lymphocytes after the cytokine downregulation as a consequence of the antigen clearance¹⁴⁴.

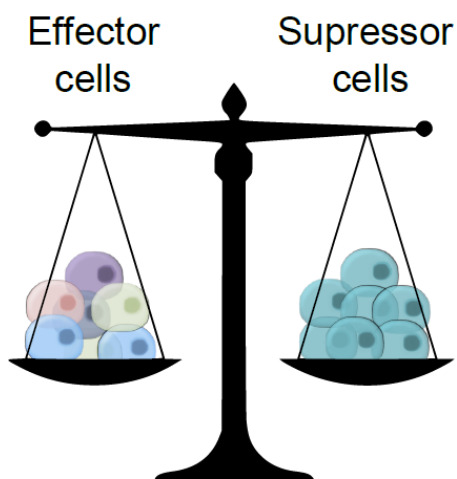


Figure 8 Modulation of both effector and suppressor cell populations is crucial to maintain the immune homeostasis. Increase of effector cells might result in chronic inflammation and autoimmunity, whereas increase of suppressor cells supposes vulnerability against pathogens and tumor cells.

2.3.1. Function of immune system

The regulation of the size of different cell subsets of the immune system is crucial for its homeostasis. In healthy conditions, the immune system is resting, vigilant and able to recognize a threat, get activated and eliminate the threat. Besides physicochemical barriers, defense against threats occurs at two different, but connected levels. Firstly, the immune system has specialized populations that are able to recognize specific molecules like the pathogen associated molecular patterns (PAMP) of microorganisms or “kill-me” signals from unwanted cells^{145–147}. As a result, the immune system is able to react quickly to the threat. Moreover, some of these cells, such as DCs and macrophages are capable to process and present antigens coming from undesirable cells or pathogens¹⁴⁸. Cells of the adaptive immune system recognize these antigens and are able to mount a second line of defense against the threat. A stochastic rearrangement of the gene segments encoding immunoglobulin (Ig) and TCR α/β chains give the capability to T and B cells to have a quasi-unlimited receptor repertoire against any antigen¹⁴⁹. Moreover, another advantage of the adaptive immunity is that a group of antigen-experienced cells remains as memory cells after the antigen clearance, to ensure a quick and effective response against a second encounter with the same threat^{150,151}.

2.3.2. Lymphocyte development

Due to the random genetic reorganization of the α/β TCR and Ig chains, any antigen is susceptible to be recognized by these cells, including self-antigens and antigens from the food or the microflora¹⁵². In such circumstances, the immune system needs mechanisms to tolerate those non-harmful antigens, in order to preserve the immune homeostasis and avoid the development of allergic reactions or autoimmunity. Given that autoantibody producing B cells appear during early stages of their development, the requirement of a mechanism to avoid or ameliorate the emergence of these cells is essential¹⁵³. These cells are forced to undergo a process of receptor editing, to enter into an anergic, i.e. unresponsive, state or undergo apoptosis^{154,155}. Furthermore, autoreactive B cells can escape from these checkpoints or newly arise from nonautoreactive B cells. To prevent the progression of these cells, there are similar mechanisms to regulate the malfunction of the B cells in peripheral organs^{154,156}.

Analogous to B cells, mechanisms to prevent T cell-derived autoimmunity are needed. Firstly, an “educational program” for T cells occurs in the thymus. This process of

central tolerance begins when the cell precursor enters in the thymus¹⁵⁷. At this stage, the thymocytes do not express neither the co-receptors CD4 nor CD8¹⁵⁷. Then, the stochastic rearrangement of the α and β genetic segments takes place, the pre-receptor is assembled and both co-receptors are expressed, giving the conformation of double positive (DP) to the thymocytes^{158,159}. In this stage, the TCR interacts with a self-antigen—MHC complex from DCs and thymic epithelial cells (TEC). The self-peptides presented are either exported by migratory DCs or generated by TECs thanks to the ability given by the transcription factor AIRE to generate self-tissue proteins. If the TCR-MHC interaction is impaired, the cell undergoes programmed cell death in a process known “death by neglect”. More than 90% of the thymocytes die through that mechanism due to the expression of “useless” TCR. If the TCR-MHC engagement is made correctly, the thymocyte downregulates one of the co-receptor becoming CD4⁺ helper or CD8⁺ cytotoxic cell. Additionally, the tolerance to self-antigen is checked from DP to single positive stage. The TCR interacts with self-antigen-MHC complexes continuously in the thymus. If one of these interactions happens with high affinity, then the thymocyte is deleted in a process called “negative selection”. In the end, only thymocytes with a correct engagement and low affinity for self-antigens reach the “positive selection” stage and migrate from the thymus to the periphery. This mechanism aims to ensure that functional but not dangerous T cells are generated.

2.3.3. Treg development

Since negative selection does not ensure the complete elimination of all the autoreactive T cells, some potential harmful cells can escape from the thymus. Consequently, there is a second level of regulation known as peripheral tolerances that counterbalance the occasional breakout of autoreactive T cells, contributing to keep immune homeostasis¹⁶⁰. Apart from the secretion of suppressive cytokines in certain tissues, the main mediators of the peripheral tolerance are the regulatory T cells (Tregs)^{161,162}. This cell type represents about 10 % of the total CD4⁺ compartment in the periphery and they express the interleukin 2 receptor α chain (CD25) and the forkhead box P3 transcription factor (Foxp3)^{162,163}. Tregs originate in the thymus, like other $\alpha\beta$ -T cells. However, during the thymic selection process, Tregs manifest higher TCR-peptide-MHC affinity than positive selected T cells¹⁶⁴⁻¹⁶⁶. This fact would entail the elimination of the Tregs by negative selection. Conversely, these cells are reprogrammed to avoid the cell death and become suppressive cells¹⁶⁷.

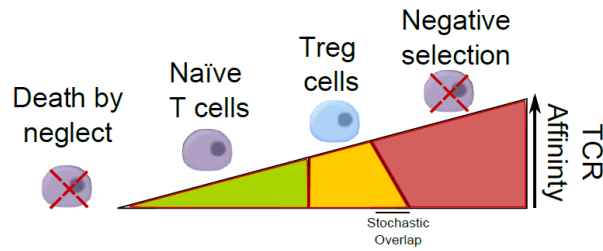
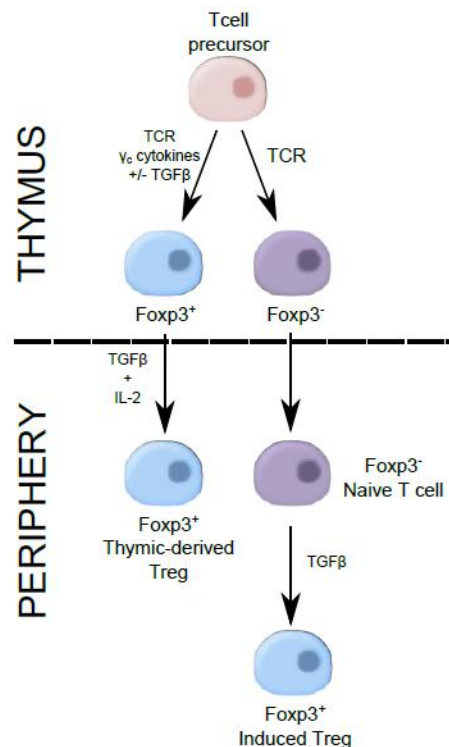


Figure 9. Cell fate during thymic selection is determined by the interaction strength between the TCR and the peptide-MHC complex. Deficient interactions result in the death of the cell through a mechanism known as death by neglect. Moreover, interactions trigger the negative selection, controlled by the pro-apoptotic protein BIM, which promotes cell apoptosis to avoid the development of potential autoreactive cells. Weak TCR-peptide-MHC interactions are needed to protect the thymocytes, promoting the positive selection and the development of naïve T cells. The development of Treg cells occurs within a range of interactions between the positive and negative selection. Therefore, Treg cells present a TCR repertoire with higher affinity to self-peptides compared to naïve T cells, sharing an affinity range with the potential autoreactive cells. Adapted from Klein et al. 2014¹⁶⁰

In addition, the differentiation under appropriate stimuli of naïve T cells to Tregs represents another source of Treg generation. The cytokine transforming growth factor beta (TGF- β) results crucial to achieve this T cell polarization to induced Tregs (iTregs) in the periphery¹⁶⁸.

Figure 10. Thymus-derived Treg cells (also called “natural Tregs”) initiate the expression of the transcription factor Foxp3 mediated by cytokine signals through thymic epithelial cells interactions as well as signals from the common cytokine-receptor- γ chain subunit. Alternatively, Treg can develop in the periphery from naïve T cells through antigen encounter and IL-2/TGF- β stimulation. Adapted from Hühn et al. 2009²³⁴



Strikingly, dysfunction of Treg cells leads to autoimmune diseases¹⁶⁹. The complete loss of function of the Tregs causes in humans the idiopathic polyendocrinopathy X-linked (IPEX) syndrome, characterized by a fatal systemic autoimmune disease¹⁷⁰. Moreover, Treg cell depletion or the presence of a nonfunctional transcription factor Foxp3 in the Treg cells generates a similar phenotype in mice, which is called *scurfy*^{171–173}. These mice present runting, scaly skin, ears and eyelids, splenomegaly, lymph nodes enlargement and premature death¹⁷⁴.

2.3.4. Treg function

Tregs have different mechanisms of action to mediate the suppression. They can secrete inhibitory cytokines, such as TGF- β , IL-10, and IL-35 to diminish the effector activity of the immune system^{175–178}. Moreover, Tregs have cytolytic activity inducing apoptosis in a perforin-, granzyme-A- and granzyme-B-dependent manner¹⁷⁹. For instance, Tregs can suppress B cell function by killing these cells via apoptosis¹⁸⁰. Tregs use also metabolic disruption mechanisms to inactivate or kill other effector cells. On the one hand, Tregs consume IL-2 by the expression of CD25 and compete with other cells for this cytokine¹⁶³. IL-2 reduction causes a deprivation of this resource in activated T cells that produces the activation of the intrinsic apoptosis in these cells^{181,182}. On the other hand, release of adenosine nucleosides represses T cell functions through the activation of the adenosine receptor 2A, it promotes TGF- β secretion and inhibits IL-6 production^{183,184}. This cytokine blocks Treg generation and polarizes naïve T cells to T helper (Th) 17 differentiation¹⁸⁵. Therefore, IL-6 repression facilitates an immunosuppressive environment instead of the development of an inflammatory process. In addition, Tregs can transfer the inhibitory second messenger cyclic adenosine monophosphate (cAMP) through gap junctions into effector T cells¹⁸⁶. Furthermore, another cell target of the Treg suppression are the antigen-presenting DCs, which are mediators of the T cell activation¹⁸⁷. Tregs restrain DCs through the lymphocyte-activation gene 3 (LAG3)-MHC and the cytotoxic T-lymphocyte antigen 4 (CTLA4)-CD80/CD86 interaction^{188–190}. Besides the inhibition of the DC function and maturation, this mechanism produces the release of indoleamine 2,3-dioxygenase (IDO) by the DCs, which is a potent inhibitor of the T cell effector function¹⁹¹.

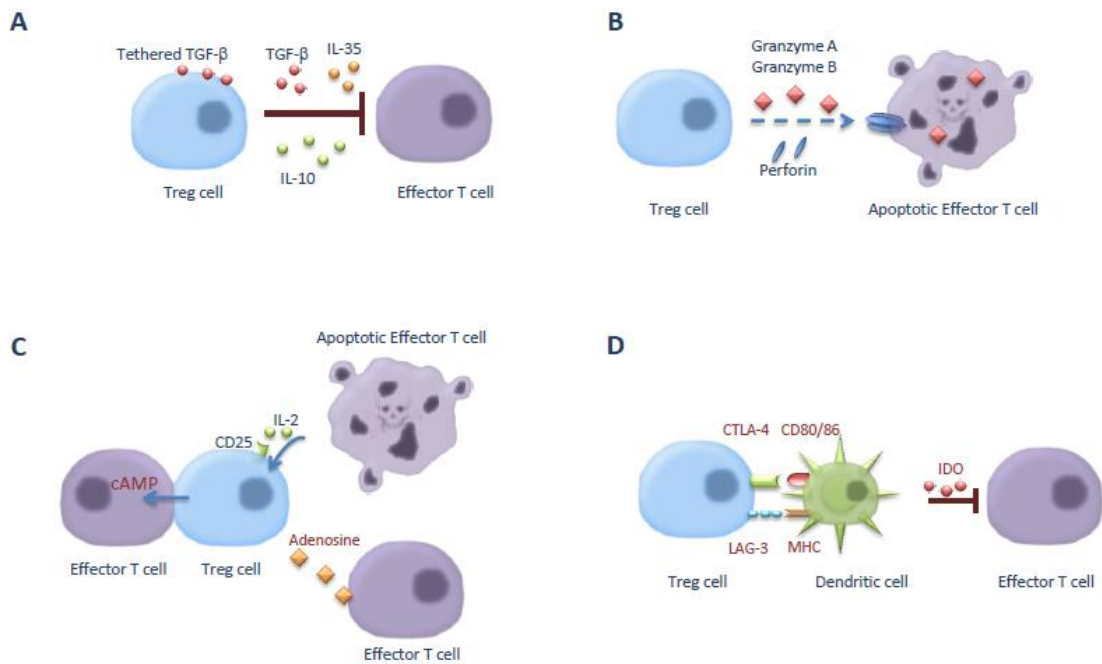


Figure 11. A. Release of inhibitory cytokines, such as TGF- β , IL-10 and IL-35 repress the activity of effector cells. B. Induction of granzyme-mediated apoptosis produces the cytolysis of target effector cells. C. Metabolic disruption includes IL-2 consumption, promoting the apoptosis initiation due to cytokine deprivation. Moreover, adenosine and cAMP production by Treg cells causes inhibition of effector cells and immunosuppression. D. Modulation of the function and maturation of dendritic cells (DC) by CTLA-4-CD80/86 and LAG-3-MHC interactions are effective methods to mediate immunosuppression as well as the induction of the production of the immunosuppressive molecule indoleamine 2,3-dioxygenase (IDO) by DCs. Adapted from Vignali et al.2008²³⁵

2.3.5. Treg homeostasis

The suppressive function of the Tregs constitutes a key factor in the balance of the immune homeostasis. The Treg population is regulated by different mechanisms contributing to the Treg homeostasis and, in consequence, influencing in the regulation of the immune system. In contrast to initial studies indicating that Tregs manifest an anergic condition^{192,193}, Tregs are in a semi-activated state, probably due to the TCR self-reactivity, which produces an elevated basal proliferation rate compared to conventional T cells (Tcons)^{194–197}. The high proliferation of the Tregs needs to be counterbalanced by cell elimination mechanisms in order to keep the size of the population. Recent reports connect Treg cell death to the intrinsic pathway of apoptosis. The transcription factor Foxp3 upregulates the BH3-only proteins BIM and PUMA, promoting the inhibition of BCL-2 anti-apoptotic proteins and consequently, facilitating the permeabilization of the mitochondria, initiating the intrinsic pathway of

apoptosis¹⁹⁸. Foxp3-promoted Treg lethality can be reverted by common gamma chain (γ c)-mediated cytokine signals¹⁹⁸. IL-2 signaling upregulates the anti-apoptotic protein MCL-1 in peripheral Tregs, which counterbalances the pro-apoptotic protein function of BIM¹⁹⁹. Thus, the IL-2-mediated regulation of the MCL-1-BIM axis controls the activation of the intrinsic pathway of apoptosis and therefore it plays an essential role in the Treg homeostasis.

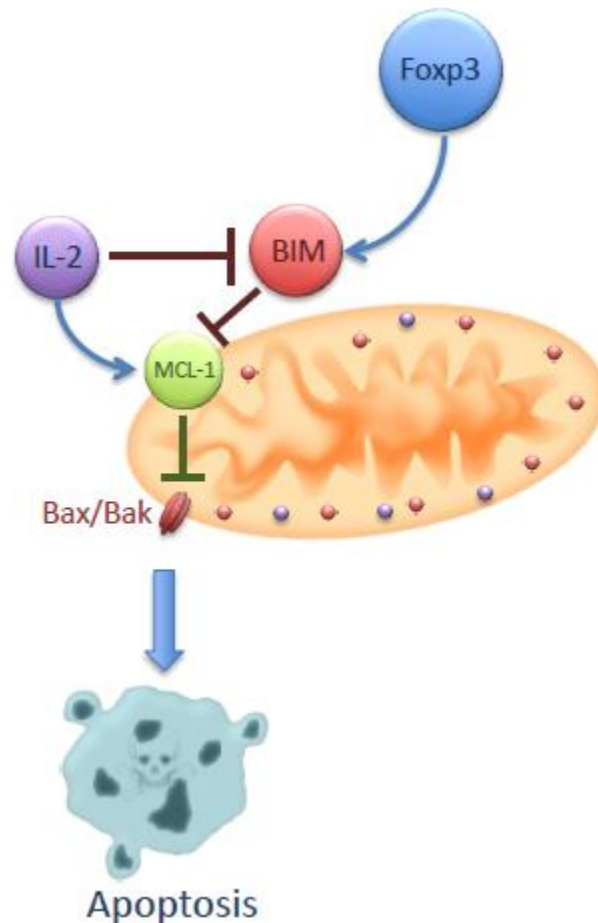


Figure 12. Intrinsic pathway controls Treg apoptosis, which is regulated by the BCL-2 family members. IL-2 counterbalances the pro-apoptotic function of Foxp3, which promotes the inhibition of MCL-1 through the pro-apoptotic protein BIM. The repression of MCL-1 facilitates the permeabilization of the mitochondria and the initiation of the intrinsic pathway of apoptosis.

2.4 Aims of the thesis

Regulatory T cells are able to suppress the immune response and, therefore, play a key role in the maintenance of immune homeostasis²⁰⁰. They represent a part of the balance that counteracts the effector response of the immune system. A shift towards the suppressor part versus the effector part supposes a weakening of the immune response, turning the organism more susceptible to infections or tumor development^{201,202}. On the other hand, the inverse situation produces a hyperactivity of the immune system facilitating the development of inflammatory processes and autoimmune diseases^{203,204}. Thus, a strict regulation of the size of the populations on both sides of the balance is necessary to keep immune homeostasis. Proliferation and cell death are two factors controlling the size of the population. Previous studies reported that Treg cells exhibit a high proliferation and apoptosis rate compared to conventional T cells, indicating the high dynamics of the suppressive cell type^{196,197,200}. Furthermore, the apoptotic mechanisms that regulate the Treg apoptosis have been investigated. The studies reveal that the transcription factor Foxp3 promotes apoptosis in the Tregs by means of the pro-apoptotic protein BIM¹⁹⁸. This mechanism is dampened by the IL-2-mediated upregulation of the anti-apoptotic protein MCL-1¹⁹⁹. However, to date, all investigations give emphasis on the regulation of the Treg apoptosis by the intrinsic pathway, neglecting a possible contribution of the extrinsic pathway to the apoptosis of this cell type. The aim of this thesis was to address whether the extrinsic pathway of apoptosis is relevant in the regulation of the Treg apoptosis. The first part of the thesis aimed to demonstrate, by *ex vivo* analyses, that the Treg cells display a higher cell death rate compared to conventional T cells and by which death mechanism Treg cells die. Additionally, the role of the anti-apoptotic protein cFLIP in Treg cell homeostasis was investigated by deleting the cFLIP-encoding gene specifically in murine Treg cells. Furthermore, the impact of the different death ligands and the contribution of the cFLIP isoforms on death receptor-mediated Treg cell death were studied.

3. Materials

3.1. Chemicals

If not mentioned otherwise, chemicals used to perform the experiments were purchased from Roth (Karlsruhe, Germany), Sigma Aldrich (Munich, Germany) or Merck (Darmstadt, Germany).

3.2. Cell culture material and devices

Cell culture work was performed using 6-well, 12-well, 24-well and 96-well plates obtained from NUNC - Thermo Fisher scientific (Rochester, USA). Sterile 10 μ l, 200 μ l and 1000 μ l filtered pipette tips were obtained from Starlab (Ahrensburg, Germany). Greiner bio-one (Frickenhausen, Germany) provided 15 ml and 50 ml conical tubes. 5 ml, 10 ml and 25 ml pipettes were purchased from Sterilin – Thermo Fisher Scientific (Rochester, USA). 20 μ m and 45 μ m sterile syringe filters were provided by Becton Dickinson (Heidelberg, Germany) and Millipore (Waltham, USA).

Cells were settled down using a 5810R centrifuge from Eppendorf (Hamburg, Germany) and were handled in a Sterile Guard III from The Baker Company (Sanford, USA). HERAcell 240i (Thermo Scientific) incubators were used for cell culture at 37°C, 5% CO₂ and 95% air humidity. Cell number was determined using a Cellometer Auto T4 by Nexcelom Bioscience (Lawrence, USA).

3.2.1. Cell culture media and supplements

Reagent	Lot. No.	Order No.	Company
RPMI 1640	1003068	41965	GIBCO - Life Technologies (Grand Island, USA)
Fetal Calf Serum (FCS)	A10108- 2367	A15-101	PAA (Pasching, Austria)
Sodium-pyruvate (100 mM)	749750	11360	GIBCO - Life Technologies
Non-essential amino acids (100x)	930229	11140	GIBCO - Life Technologies
Penicillin / Streptomycin (5 µg/ml)	918582	15070	GIBCO - Life Technologies
β-Mercaptoethanol (50 mM)	806672	31350	GIBCO - Life Technologies

3.2.2. Medium for cell culture

T cells and thymocytes were cultured in RPMI 1640, supplemented with 10% FCS, 1 mM Sodium-pyruvate, 1x non-essential amino acids, 50 µg/ml Penicilline/Streptomycin and 50 µM β-Mercaptoethanol.

3.2.3. Reagents, antibodies and cytokines used for cell stimulation

Reagent	Lot. #	Order #	Company
Anti-murine CD3 (Clone 145-2C11)	B133074	100314	Biolegend (San Diego, USA)
Phorbol 12-myristate 13-acetate (PMA)	16561-29-8	P8139	Sigma Aldrich
Ionomycin	56092-82-1	I-0634	Sigma Aldrich
Murine interleukin-2	MX1210031	402-ML	R&D Systems (Minneapolis, USA)
CD95L (scErbB2)	-	-	Self-produced (HEK293 cells)
TRAIL	810904	-	Novitec (Freiburg im Breisgau, Germany)
TNF α	-	410-MT-010	R&D (Minneapolis, USA)
FasFc	-	-	Self-purified - FPLC (HEK293 cells)
Q-VD-Oph	OPH109	03OPH10901	MP Biomedicals (Aurora, OH, USA)
Dexamethasone	-	D4902- 100mg	Sigma Aldrich

3.3. Materials, devices and reagents for flow cytometry

3.3.1. Devices

Labelled samples were analyzed on BD LSRFortessa and BD LSR II by Becton Dickinson (New Jersey, USA). Cell purification was performed using FACS Aria II (Becton Dickinson) or Moflo (Beckman Coulter, Indianapolis, USA) devices.

3.3.2. Fluorescent dyes

Reagent	Excitation	Emission	Company
LIVE/DEAD®			
Blue fluorescent reactive dye	350 nm	450 nm	Life Technologies
Tetramethylrhodamine ethyl ester (TMRE)	549 nm	574 nm	Enzo Life Sciences
7-amino-actinomycin D (7AAD)	543 nm	647 nm	BD Biosciences
Annexin V-APC	650 nm	660 nm	Becton, Dickinson

3.3.3. Flow cytometry antibodies

Reactivity	Fluorochrome	Species/Isotype	Clone	Order #	Company
humanCD2	APC	Mouse IgG1, κ	RPA-2.10	300214	Biologend
CD4	PacificBlue	Rat IgG2A, κ	RM4-5	100531	Biologend
CD8	PE-Cy7	Rat IgG2A, κ	53-6.7	100722	Biologend
CD25	APC	Rat IgG2A, λ	PC61.5	17-0251	Biologend
CD44	APC	Rat IgG2A, κ	IM7	103012	Biologend
CD62L	PerCP/Cy5.5	Rat IgG2A, κ	MEL-14	45-0621-82	eBioscience
Ki67	PE	Mouse IgG1, κ	B56	556027	Becton, Dickinson
Foxp3	AlexaFluor 488	Rat IgG2A, κ	FJK-16s	53-5773-82	eBioscience
Foxp3	PE	Rat IgG2A, κ	FJK-16s	12-5773-80	eBioscience
CD95	PE	Armenian Hamster IgG	MFL3	106605	Biologend
CD262 (DR5)	PE	Armenian Hamster IgG	MD5-1	119905	Biologend

Reactivity	Fluorochrome	Species/Isotype	Clone	Order #	Company
TNFR1	PE	Armenian Hamster IgG	55R-286	113003	Biolegend
Isotype control	PE	Armenian Hamster IgG	Ha4/8	553965	BD Pharmingen
CD16/CD32 (FcBlock)	-	Rat IgG2B, κ	2.4G2	553142	BD

*Antibodies have mouse reactivity, if not stated otherwise.

3.4. Reagents and materials used for Western blotting

PVDF membrane and photosensitive Hyperfilms® were purchased from GE Healthcare (Buckinghamshire, UK). Blotting and transfer devices from Bio-Rad Laboratories (Hercules, USA) were used for SDS-PAGE and protein transfers.

3.4.1. Primary antibodies

Antibody	Reactivity	Isotype	Species	Clone	Company
Anti- β - Actin	Mouse, Human	IgG2A	Mouse	AC-74	Sigma-Aldrich
Anti- Cleaved Caspase 3	Mouse, Human, Rat, Monkey	IgG	Rabbit		Cell Signaling (Massachusetts, USA)
Anti-Foxp3	Mouse, Human	IgG1	Mouse	eBio7979	eBioscience

3.4.2. Horseradish peroxidase-conjugated secondary antibodies

Reactivity	Species	Clone	Company
Mouse IgG1	Goat	1070-09	Southern Biotechnology (Birmingham, USA)
Mouse IgG2a	Goat	1080-05	Southern Biotechnology
Rabbit IgG	Goat	5030-05	Southern Biotechnology

3.5. Reagents and devices for confocal microscopy

Fluorescent microscopic pictures were taken with a Nikon Eclipse Ti (Düsseldorf, Germany) microscope, equipped with an UltraViewVox Spinning Disc module by Perkin Elmer (Waltham, USA)

3.5.1. Reagents for microscopy

3.5.1.1. Fluorescent dyes

Reagent	Excitation	Emission	Order #	Company
CellEvent® Caspase-3/7 Green Detection Reagent	503 nm	530 nm	C10423	Life Technologies

3.5.1.2. Fluorochrome-labeled antibodies

Reactivity	Fluorochrome	Species	Clone	Order #	Company
humanCD2	APC	Mouse IgG1, κ	RPA- 2.10	300214	Biolegend
CD4	PacificBlue	Rat IgG2A, κ	RM4-5	100531	Biolegend

3.6. Reagents for *in vivo* treatments

Reagent	Clone	Order #	Company
Anti-murine CD95L	MFL3	106608	Biolegend
Anti-murine CD95L	3C82	*	
Q-VD-OPh	-	SML0063- 5MG	Sigma Aldrich

*This antibody was a kind gift of Prof. Dr. Klaus Schultze-Ostoff from Universität Tübingen.

3.7. Frequently used buffers

Group	Buffer	Components
Cellular buffers	PBS	138 mM NaCl, 8.1 mM Na_2HPO_4 , 2.7 mM KCl, 1.5 mM K_2HPO_4 , pH7.4
	FACS Buffer	2% w/v BSA in PBS
	10x Annexin V binding buffer	0.1 mM HEPES / NaOH, 1.4M NaCl, 25 mM CaCl_2 , pH 7.4
Lysis buffers	TPNE	1% v/v Triton X-100, 2 mM EDTA, in PBS ad 300 NaCl mM, pH 7.4
	100x protease inhibitors	100 $\mu\text{g/ml}$ Apotinin, 100 $\mu\text{g/ml}$ Leupeptin, 100 $\mu\text{g/ml}$ Chymostatin, 100 $\mu\text{g/ml}$ Pepstatin
Western blot buffers	5x Laemmli	50 mM Tris, pH 6.8, 10% w/v SDS, 25% v/v β -Mercaptoethanol, 50% v/v Glycerol, 0.25 mg/ml Bromphenolblue
	Running buffer	25 mM Tris, pH 8.0, 192 mM Glycerin, 1% v/v SDS
	Transfer buffer	25 mM Tris, pH 8.0, 192 mM Glycerin, 20% v/v Methanol
	Blocking buffer	5% w/v non-fat dry milk, 0.2 % v/v Tween-20 in PBS
	TBS	137 mM NaCl, 2.68 mM KCl, 24.76 mM Tris, pH 7.4
	Washing buffer	0.05% v/v Tween-20 in TBS

3.8. Oligonucleotides

HPLC-purified oligonucleotides were supplied by Eurofins MWG Operon (Ebersberg, Germany).

3.8.1. Oligonucleotides for quantitative RT-PCR

Name	Sequence (5'→3')
UBC fwd	AAGAGAATCCACAAGGAATTGAATG
UBC rev	CAACAGGACCTGCTGAACACTG
cFLIP fwd	ACCCTCACCTGGTTTCTGATT
cFLIP rev	TCGTTCTGATCTAAGCTCTCACC
cFLIP _L fwd	GCAGAAGCUCUCCCAGCA
cFLIP _L rev	UUUGUCCAUGAGUUCAACGUG
cFLIP _R fwd	UCCAGAAGUACACCCAGUCCA
cFLIP _R rev	CACUGGCUCCAGACUCACC

3.8.2. Oligonucleotides for mouse genotyping

Name	Sequence (5'→3')
Foxp3 WT fwd	CCTAGCCCCTAGTTCCAACC
Foxp3 WT rev	AAGGTTCCAGTGCTGTTGCT
Foxp3 Mut fwd	AGGATGTGAGGGACTACCTCCTGTA
Foxp3 Mut rev	TCCTTCACTCTGATTCTGGCAATTT
FLIP flox fwd	CATGAGCACTGAGGGACACA
FLIP flox rev	GCGGAGTTTGCTACAGGAAG

3.9. Mouse strains

Foxp3^{tm1(CD2/CD52)Shori} mice²⁰⁵, referred to as Foxp3-hCD2 and C57BL/6-Tg(Foxp3-GFP)90Pkraj/J mice²⁰⁶, referred to as Foxp3-GFP were used as Treg reporter mice. B6.129(Cg)-Foxp3^{tm4(YFP/cre)Ayr/J} mice, referred to as Foxp3^{Cre}, were previously described²⁰⁷. B6.129-Cflar^{tm1Ywh/J} mice, referred to as *Cflar*^{fl}, were previously described¹³⁶. The two previous mouse strains were used to generate the *Cflar*^{ΔFoxp3} mouse strain. If not stated otherwise, experiments were performed using littermate controls animals. The mice were kept under specific pathogen free conditions in the animal facility of the Helmholtz Centre for Infection Research, Braunschweig, Germany. All breeding and experiments were performed in accordance with the guidelines of national and local authorities.

4. Experimental procedures

4.1. Molecular biology methods

4.1.1. RNA isolation

Cell lysis was performed by means of QIAshredder columns from Qiagen (Hilden, Germany). RNA of eukaryotic cells was purified using RNeasy Kit from Qiagen. Both procedures were done according to manufacturer's instructions.

4.1.2. Photometric determination of DNA/RNA concentration

DNA/RNA concentrations were determined by means of a Nanodrop 2000c (Thermo Scientific). Lambert-Beer function was used for calculations.

$$c = \varepsilon \times d \times E^{-1}$$

c = concentration (mol/l)

ε = coefficient of extinction ($M^{-1} \times cm^{-1}$)

d = density of the cuvette (cm)

E = extinction

4.1.3. Reverse transcription

100 ng of purified RNA were used as template to generate a complementary DNA (cDNA) strand by means of Revert™ Premium First Strand cDNA Synthesis Kit (Thermo Scientific). Oligo(dt)₁₈ primers were used for the RNA transcription according to supplier's protocol. Incubations were done in peqSTAR thermocycler from PEQLAB (Erlangen, Germany).

4.1.4. Polymerase chain reaction (PCR)

DNA obtained from mouse tissue by means of KAPA Express Extract (PEQLAB), was used for mouse genotyping. DNA amplification was performed using 2x KAPA Fast ReadyMix (PEQLAB) according to the following pattern:

Component	Amount
DNA template	1 µl (50-100 ng)
2x Ready-to-use mix	12.5 µl
Forward primer	1 µl (100 pmol)
Reverse primer	1 µl (100 pmol)
H ₂ O	9.5 µl

PeqSTAR thermocycler (PEQLAB) was used for incubation according to the following program:

Time	Temperature	Function	Cycles #
5 minutes	94 °C	Initial denaturation	1
30 seconds	94 °C	Denaturation	} 25-32
30 seconds	60° C (+/- x)*	Hybridization	
30 seconds	72° C	Elongation	
10 minutes	72° C	Terminal elongation	1

*Hybridization temperature was chosen 3° C under the T_M of the respective primer combination

4.1.5. Analytic agarose gels

1-2% agarose gels were used to separate DNA fragments, according to their length, by means of an electric field of 150 mA in the horizontal gel-electrophoresis system perfectBlue M (PEQLAB) in TAE buffer (40 mM Tris pH 8, 20 mM acetic acid, 1 mM EDTA) with 0.5 µg/ml ethidiumbromide. 1kB DNA ladder by PEQLAB was used as standard. The ethidiumbromide-DNA was visualized by UV-light ($\lambda = 254\text{nm}$).

4.1.6. Quantitative real-time polymerase chain reaction (qRT-PCR)

cDNA obtained from RNA of eukaryotic cells (see 4.1.1., 4.1.2. and 4.1.3.) was used for amplification in order to determine gene expression by means of qPCR analysis. SYBR Green I Master, 2x concentrated by Roche (Mannheim, Germany) was used to detect double strand DNA during qPCR amplification in a LightCycler® 96 System device from Roche. Gene expression was determined by relative quantification using Ubiquitin-conjugating enzyme E2D 2A (UBC) as reference gene. DNA Amplification and fluorescence measurement was done using the following program:

Time	Temperature	Function	Cycles #
1 minute	95 °C	Preincubation	1
10 seconds	95 °C	Single Mode of Acquisition	45
10 seconds	60° C		
10 seconds	72° C		
10 seconds	95° C	Continuous Mode of Acquisition	1
60 seconds	65° C		
1 second	97° C		

4.2. Protein biochemical methods

4.2.1. Cell lysis

TPNE lysis buffer supplemented with leupeptin, aprotinin, chymostatin and pepstatin A was used to get whole cell extracts. Cells were incubated on ice for 20 minutes and centrifuged (20.000g) for 15 minutes. After the incubation, supernatant was transfer to a prechilled tube.

4.2.2. Determination of protein concentration

Bicinchoninic acid (BCA) assay, provided by Pierce – Thermo Fisher Scientific, was used to determine total protein amount of lysates generated as indicated in 4.2.1. according to supplier's instructions. Absorption was as measured at 562 nm determined in a TECAN infinite 200M device (Männedorf, Switzerland).

4.2.3. SDS-Polyacrylamide gel electrophoresis (SDS-PAGE)

20 µg of protein lysate was mixed with 5x Laemmli buffer to a 1x final concentration and incubated at 95° C for 5 minutes. Biorad "Tetra cell" was used to separate the proteins in a 12% polyacrylamide gel at 33mA and 80V.

4.2.4. Western blotting

Biorad "Criterion Blotter" was used to transfer the proteins from SDS-PAGE to a PVDF membrane (GE healthcare) in 1x Transfer buffer at 500 mA at 80 V for 90 minutes. Afterwards, the membrane was incubated in blocking buffer for 1 hour at room temperature (RT) with constant agitation. Subsequently, the membrane was transferred into blocking buffer solution containing the primary antibody, diluted according to supplier's instructions, and incubated overnight. After the incubation, the membrane was washed 3 times with washing buffer and incubated with the secondary antibody for one hour at RT with agitation. Afterwards the membrane was washed 3 times with washing buffer and proteins were detected using SuperSignal West Dura substrate from Pierce - Thermo Fisher Scientific.

4.3. Mouse surgery and cellular methods

4.3.1. Isolation of mouse organs

Mice were sacrificed by cervical dislocation or CO₂. Thymus, spleen and peripheral lymph nodes were isolated from mice. Peripheral lymph nodes included cervical, axillar, brachial and inguinal lymph nodes. Lymphoid organs were milled through a 45 µm filter. Resulting cells were resuspended in PBS.

4.3.2. Flow cytometry analysis

For *ex vivo* analysis, 1×10^6 cells were washed twice with PBS, resuspended in 100 µl PBS and stained with LIVE/DEAD® Blue fluorescent reactive dye, diluted according to manufacturer's protocol. After 30 minutes incubation at 4° C in the dark, cells were washed twice with PBS, resuspended in FACS buffer containing FcBlock antibodies and incubated for 15 minutes at 4°C in the dark. Subsequently, cells were washed twice with FACS buffer, resuspended in 100 µl of FACS buffer and stained with the respective surface antibodies. After incubation for 15 minutes at 4°C in the dark, cells were washed twice with FACS buffer. In the case of intracellular marker determinations, cells' fixation and permeabilization was performed using FoxP3 Staining Buffer Set by Miltenyi Biotec (Mönchengladbach, Germany) following supplier's instructions.

For studies of viability/apoptosis determined by flow cytometry, cells were firstly stained with the respective surface markers according to the indications mentioned above. Next, TMRE or Annexin V/7AAD staining was performed for cell viability determination. For TMRE staining, cells were resuspended in 250 µl of FACS buffer, stained with TMRE and incubated for 20 minutes at RT in the dark. Then, 250 µl of FACS buffer was added to stop the staining and samples were analyzed by flow cytometry. For Annexin V/7AAD staining, cells were resuspended in 250 µl of 1x Annexin V binding buffer containing 3 µl of Annexin V and 1.5 µl of 7AAD, and incubated for 20 minutes at RT in the dark. After the incubation, 250 µl of 1x Annexin V binding buffer was added to stop the staining and samples were analyzed by flow cytometry.

4.3.3. Cell isolation by flow cytometry

Primary cells were stained with the respective surface markers as mentioned in 4.3.2. and were sorted by means of a FACS Aria II or Moflo device and collected in tubes containing PBS. This procedure was performed in cooperation with Dr. Lothar Gröbe, head of the flow cytometry and cell sorting facility at the Helmholtz Center for Infection Research (Braunschweig, Germany).

4.3.4. Viability studies in Tcon and Treg cells

Tcon and Treg cells were sorted from lymph nodes and spleen of Foxp3-GFP reporter mice. The cells were seeded in primary T cell medium (see 3.2.2.) and incubated for different time points (0, 24, 48, 72 hours) in the absence or presence of coated anti-CD3 (10 µg/ml), IL-2 (50 ng/ml), QVD (10 µM) and dexamethasone (0.5 µM). After incubation, cells were harvested, stained with Annexin V/7AAD and analyzed by flow cytometry.

4.3.5. Active caspase 3 detection by Western blot

Tcon and Treg cells were sorted from lymph nodes and spleen of Foxp3-GFP reporter mice. The cells were seeded in primary T cell medium (see 3.2.2.) and incubated for 2 hours in the absence or presence of PMA (10 ng/ml), ionomycin (1 µM), and anti-IL 2 (50 ng/ml). Then, the cells were harvested and protein lysates were obtained for Western blotting analysis.

4.3.6. *In vitro* stimulation with death ligands

Sorted Tcon and Treg from Foxp3-GFP mice cells were stimulated with 20 ng/ml CD95L, 20 ng/ml TRAIL, 20 ng/ml TNF α (R&D) or 0.5 µM dexamethasone for 16 hours. A FasFc fusion protein (50 µg/ml) was used to block CD95L-induced cell death. Primary cells from the thymus of *Cflar* ^{Δ Foxp3} and control mice were incubated for 16 hours with 200 ng/ml CD95L, 20 ng/ml TRAIL, 20 ng/ml TNF α and 0.5 µM dexamethasone, respectively. After incubation, cells were harvested, stained with Annexin V/7AAD and analyzed by flow cytometry.

4.3.7. Active caspase 3/7 determination by confocal microscopy

Primary cells from lymph nodes stained with anti-CD4-PacificBlue and hCD2-APC antibodies as in 4.3.2. Subsequently, cells were washed with PBS, resuspended in 1ml PBS and incubated with 50 µl of CellEvent® Caspase-3/7 Green Detection Reagent for 10 minutes at RT in the dark. Finally, samples were transferred to an 8-well cell culture chamber (Sarstedt, Germany) and analyzed by confocal microscopy.

Tcon and Treg cells were purified from Foxp3-hCD2 mice and stimulated with death ligands as in 4.3.6. for 16 hours. After incubation, both cell types were stained with CellEvent® Caspase-3/7 Green Detection Reagent as mentioned above and analyzed by confocal microscopy.

4.3.8. Histology and immunohistochemistry

Cflar^{ΔFoxp3} and control mice were sacrificed and lung, skin, pancreas and spleen tissue was isolated. Samples were fixed with 4% formaldehyde and embedded in paraffin. 3 µm sections were cut, deparaffinized and stained with hematoxylin and eosin for histological analysis. Furthermore, thymus, spleen and lymph node sections were stained with Foxp3 antibody. Histological analysis and immunohistochemistry determinations were done in cooperation with Dr. Marina Pils, head of the mouse pathology facility at the Helmholtz Center for Infection Research (Braunschweig, Germany).

4.3.9. Determination of cytokines in serum

Blood was obtained by means of the final heath puncture method. Samples were incubated at 37°C for 1 hour, then 10 minutes at 4°C and finally centrifuged. The supernatant was transferred to another tube and stored at -80°C. Cytokine levels from serum were determined using Th1/Th2 Mouse 6-Plex Panel (LifeTechnologies) in a Luminex® Instrument of the Luminex Corporation (Austin, USA) following supplier's protocol.

4.3.10. Autoantibodies determination

20 µg of liver and kidney extracts from RAG2-deficient mice were loaded onto a 12 % SDS-polyacrylamid gel and a Western blot analysis was implemented. PVDF membrane was incubated with serum diluted to a protein concentration of 5 µg/ml from *Cflar*^{ΔFoxp3} and control mice for autoantibody detection in the respective serum.

4.3.11. *In vivo* treatments

Cflar^{ΔFoxp3} and control mice were treated with 100 µg of anti-CD95L via intraperitoneal injection at days 7, 9 and 11 after birth. Mice were sacrificed at day 12 after birth for lymphoid organ isolation and flow cytometry analysis.

Cflar^{ΔFoxp3} and control mice were treated with 100 µg of QVD via intraperitoneal injection at days 8, 9 and 10 after birth. Mice were sacrificed at day 11 after birth for lymphoid organ isolation and flow cytometry analysis.

4.4. Statistical Analysis

Statistical analyses were performed by Mann-Whitney-tests to determine statistical significance, using Graph Pad Prism (Graph-Pad-Software Inc., La Jolla, CA, USA). Standard error of the mean (SEM) were represented as error bars in the graphs.

5. Results

5.1 Regulatory T cells manifest a higher apoptosis rate than conventional T cells

Treg cells are considered as a very dynamic population with a high turnover. Some studies support this idea showing a high basal proliferation rate in this T cell subset^{195,199}. Hence, a compensatory mechanism is needed in order to maintain the size of the population. It would seem logical to think that Treg cells have also a high cell death rate to compensate the high proliferation rate. However, to date, only few studies have been performed corroborating that fact^{199,208,209}. Thus, the analysis of the apoptosis rate in Treg cells is a pertinent study in order to corroborate previous findings, which indicated that Treg cells are a dynamic population. One consequence of apoptosis is the mitochondrial permeabilization leading to the loss of mitochondrial membrane potential (MMP)²¹⁰. It is possible to take advantage of this fact in order to measure cell apoptosis using tetramethylrhodamine ethyl ester (TMRE). Since TMRE is permeable to the mitochondrial membrane and a positively-charged red dye, it can be incorporated by active mitochondria. Thus, depolarized mitochondria, having decreased membrane potential, are less efficient in the incorporation of TMRE and therefore they show reduced staining. *Ex vivo* Treg and conventional T (Tcon) cells from thymus, spleen, peripheral lymph nodes (pLN) and mesenteric lymph nodes (mLN) of Foxp3-GFP mice were stained with TMRE and analyzed by flow cytometry. Since TMRE staining is not compatible with cell fixation, the cells were obtained from Foxp3-GFP mice, which express green fluorescent protein (GFP) in Foxp3-expressing cells, allowing discrimination between Foxp3 positive and negative cells. The TMRE_{low} subpopulations were significantly higher in Tregs compared to Tcon cells, indicating increased mitochondrial depolarization and suggesting higher apoptosis in the Treg population (Figure 13).

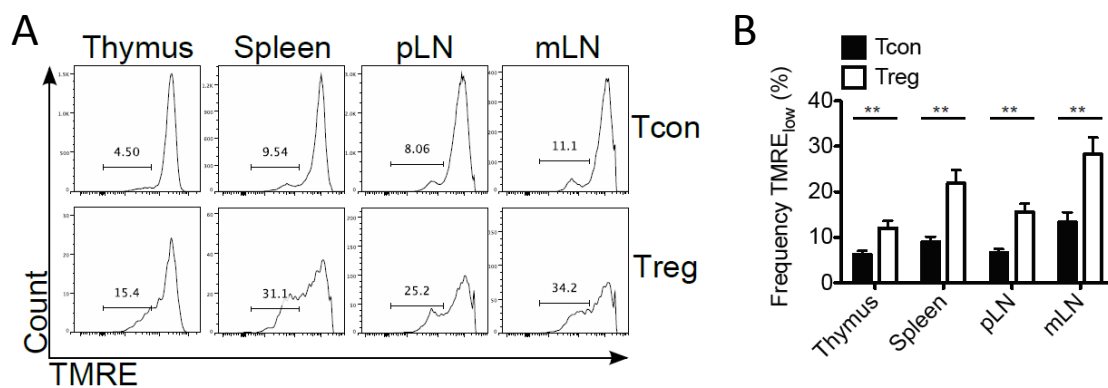


Figure 13. Treg cells have higher frequencies of TMRE_{low} than Tcon cells

(A) Representative histograms of TMRE stainings of thymus, spleen, pLN and mLN of Foxp3-GFP. (B) Bar graph of the percentages of TMRE_{low} subpopulations within Tcon and Treg cells (n=20 for thymus and spleen; n=19 for pLN and mLN). Bar graphs represent the mean; error bars represent SEM. Statistical analyses were performed by two-tailed Mann-Whitney tests; **p<0.01.

Since changes in the mitochondrial membrane potential are not an exclusive process of T cell apoptosis²¹¹, alternative methods were used to assess the apoptosis rate in Tcon and Treg cells. During the apoptotic cell demolition, phosphatidylserine (PS) molecules, which are normally in the inner layer of the plasma membrane, are exposed on the cell surface. It is possible to detect exposed PS molecules on cells using the protein Annexin V, which binds specifically to PS¹⁶, coupled with a fluorochrome. Moreover, the combination of Annexin V and a fluorescent DNA intercalator dye, like and 7-aminoactinomycin D (7AAD), allows discrimination between live cells, early apoptotic cells, which are only stained with Annexin V, and late apoptotic/necrotic cells, which are double positive for 7AAD and Annexin V by flow cytometry. In line with the previous results, higher frequencies of apoptotic cells, detected by their PS exposure, were found within the Treg population compared to Tcon cells in thymus, spleen, pLN and mLN of Foxp3-GFP mice (Figure 14).

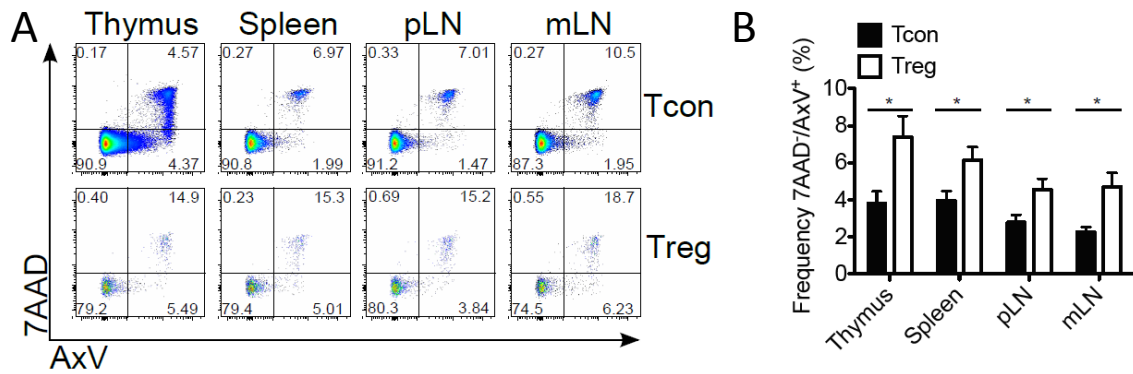


Figure 14. Annexin V (AxV) frequencies are higher in Treg than in Tcon cells.

(A) Representative dot plots of AnnexinV/7AAD staining of Tcon and Treg cells from thymus, spleen, peripheral and mesenteric lymph nodes of Foxp3-GFP mice (n=12 for thymus, spleen and pLN; n=11 for mLN). AxV⁻/7AAD⁻ cells are living cells, AxV⁺/7AAD⁻ are early apoptotic cells, and AxV⁺/7AAD⁺ are late apoptotic/necrotic cells. (B) Bar graph summary of AxV⁺/7AAD⁻ (early apoptotic) cells of Tcon and Treg cells from thymus, spleen, pLN and mLN of Foxp3-GFP mice. Bar graphs represent the mean; error bars represent SEM. Statistical analyses were performed by two-tailed Mann-Whitney tests; *p < 0.05.

A characteristic feature of apoptosis is the activation of caspase, such as the effector caspases 3 and 7¹³. The presence of active caspase 3/7 was tested in Tcon and Treg cells from lymph nodes of Foxp3-hCD2 reporter mice, using a fluorogenic substrate, which is processed by the active form of caspase 3 and 7 and stains the cell nucleus. Human CD2 (hCD2) expression on the cell surface correlated with Foxp3 expression, allowing the detection of Treg cells with a surface reporter marker. Consistently with the previous results, higher frequency of active caspase positive events was found by confocal microscopy in Treg compared to Tcon cells (Figure 15).

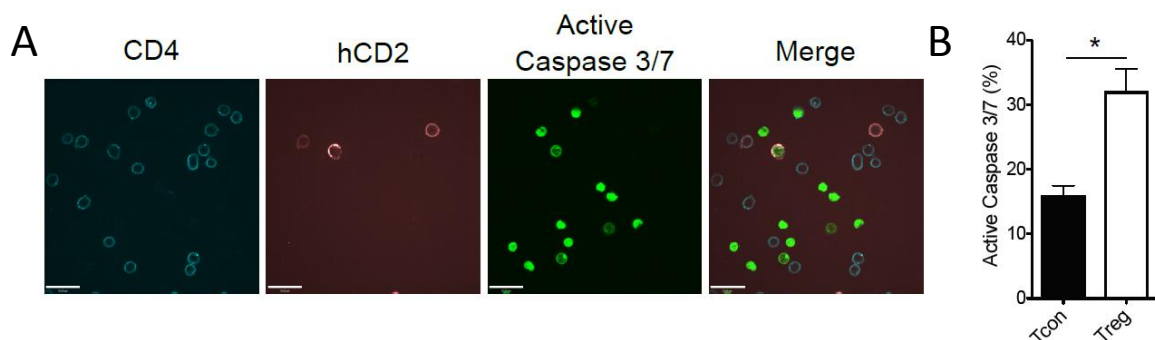


Figure 15. Active caspase 3/7 frequencies are higher in Treg than in Tcon cells.

(A) Representative confocal images of CD4, hCD2 (Foxp3) and active caspase 3/7 staining. Scale bars= 19 μ m. (B) Summary graph of frequencies of active caspase 3/7 in Tcon and Treg cells (n=5). Bar graphs represent the mean; error bars represent SEM. Statistical analyses were performed by two-tailed Mann-Whitney tests; *p < 0.05

Taken together, the results of the mitochondrial depolarization (TMRE defective uptake), plasma membrane disorganization (Annexin V exposure), and caspase activation, indicate higher apoptosis rate in Treg cell compared to Tcon cells, determined by *ex vivo* analysis.

5.2 Pan-caspase inhibitor and IL-2 improves Treg viability

After providing evidence that the cell death rate is higher in Treg cells compared to Tcon cells, an apoptotic inhibitor was used in order to determine whether apoptosis participates in Treg cell death. For this purpose, Treg cells were purified from Foxp3-GFP mice by sorting and cultivated in the absence and presence of IL-2, Q-VD-OPh (QVD) or dexamethasone for different time points (24, 48 and 72 hours). IL-2 was previously described as an important pro-survival factor for Treg cells. This cytokine, through the activity of anti-apoptotic proteins, blocks the mitochondrial permeabilization and the initiation of the intrinsic pathway of apoptosis¹⁹⁸. On the other hand, QVD is a pan-caspase inhibitor, and therefore prevents cell apoptosis²¹². Finally, the synthetic glucocorticoid dexamethasone was used as positive control because of its known potent apoptotic activity in T cells^{213,214}. Cell viability was assessed using Annexin V-7AAD staining by flow cytometry. IL-2 as well as QVD treatment increased Treg cell viability compared to untreated cells. Remarkably, QVD was more efficient blocking apoptosis than IL-2 treatment. As expected, dexamethasone treatment induced efficiently massive cell death in the cell cultures. All these data corroborate the key role of apoptosis in Treg cell death (Figure 16).

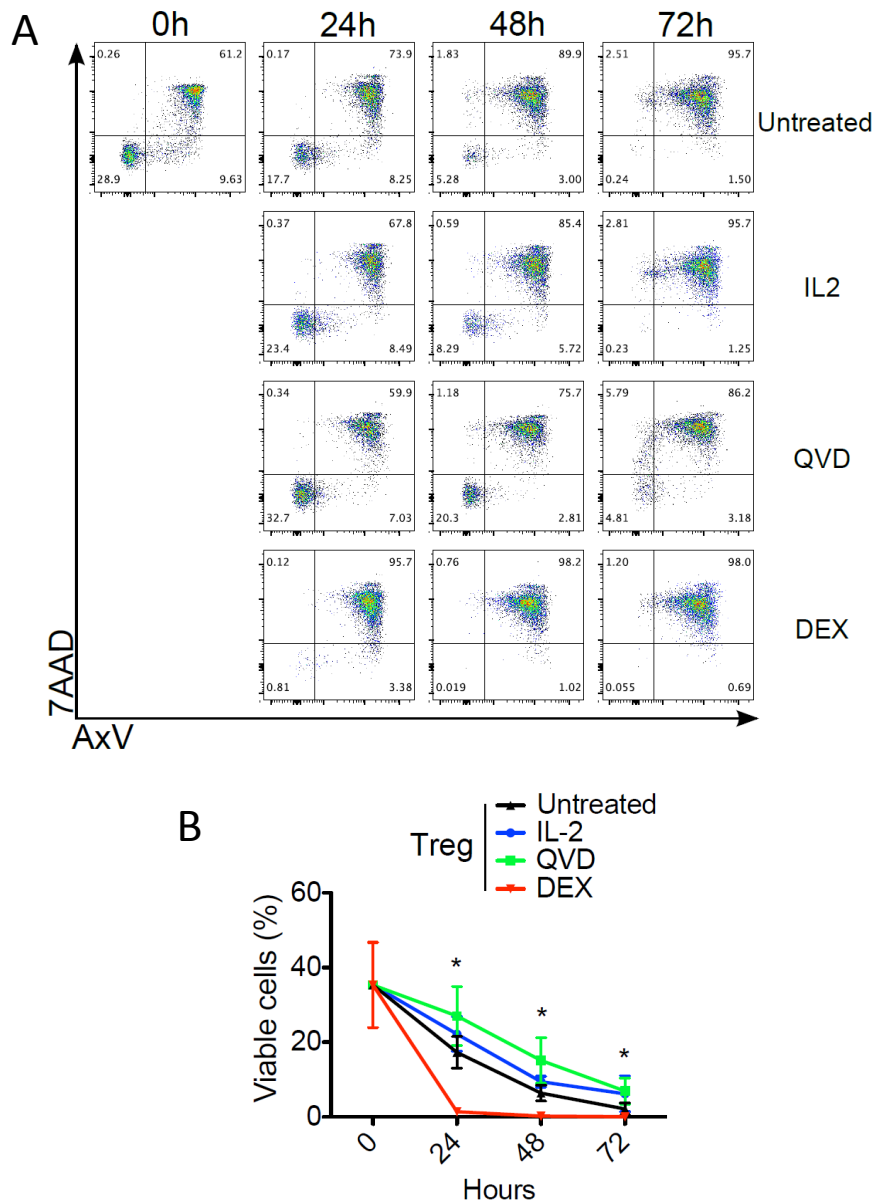


Figure 16. *In vitro* Treg viability improved upon QVD and IL-2 stimulation.

(A) Representative dot plots and (B) kinetics of Treg cell viability determined by AnnexinV/7AAD staining. Cells were purified from GFP-Foxp3 reporter mice by FACS sorting. They were cultivated without stimulation and in the presence of IL-2, QVD, and dexamethasone (DEX). AxV⁺/7AAD⁻ cells are viable cells (n=6). Each point represents the mean and error bars represent SEM. Statistical analyses comparing untreated vs. QVD samples were performed by one-tailed Mann-Whitney tests; *p< 0.05.

Furthermore, sorted Treg cells were also stimulated with anti-CD3 in order to induce cell death. T cell receptor (TCR) stimulation, in the absence of co-stimulatory signals, promotes apoptosis^{143,215}. However, TCR stimulation together with co-stimulatory CD28-derived signals, which regulates the anti-apoptotic protein BCL-XL, promotes cell activation instead of cell death²¹⁶⁻²¹⁸. For this purpose, anti-CD3 coated plates were used to cultivate the cells. Comparable to the previous data, IL-2 could improve Treg viability whereas QVD was even more efficient than IL-2 blocking apoptosis. Like in the previous experiment, dexamethasone killed massively activated Treg cells (Figure 17).

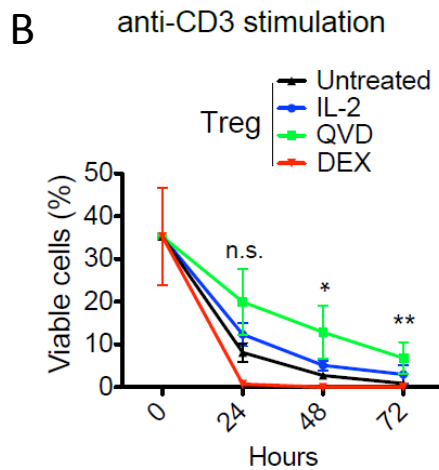
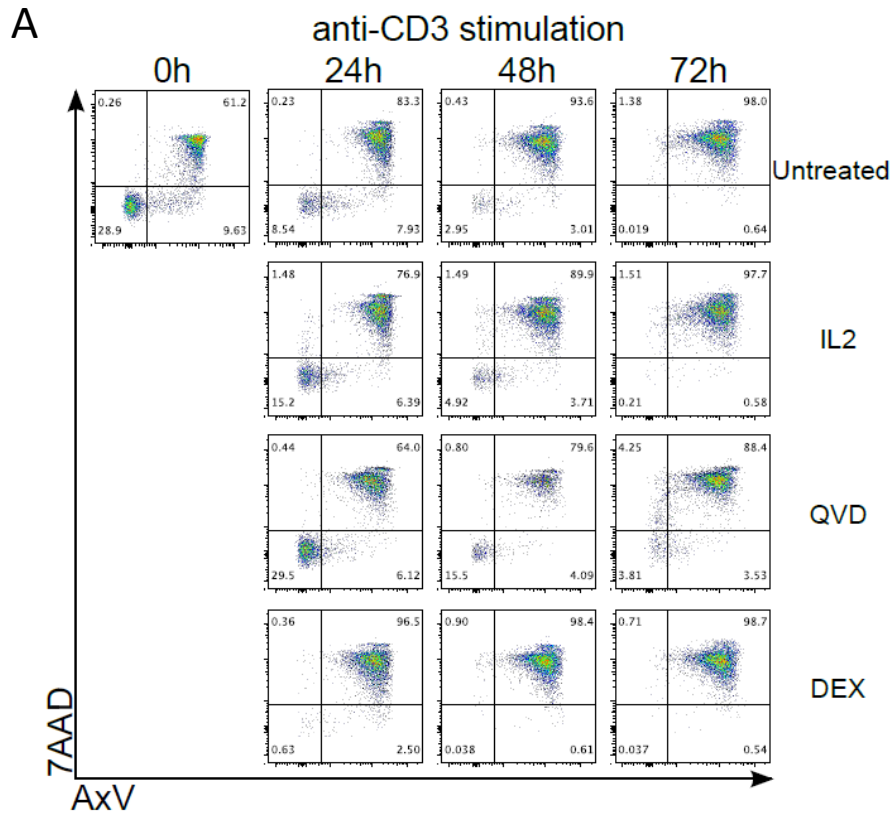


Figure 17. Viability of anti-CD3-stimulated Treg cells improved by QVD and IL-2 *in vitro* stimulation.

(A) Representative dot plots and (B) kinetics of Treg cell viability determined by AnnexinV/7AAD staining. Cells were purified from GFP-Foxp3 reporter mice by FACS sorting. They were cultivated in anti-CD3 coated plates in absence and presence of IL-2, QVD, and dexamethasone (DEX). AxV⁺/7AAD⁻ cells are viable cells (n=6). Each point represents the mean and error bars represent SEM. Statistical analyses comparing untreated vs. QVD samples were performed by one-tailed Mann-Whitney tests; *p< 0.05, **p<0.01; n.s., not significant.

Parallel to the Treg cell cultures, sorted Tcon cells were cultivated also in the presence of IL-2, QVD and dexamethasone. Unlike the Treg cells, the viability of the Tcon cells was not affected by either IL-2 or QVD stimulation (Figure 18).

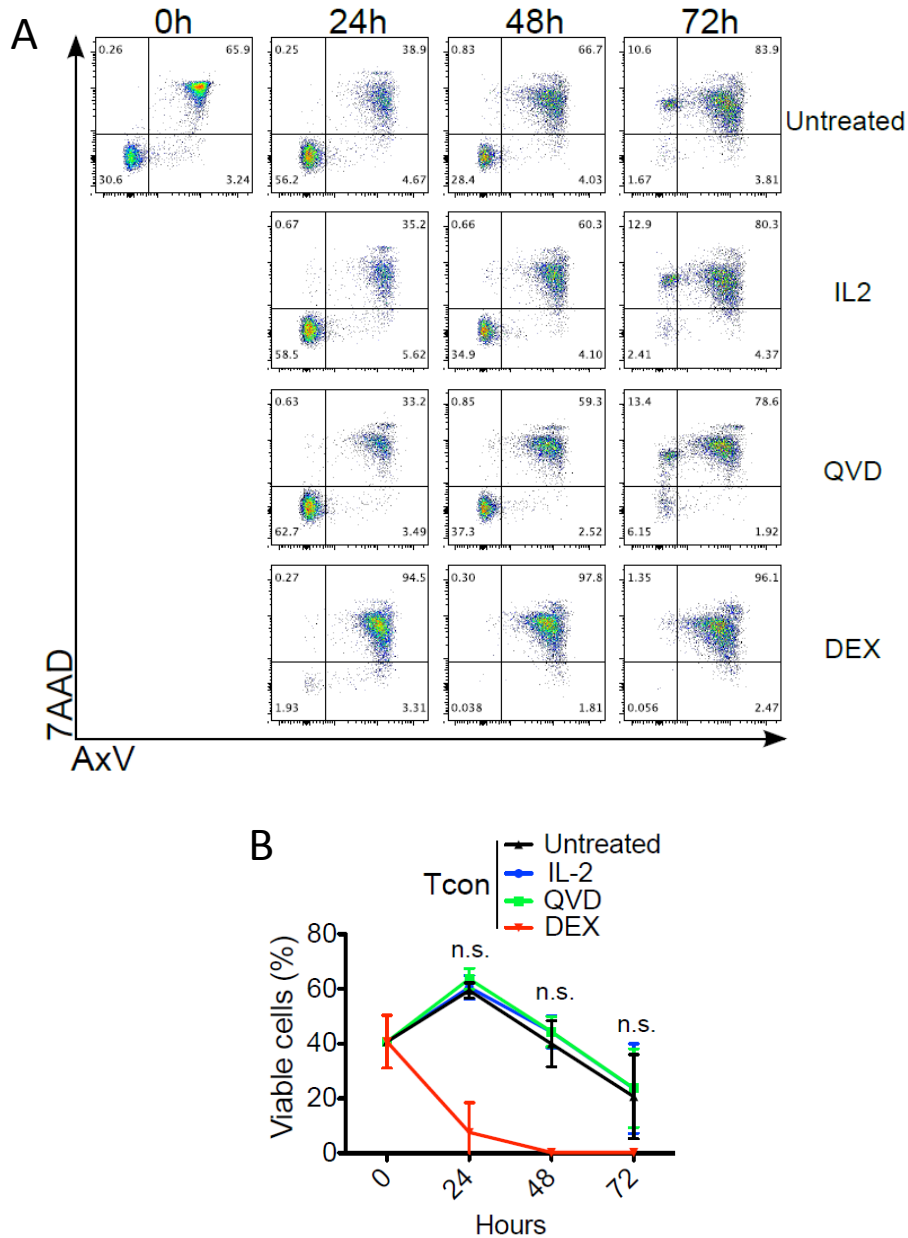


Figure 18. *In vitro* Tcon viability did not improve upon QVD and IL-2 stimulation. (A) Representative dot plots and (B) kinetics of Tcon cell viability determined by AnnexinV/7AAD staining. Cells were purified from GFP-Foxp3 reporter mice by FACS sorting. They were cultivated without TCR triggering and in the presence of IL-2, QVD, and dexamethasone (DEX). AxV/7AAD⁻ cells are viable cells (n=6). Each point represents the mean and error bars represent SEM. Statistical analyses comparing untreated vs. QVD samples were performed by one-tailed Mann-Whitney tests; n.s., not significant.

When the Tcon cells were cultivated in anti-CD3 coated plates and stimulated with IL-2 and QVD, the viability of Tcon cells improved by QVD treatment. In contrast, IL-2 did not improve the Tcon cell viability (Figure 19).

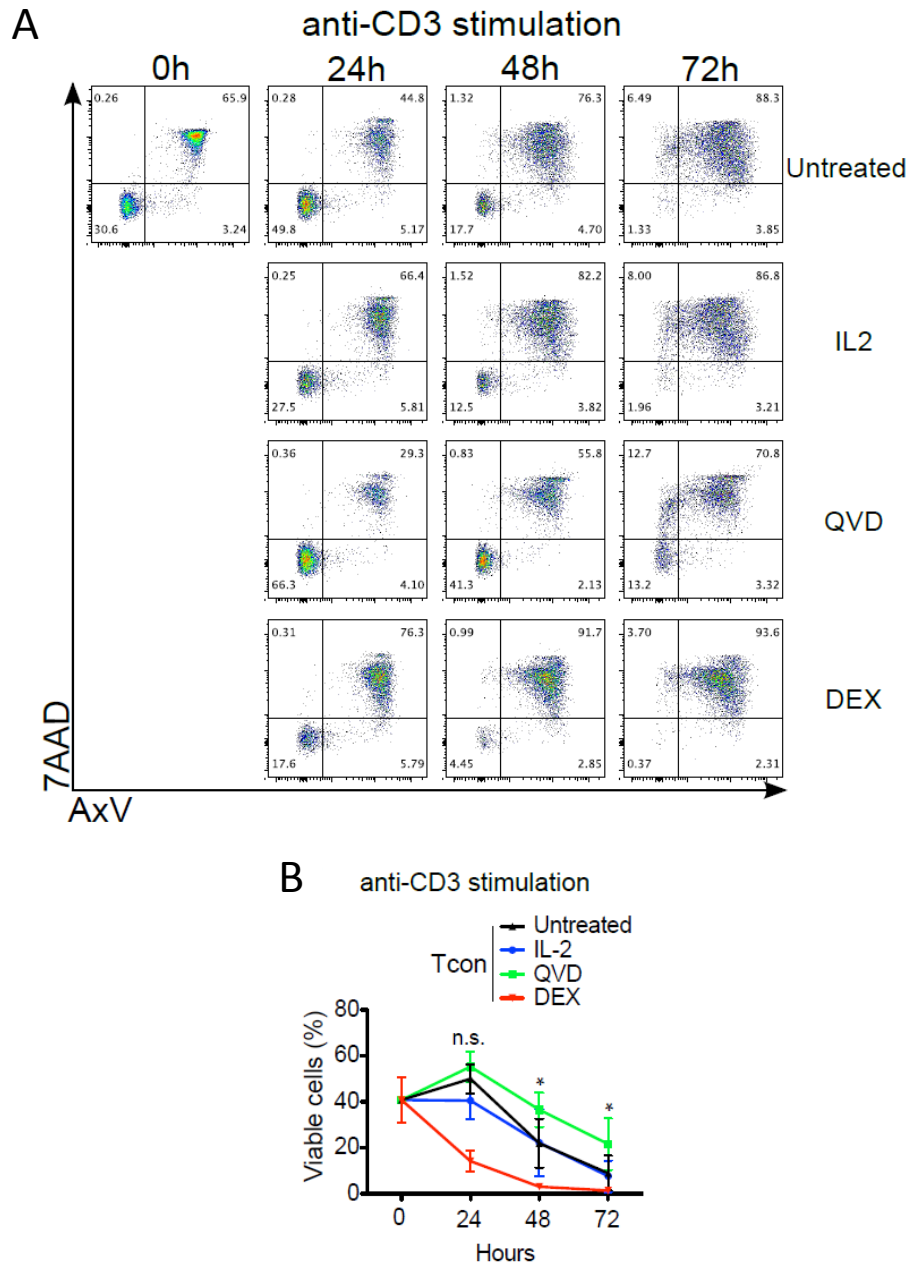


Figure 19. Viability of anti-CD3-stimulated Tcon cells improved upon QVD but not IL-2 *in vitro* stimulation.

(A) Representative dot plots and (B) kinetics of Tcon cell viability determined by AnnexinV/7AAD staining. Cells were purified from GFP-Foxp3 reporter mice by FACS sorting. They were cultivated in anti-CD3 coated plates in absence and presence of IL-2, QVD, and dexamethasone (DEX). AxV⁻/7AAD⁻ cells are viable cells (n=6). Each point represents the mean and error bars represent SEM. Statistical analyses comparing untreated vs. QVD samples were performed by one-tailed Mann-Whitney tests; *p< 0.05; n.s., not significant.

All these data together indicate that Treg cells, contrary to Tcon cells, were prone to die and they needed anti-apoptotic stimuli to remain viable. Moreover, Tcon cells became sensitive to apoptosis, like Treg cells, upon activation stimuli. On the other hand, the viability of Tcon and Treg cells at time point 0 hours was remarkable low. This fact was due to the inflation of necrotic cells, detected as AxV⁺/7AAD⁺, caused by the cell sorting and sample preparation. Most of the necrotic cells in the further time points are probably degraded and therefore out of the detection limit set for the flow cytometric analysis.

In addition, Treg cells sorted from Foxp3-GFP mice and cultured for two hours, showed the active form of caspase-3 in contrast to Tcon cells. Phorbol 12-myristate 13-acetate (PMA), through protein kinase C activation, and ionomycin, which raises the intracellular levels of calcium, mimic TCR-CD28 T lymphocyte activation. Remarkably, the activation of caspase-3 in the Treg cells was reverted upon IL-2, PMA and ionomycin stimulation during two hours (Figure 20).



Figure 20. PMA, ionomycin and IL-2 stimulation repressed spontaneous caspase 3 activation in Treg cells after 2 hours in culture.

Immunoblot analysis of active caspase-3 presence in Tcon and Treg cells after 2 hours of culture in the presence or absence of IL-2, phorbol myristate acetate (PMA) and ionomycin. Cells were purified from Foxp3-GFP reporter mice using FACS sorting.

5.3 cFLIP deficiency in Treg cells caused autoimmune disease in mice

Once confirming that cell death was prominent in Treg cells and is mainly caused by apoptosis, the next question was how this mechanism is mediated. Studies published in the last years implicated the intrinsic pathway in the regulation of the Treg apoptosis^{198,199,208}. However, nothing is known so far about the possible contribution of the death receptor-mediated pathway to the Treg homeostasis. The usage of the Cre-Lox system allows deleting target genomic sequences flanked by Lox sequences by

recombination²¹⁹. To study the impact of the extrinsic pathway on Treg cell death, the inhibitor of the extrinsic pathway c-FLIP was deleted specifically in Treg cells. To this end, a mouse line was generated crossing mice expressing the recombinase enzyme Cre under the control of the *Foxp3* promoter with mice containing loxP sites surrounding *Cflar*, the gene encoding cFLIP. *Cflar*^{fl/wt} - *Foxp3*^{Cre/wt} female mice and *Cflar*^{fl/wt} - *Foxp3*^{Cre/Y} male mice were used to generate the deletion of *Cflar* in regulatory T cell. Multiple genotype combinations resulted from the crossing of these mice, however only *Cflar*^{fl/fl} - *Foxp3*^{Cre/Cre} females and *Cflar*^{fl/fl} - *Foxp3*^{Cre/Y} males, hereafter referred to as *Cflar*^{ΔFoxp3}, showed a different phenotype compared to the rest of the resulting genotypes, which were later grouped and considered as control mice (Figure 21).

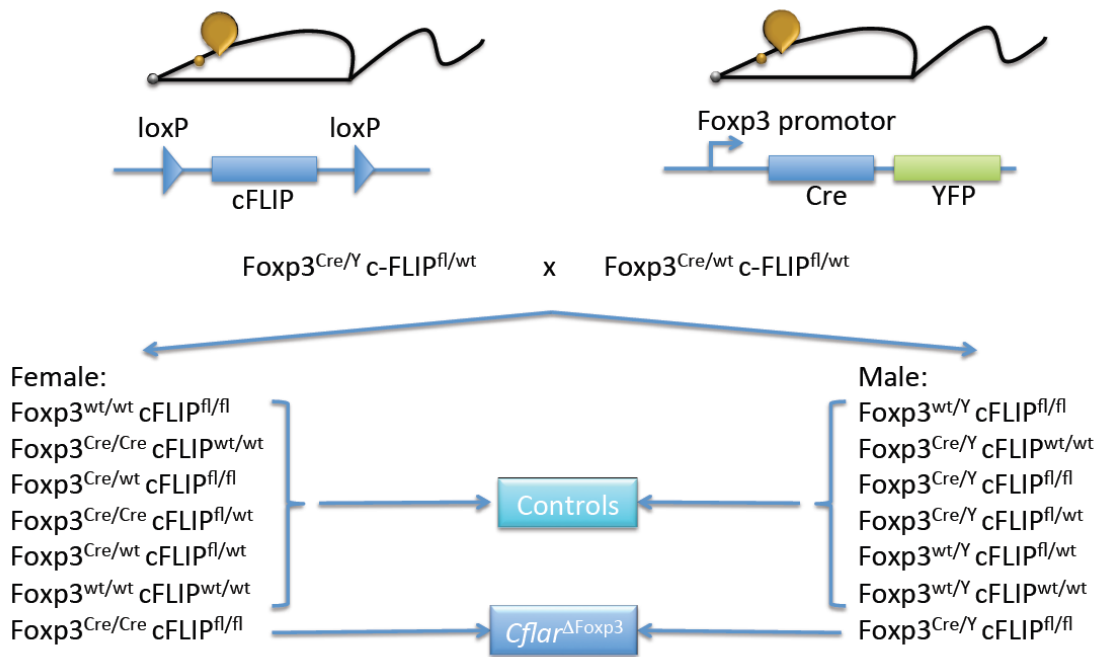


Figure 21. Breeding strategy and resulting genotypes to generate *Cflar*^{ΔFoxp3} mice

A consequence of the deletion of cFLIP in the Treg cells of *Cflar*^{ΔFoxp3} mice was that the Treg cells were barely detectable in the periphery (spleen and lymph nodes). Remarkably, thymic Treg production was not impaired in the *Cflar*^{ΔFoxp3} (Figure 22).

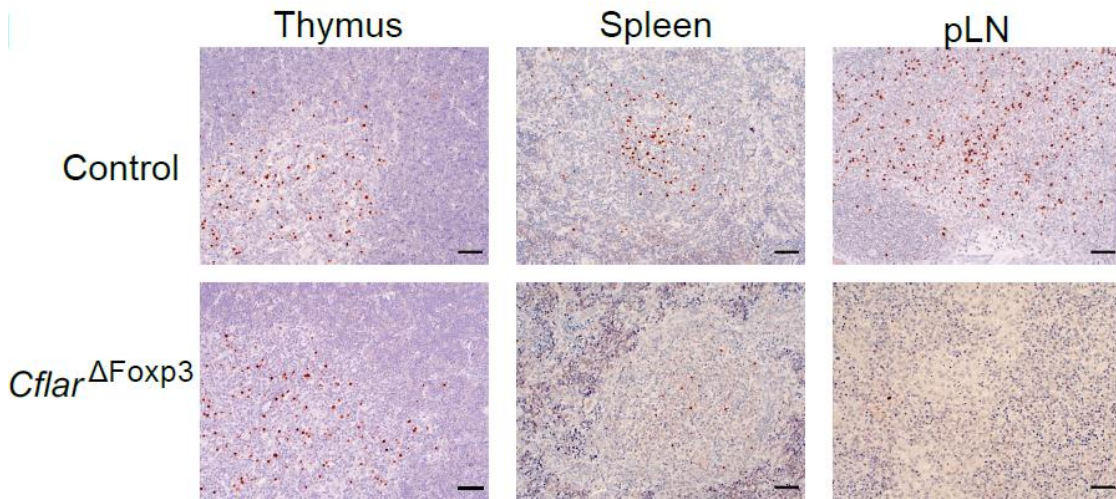


Figure 22. Treg cells were present in the thymus of *Cflar*^{ΔFoxp3} mice but absent in the spleen and lymph nodes.

Representative Foxp3 immunostaining of thymus, spleen and peripheral lymph nodes sections of 2 weeks old *Cflar*^{ΔFoxp3} mouse and littermate control.

Confirming the results of the histological analysis, Treg cell frequencies, measured by flow cytometry, were extremely low in spleen and lymph nodes of *Cflar*^{ΔFoxp3} mice (Figure 23A and 23B). Again Treg cells in the thymus showed comparable frequencies to the controls (Figure 23A and 23B). Treg cell absolute numbers followed similar differences in the spleen and lymph nodes, being always much lower in the *Cflar*^{ΔFoxp3} mice (Figure 23C). Nevertheless, although the Treg cell frequencies in the thymus were comparable in *Cflar*^{ΔFoxp3} and control mice, the absolute numbers in the thymus were substantially lower in *Cflar*^{ΔFoxp3} mice due to reduced organ size in these mice (Figure 23).

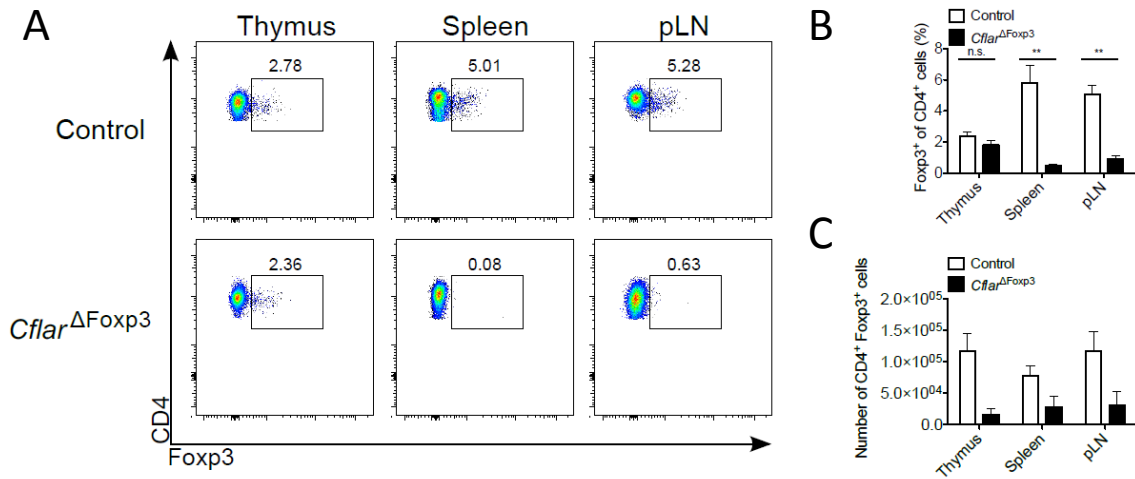


Figure 23. Treg cells showed normal frequencies in thymus but were barely detectable in the periphery of *Cflar*^{ΔFoxp3}.

(A) Representative flow cytometric dot plots, (B) percentages and (C) absolute numbers of Foxp3⁺ Treg cells within the CD4⁺ CD8⁻ population from thymus, spleen and peripheral lymph nodes of 2-3 weeks old *Cflar*^{ΔFoxp3} mice and littermate control mice are shown (n=7 each; except thymus *Cflar*^{ΔFoxp3} which is n=4). Bar graphs represent the mean; error bars represent SEM. Statistical analyses were performed by two-tailed Mann-Whitney tests; *p<0.05, **p<0.01.

In the case of females, the genotype *Cflar*^{fl/fl} - Foxp3^{Cre/wt} was included within the control mice, since they showed comparable phenotype to the other genotypes included in the control group. Despite containing loxP sites in both *Cflar* alleles and one X chromosome containing the Cre recombinase, they did not develop abnormalities like the *Cflar*^{ΔFoxp3} genotypes.

In order to check the effect of the random X chromosome inactivation in female mice, Cre-YFP expression, within the Treg compartment of *Cflar*^{fl/fl}-Foxp3^{Cre/wt}, *Cflar*^{fl/wt}-Foxp3^{Cre/wt} and *Cflar*^{wt/wt}-Foxp3^{Cre/wt}, was analyzed by flow cytometry. Since YFP fluorescence is affected by the cell fixation/permeabilization during the staining process, the CD25 cell surface marker was used to identify Treg cells from LNs of these mice, instead of the intracellular marker Foxp3. The Treg population of *Cflar*^{fl/fl}-Foxp3^{Cre/wt} females was YFP, i.e. Cre negative, whereas about 9% of the Treg cells of *Cflar*^{fl/wt}-Foxp3^{Cre/wt} females were YFP positive and almost 30 % of *Cflar*^{wt/wt}-Foxp3^{Cre/wt} females were YFP positive (Figure 24).

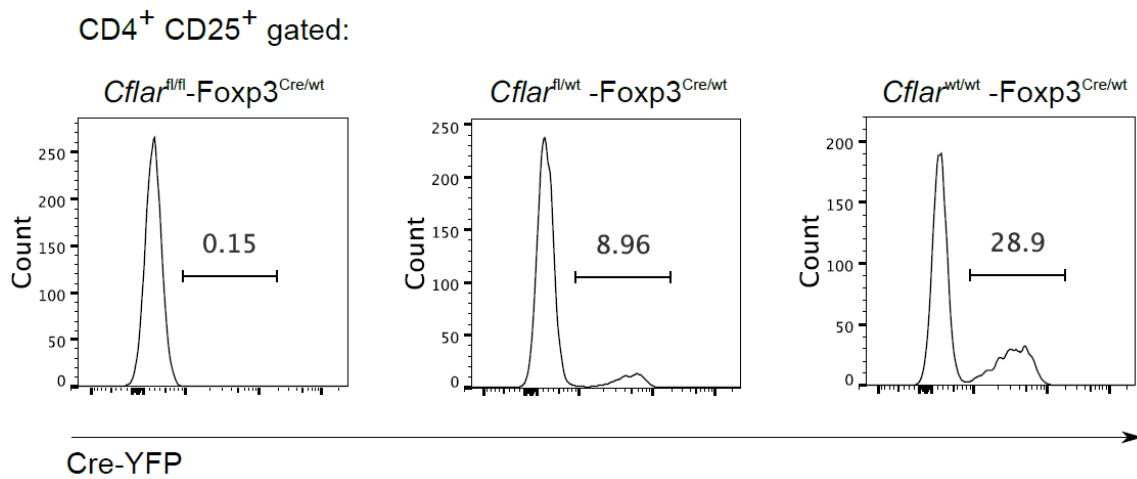


Figure 24. X chromosome random inactivation caused Treg chimeric females.

Histogram graphs of YFP-Cre expression analyzed within the Treg compartment (CD4⁺ CD25⁺ pre-gated) from LN cell suspension by flow cytometry.

Cflar^{ΔFoxp3} mice presented remarkable differences from the second week of life onwards compared to control mice, such as stunting, body weight reduction, crusting and scaliness in tails, ears and eyelids (Figure 25).



Figure 25. *Cflar*^{ΔFoxp3} mice showed macroscopic abnormalities and body weight reduction.

(A) Picture of 24 days old *Cflar*^{ΔFoxp3} mouse. (B) Comparative picture of 12 days old *Cflar*^{ΔFoxp3} mouse and littermate control in ventral decubitus position. (C) Scatter dot plot of body weight comparison between 2-3 weeks old *Cflar*^{ΔFoxp3} mice and respective control littermates (n=8). Each point represents a single mouse. Horizontal lines represent the mean; error bars represent SEM. Statistical significances were calculated by two-tailed Mann-Whitney test. Bar graphs represent the mean; error bars represent SEM. Statistical analyses were performed by two-tailed Mann-Whitney tests; ***p<0.001.

The lymphoid organs of *Cflar*^{ΔFoxp3} mice showed certain abnormalities. The thymus presented at least a 50% size reduction and peripheral lymph nodes were considerably enlarged compared to controls (Figure 26A). Furthermore, the size of the spleen was comparable, but considering the small dimensions and the reduced weight of *Cflar*^{ΔFoxp3} mice compared to the controls these mice manifest a certain degree of splenomegaly (Figure 26B).

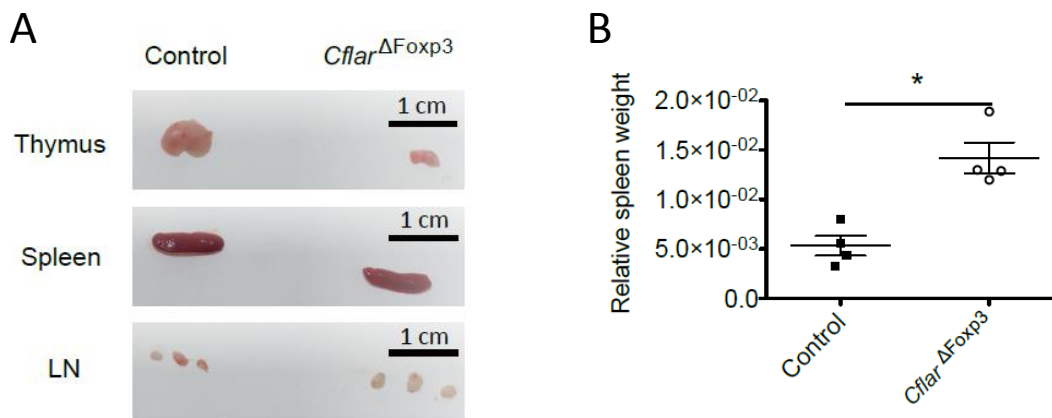


Figure 26. *Cflar*^{ΔFoxp3} mice showed morphological abnormalities in lymphoid organs. (A) Macroscopic appearance of lymphoid organs (thymus, spleen and lymph nodes) of *Cflar*^{ΔFoxp3} mouse and littermate control. (B) Scatter dot plot of relative spleen weight of 2-3 weeks old *Cflar*^{ΔFoxp3} mice and respective control littermate. Each point represents the value of a single spleen (n=4). Horizontal lines represent the mean; error bars represent SEM. Statistical significances were calculated by two-tailed Mann-Whitney test. Bar graphs represent the mean; error bars represent SEM. Statistical analyses were performed by two-tailed Mann-Whitney tests; *p < 0.05.

As Treg cells participate in the immune homeostasis by suppressing the Tcon cells, the CD4⁺ and CD8⁺ T cell subpopulations in these mice were examined by flow cytometry. Thymus of *Cflar*^{ΔFoxp3} mice manifest a strong reduction of the CD4⁺ CD8⁺ double positive thymocytes resulting in the accumulation of the CD4⁺ and CD8⁺ single positive populations (Figure 27A, 27B and 27C). Likewise, the spleen of *Cflar*^{ΔFoxp3} mice also showed higher frequencies of helper and cytotoxic T cells (Figure 27A, 24B and 27 C). Conversely, the frequencies of T cells were comparable in the peripheral lymph nodes of *Cflar*^{ΔFoxp3} mice and control mice (Figure 27A, 27B and 27C). In contrast to the frequencies, the absolute numbers of CD4⁺ and CD8⁺ single positive cells were

significantly higher in the control mice, despite the frequencies were higher in the *Cflar*^{ΔFoxp3} mice (Figure 27D and 27E). The strong reduction of the thymic size in *Cflar*^{ΔFoxp3} mice explains the low absolute numbers of CD4⁺ and CD8⁺ single positive thymocytes in spite of showing higher frequencies than control mice. Regarding the periphery, CD4⁺ and CD8⁺ T cells showed higher frequencies in the spleen of *Cflar*^{ΔFoxp3} mice, whereas the percentages of both cell types were very similar in the pLNs (Figure 27A, 27B and 27C). The absolute number of CD4⁺ and CD8⁺ T cell was higher in the spleen of *Cflar*^{ΔFoxp3} mice, especially in the case of CD8⁺ T cells. In the case of pLN, the absolute cell numbers of both CD4⁺ and CD8⁺ T cells were slightly lower in *Cflar*^{ΔFoxp3} mice compared to the controls (Figure 27D and 27E).

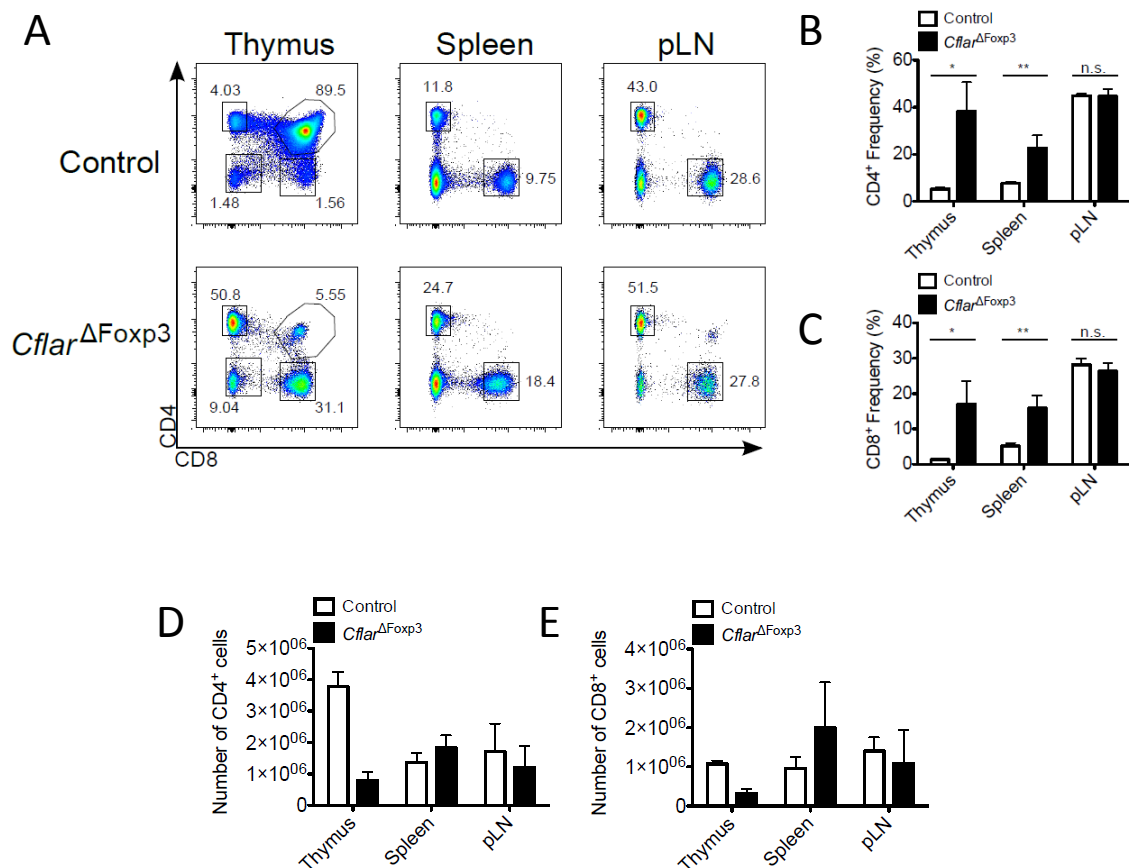


Figure 27. CD4⁺ and CD8⁺ T cell cellularity was altered in *Cflar*^{ΔFoxp3} mice.

(A) Representative flow cytometric dot plots, (B and C) percentages and (D and E) absolute numbers of CD4⁺ and CD8⁺ (both single positive) T cells respectively from thymus, spleen and peripheral lymph nodes of 2-3 weeks old *Cflar*^{ΔFoxp3} mice and littermate control mice are shown (n=7 each; except thymus *Cflar*^{ΔFoxp3}, n=4). Bar graphs represent the mean; error bars represent SEM. Statistical analyses were performed by two-tailed Mann-Whitney tests; *p< 0.05, **p<0.01, n.s., not significant.

Furthermore, the LNs of *Cflar*^{ΔFoxp3} mice showed an unusual FACS forward/side scatter dot plot picture. The lymphocytes, analyzed by flow cytometry, presented reduced size and augmented cellular granularity. Moreover, the viability of the lymphocytes was considerably lower in *Cflar*^{ΔFoxp3} mice compared to control mice.

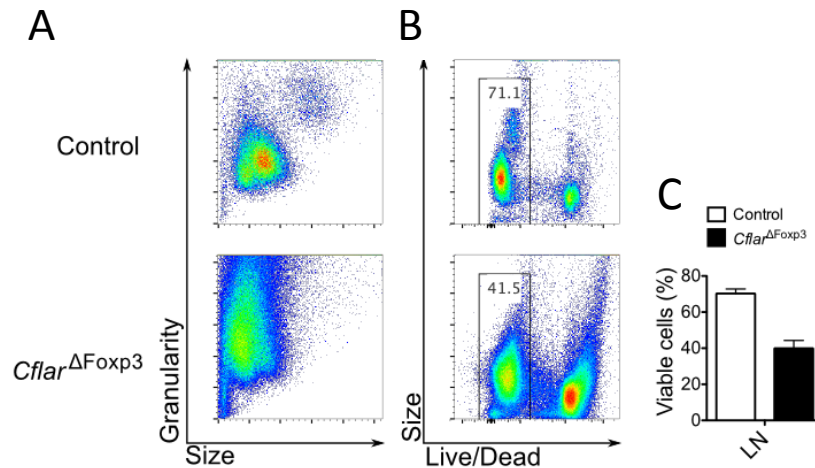


Figure 28. Reduced viability in lymphocytes of *Cflar*^{ΔFoxp3} mice.

(A) Representative FSC(Size)/SSC(Granularity) flow cytometric dot plots, (B) representative FSC(Size)/Live/Dead flow cytometric dot plots and (C) summary of viability from lymph nodes of *Cflar*^{ΔFoxp3} mice and controls (n=7, each).

Besides the remarkable variation in the T cell population of these mice, the condition of such cells was also altered in *Cflar*^{ΔFoxp3} mice. Cell adhesion molecule CD62L and the CD44 molecule are typically used as markers to characterize the resting versus activation status of T cells. The CD62L homing receptor allows resting naïve T cells to enter into secondary lymphoid tissues. Alternatively, CD44 participates in the activation and recirculation of T cells, being a marker to identify effector-memory T cells. Both molecules are co-expressed in central memory T cells. The combination of CD62L and CD44 allows the discrimination between naïve, central-memory and effector-memory T cells. Flow cytometric analysis of CD4⁺ T helper and CD8⁺ T cytotoxic cells, using CD62L and CD44 markers, showed a clear shift from naïve T cells to effector-memory T cells in spleen and lymph nodes of *Cflar*^{ΔFoxp3} mice, in contrast to control mice where most of them were naïve T cells (Figure 29).

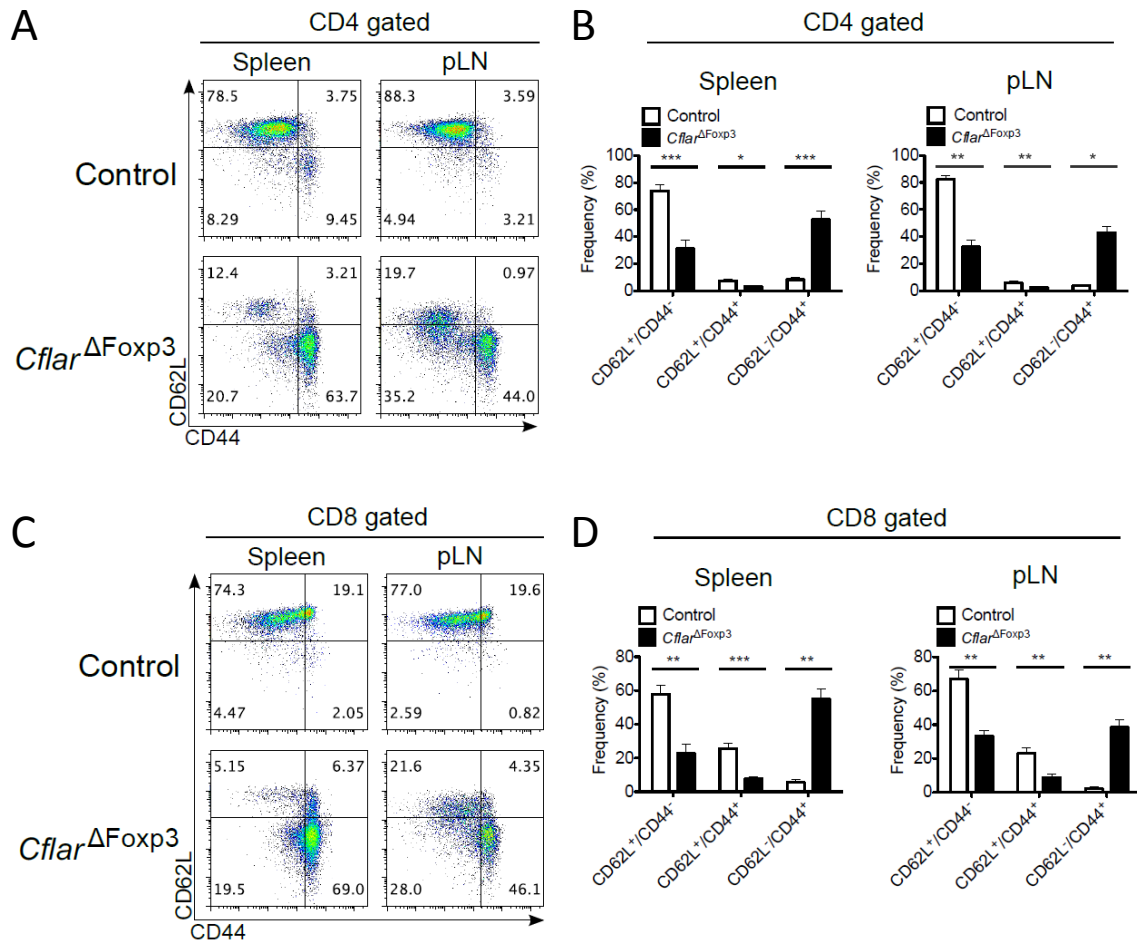


Figure 29. CD4⁺ and CD8⁺ T cell populations were altered in *Cflar*^{ΔFoxp3} mice.

(A) Representative flow cytometric dot plots (B) and percentages of T cell activation markers CD62L and CD44 in CD4⁺ T cells from spleen and peripheral lymph nodes of 2-3 weeks old *Cflar*^{ΔFoxp3} mice and littermate control mice are shown. (C) Representative flow cytometric dot plots (D) and percentages of T cell activation markers CD62L and CD44 in CD8⁺ T cells from spleen and peripheral lymph nodes of 2-3 weeks old *Cflar*^{ΔFoxp3} mice and littermate control mice are shown. CD62L⁺/CD44⁻ cells are naïve T cells, CD62L⁻/CD44⁺ cells are effector-memory T cells and CD62L⁺/CD44⁺ cells are central memory T cells (n=7 each). Bar graphs represent the mean; error bars represent SEM. Statistical analyses were performed by two-tailed Mann-Whitney tests; *p<0.05, **p<0.01, ***p<0.001.

The changes in the Treg, CD4⁺ and CD8⁺ T cell compartments as well as the T cell activation was tracked during the first days of life of *Cflar*^{ΔFoxp3} mice in order to describe the development of the *scurfy*-like phenotype produced in these animals. The Treg production in the thymus was constant and practically identical in *Cflar*^{ΔFoxp3} and control mice during the analyzed period. The gradual decrease of regulatory T cells is clearly visible between days 6 and 8 of life of *Cflar*^{ΔFoxp3} mice. From day 8 onwards, the

Treg cells were barely detectable in the spleen and lymph nodes of the deficient animals (Figure 30).

CD4⁺ Foxp3⁺ gated:

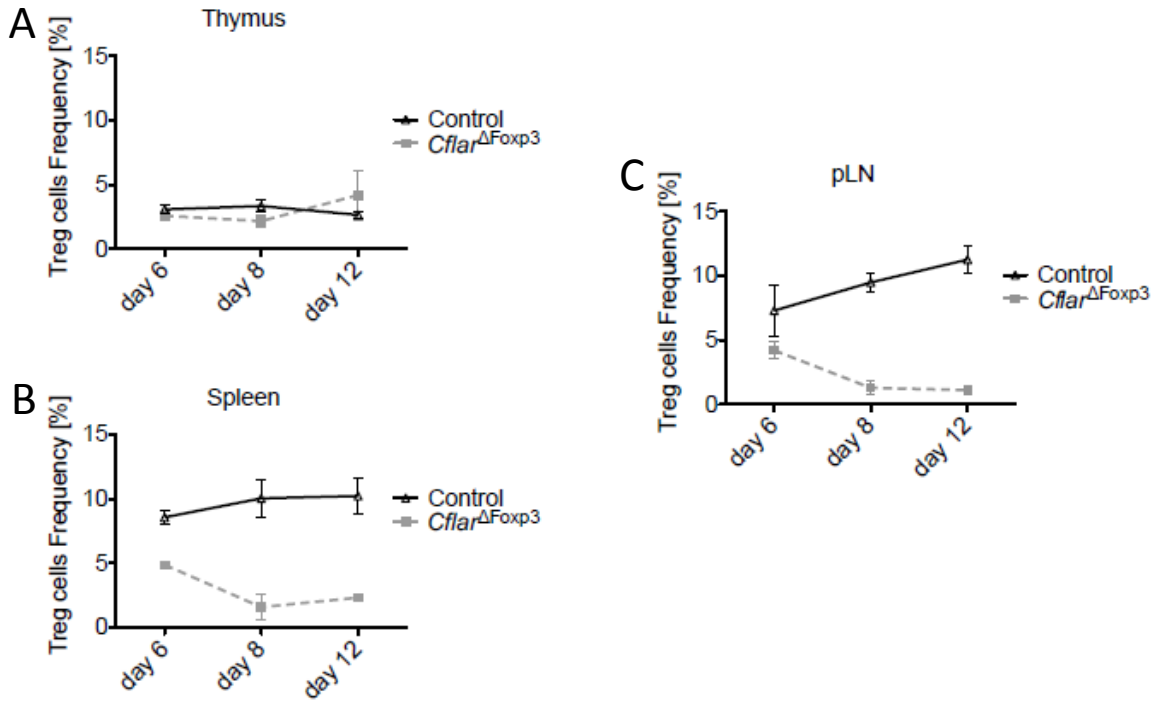


Figure 30. Treg cells progressively disappeared during the first days of life in *Cflar*^{ΔFoxp3} mice.

Frequencies of Treg cells in (A) thymus (B) spleen and (C) peripheral lymph nodes (LN) of *Cflar*^{ΔFoxp3} and control mice at day 6, 8 and 12 after birth.

Following the disappearance of Treg cells at the day 8, the frequencies of the two subpopulations of T cells, CD4⁺ and CD8⁺, were substantially higher at day 12 of life in spleen of *Cflar*^{ΔFoxp3} mice (Figure 31). Unlike the spleen, the frequencies of CD4⁺ and CD8⁺ T cells did not show relevant changes in peripheral lymph nodes compared to control animals (Figure 31).

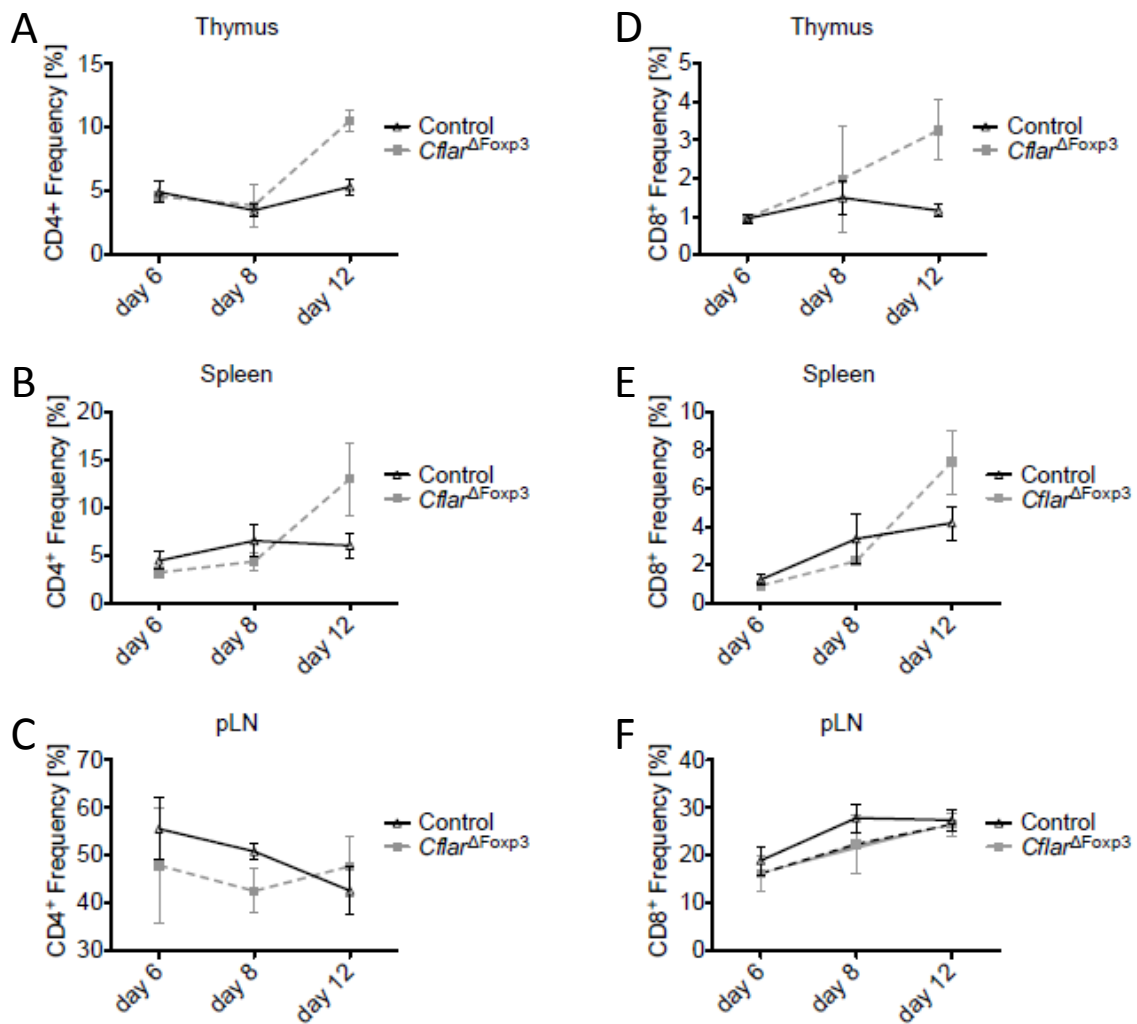


Figure 31. T cell frequencies increased in lymph nodes, but not in spleen, of *Cflar*^{ΔFoxp3} mice.

Frequencies of CD4⁺ T cells in (A) thymus, (B) spleen and (C) peripheral lymph nodes (pLN) and CD8⁺ T cells in (D) thymus, (E) spleen and (F) peripheral lymph nodes (pLN) of *Cflar*^{ΔFoxp3} and controls at day 6, 8 and 12 after birth.

Another consequence of missing Treg cells is the hyper-activation of the immune system. For this reason, the activation status of the T cell subpopulation was also tracked in the spleen and pLN of *Cflar*^{ΔFoxp3} and control mice within the first two weeks of life. In the case of *Cflar*^{ΔFoxp3} mice, the naïve CD4⁺ T cells started to decrease vertiginously from day 6 of life in both organs and, consequently, the activated CD4⁺ subpopulation rose (Figure 32). On the other hand, regarding the CD8⁺ compartment, the naïve cells decreased and the activated cells increased in the spleen of *Cflar*^{ΔFoxp3} mice at day 12. Looking at the peripheral lymph nodes of *Cflar*^{ΔFoxp3} mice, the activated CD8⁺ T cells increased considerably, whereas the naïve CD8⁺ T cells of *Cflar*^{ΔFoxp3} and control mice behave in similar manner.

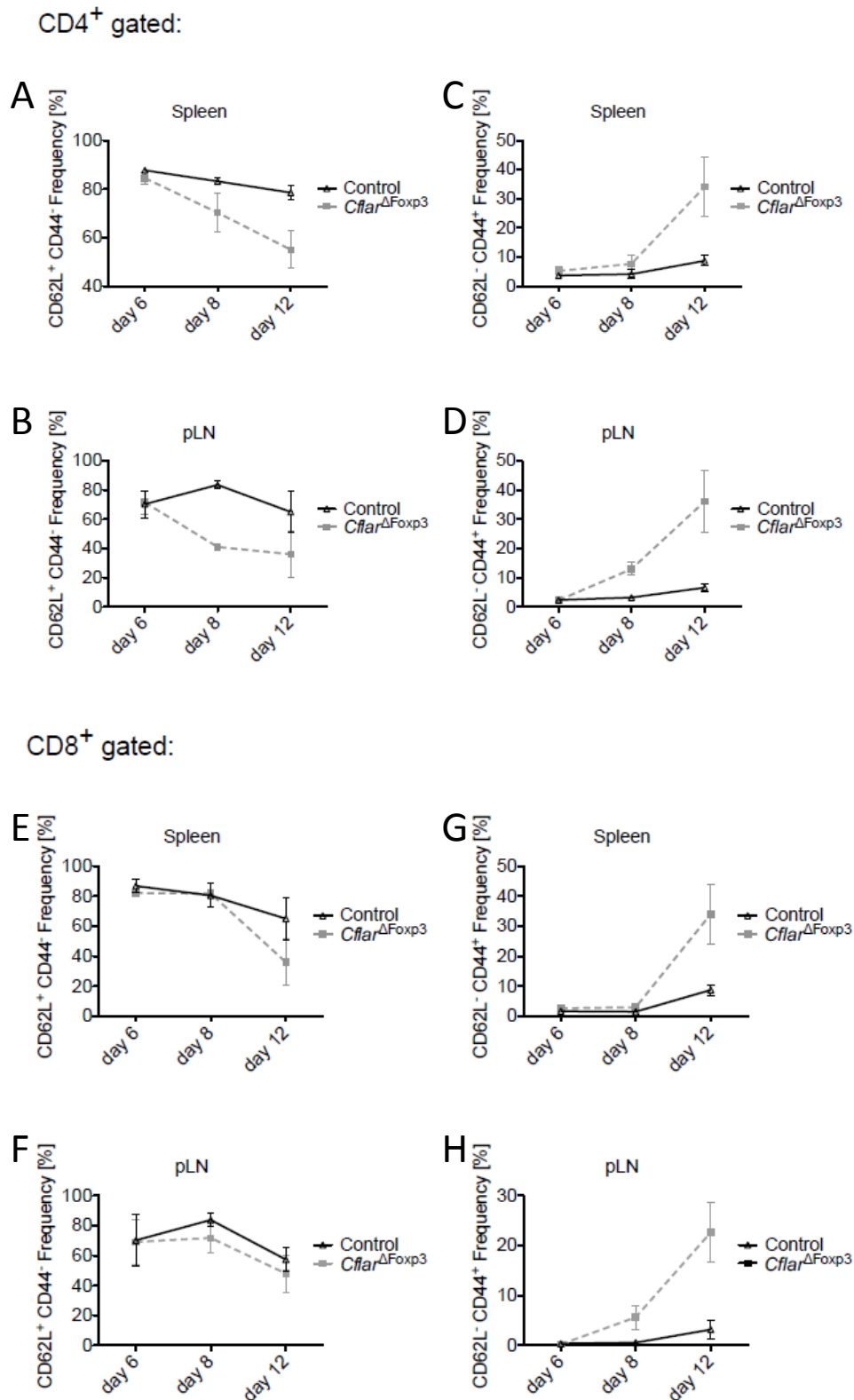


Figure 32. CD4⁺ and CD8⁺ became activated T cells in *Cflar*^{ΔFoxp3} mice. Frequencies of naïve CD4⁺ T cells (CD62L⁺, CD44⁻) in (A) spleen and (B) peripheral lymph nodes (pLN) and activated CD4⁺ T cells (CD62L⁻, CD44⁺) in (C) spleen and (D) pLN of *Cflar*^{ΔFoxp3} and control mice at day 6, 8 and 12. Frequencies of naïve CD8⁺ T cells (CD62L⁺, CD44⁻) in (E) spleen and (F) pLN, and activated CD8⁺ T cells (CD62L⁻, CD44⁺) in (G) spleen and (H) pLN of *Cflar*^{ΔFoxp3} and control mice at day 6, 8 and 12.

A consequence of the T cell activation is the production of cytokines. Therefore, cytokine levels were measured in the serum of *Cflar*^{ΔF_{oxp3}} mice and control mice. Pro-inflammatory cytokines such as IL-4, IL-5, IL-6, IFN γ , and TNF α were extraordinarily higher in the serum of *Cflar*^{ΔF_{oxp3}} mice (Figure 33). The elevated concentration of pro-inflammatory cytokines may explain the degeneration and reduction of the thymus in *Cflar*^{ΔF_{oxp3}} mice. Additionally, the presence of autoantibodies was analyzed in the serum of *Cflar*^{ΔF_{oxp3}} mice and control mice. To this end, protein extracts from liver and kidney of RAG2-deficient mice were incubated with serum from both groups. The extracts incubated with *Cflar*^{ΔF_{oxp3}} mouse serum displayed presence of antibodies against liver and kidney in contrast to the controls which were negative for such antibodies (Figure 33).

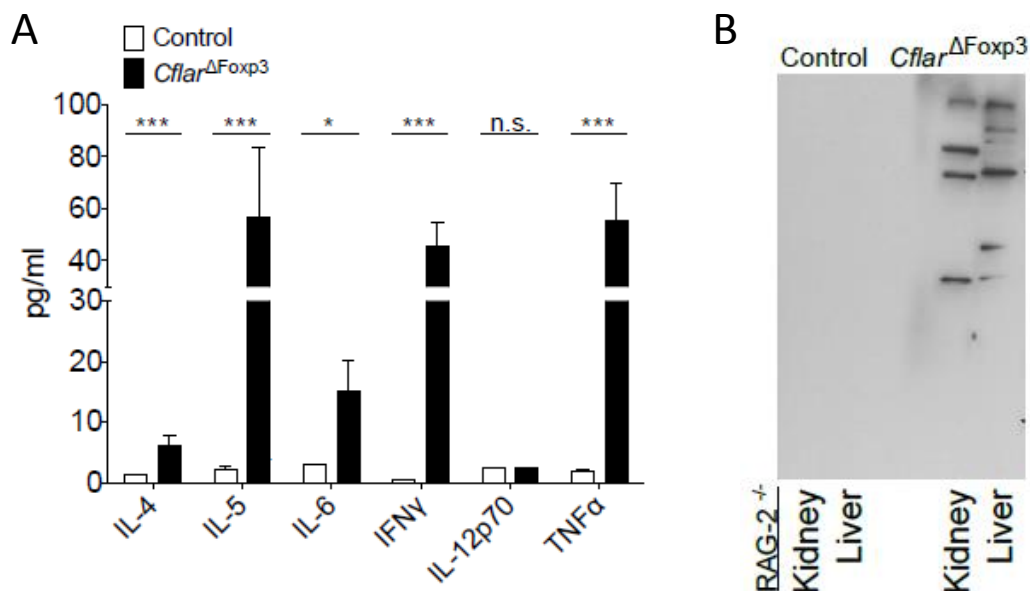


Figure 33. Sera from *Cflar*^{ΔF_{oxp3}} mice contained large amounts of pro-inflammatory cytokines and autoantibodies.

(A) Determination of the concentration of IL-4, IL-5, IL-6, IFN γ , IL-12p70, TNF α in sera of 2 weeks old *Cflar*^{ΔF_{oxp3}} mice and littermate control mice by Luminex assay (n=11 each). Bar graphs represent the mean; error bars represent SEM. Statistical analyses were performed by two-tailed Mann-Whitney tests; *p<0.05, ***p<0.001, n.s., not significant. (B) Autoantibody evaluation in sera from 2 weeks old *Cflar*^{ΔF_{oxp3}} mice and littermate control mice by incubation with protein extracts from kidney and liver of RAG-2-deficient mice.

Due to the hyper-activation of the immune system a leukocyte proliferation and tissue infiltration occurred in some organs of these mice. The following images show the structure alteration and massive infiltration occurred in liver, lung, pancreas and skin of *Cflar*^{ΔFoxp3} mice in contrast to the controls, which exhibited normal tissue architecture (Figure 34).

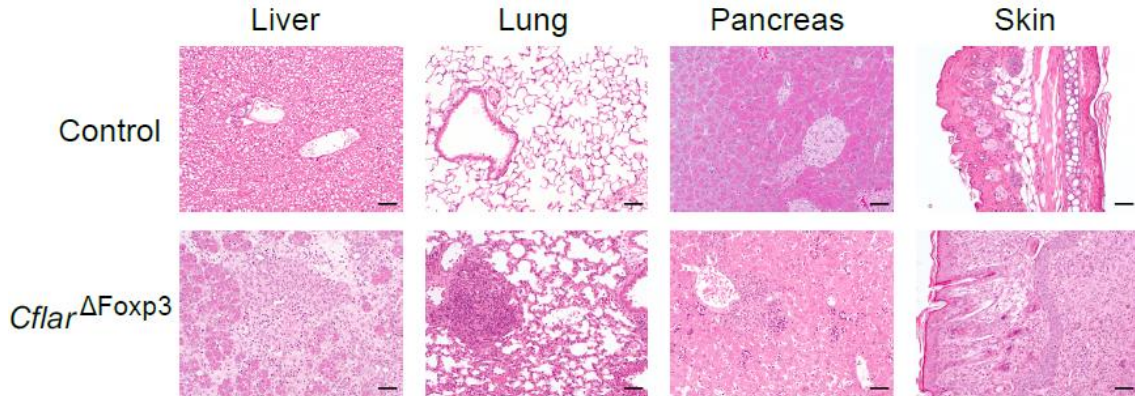


Figure 34. Massive leukocyte infiltration occurred in *Cflar*^{ΔFoxp3} mouse tissues. Representative H&E staining of liver, lung, pancreas and skin sections from 2 weeks old *Cflar*^{ΔFoxp3} mouse and littermate control are shown.

All these data together, indicate the development of a severe autoimmune disease in *Cflar*^{ΔFoxp3} mice, resulting in a drastic reduction of the life duration of these mice, which die within the first three weeks of life (Figure 35). Most of the features and development of *Cflar*^{ΔFoxp3} phenotype are comparable to *scurfy* phenotype.

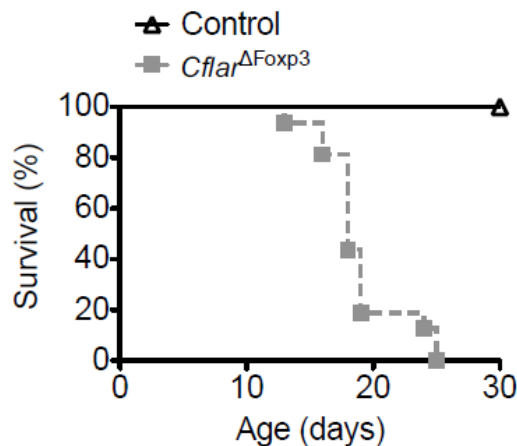


Figure 35. *Cflar*^{ΔFoxp3} mice died prematurely within the first weeks of life. Kaplan Meier plot of the *Cflar*^{ΔFoxp3} mice and littermate control mice (n=16 each group).

5.4 Treg cells are sensitive to CD95-, but not DR5- or TNFR1-induced cell death

The *Cflar*^{ΔFoxp3} animals demonstrated that cFLIP is essential to maintain Treg cell viability and therefore linking the extrinsic pathway of apoptosis to Treg cell homeostasis. However, the mechanism that explains how cFLIP protects Treg cells from cell death remained unclear. Since extrinsic apoptosis is initiated by death receptors stimulation, Treg cell death might be related specifically to one or various death receptors. In order to assess which death receptor/s produced cell death susceptibility in Treg cells, Tcon and Treg cells were purified from Foxp3-GFP reporter mice and cultured in the presence of CD95L, TRAIL, and TNF α . After 16 hours in culture, the cell viability was analyzed by flow cytometry using AxV/7AAD staining. In parallel, untreated Tcon and Treg cells were cultured in the absence of death receptor stimulation. Cell viability was determined by the frequency of AxV⁺/7AAD⁻ treated cells relative to the respective AxV⁺/7AAD⁻ untreated samples. CD95L stimulation reduced considerably Treg cell viability, in agreement with previous reports²²⁰ whereas TRAIL and TNF α did not manifest any impact on their viability (Figure 36). Moreover, Treg cells showed higher susceptibility to CD95L compared to Tcon cells, which showed a slightly reduction on its viability but not as pronounced as Treg cells (Figure 36).

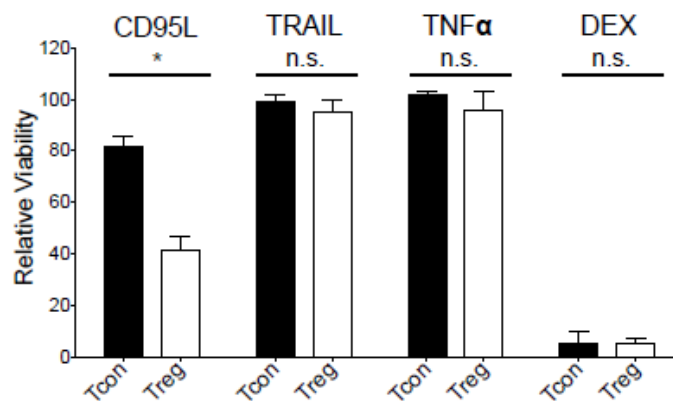


Figure 36. CD95L enhances apoptosis in Treg cells.

Statistical summary of Tcon and Treg cell viability relative to the respective untreated sample, assessed by flow cytometric analysis of AnnexinV/7AAD staining, is shown. The cell populations were purified from GFP-Foxp3 reporter mice by FACS sorting and cultivated 16 hours in the presence of CD95L (20 ng/ml), TRAIL (20 ng/ml), TNF α (20 ng/ml) and dexamethasone (DEX) (0.5 μ M) (n=4 each). Bar graphs represent the mean; error bars represent SEM. Statistical analyses were performed by two-tailed Mann-Whitney tests; *p<0.05; n.s., not significant.

To corroborate the impact of the CD95 system on Treg cell viability, sorted Tcon and Treg cells from Foxp3-GFP mice were stimulated with CD95L in the absence and presence of FasFc, which is a recombinant fusion protein of the immunoglobulin heavy-chain constant region with the extracellular domain of the CD95 receptor, which is able to capture CD95L molecules. Untreated Tcon and Treg samples were used as reference to calculate the relative viability. Flow cytometric analysis based on AnnexinV/7AAD determination revealed that the cells treated with FasFc showed a significant improved viability, indicating that FasFc competed with the added CD95L and reduced the input on CD95 receptor. Dexamethasone treatment induced efficiently massive cell death (Figure 37).

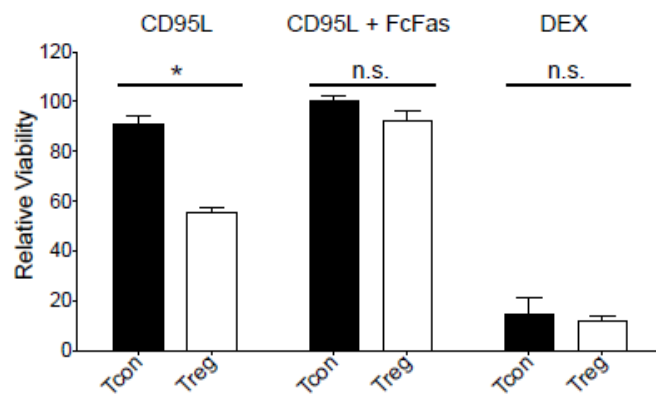


Figure 37. CD95-mediated apoptosis is repressed by FasFc.

Statistical summary of Tcon and Treg viability relative to the respective untreated samples, assessed by flow cytometric analysis of AnnexinV/7AAD staining, is shown. The cell populations were purified from Foxp3-GFP reporter mice by FACS sorting and cultivated 16 hours in the presence of CD95L (20 ng/ml), CD95L (20 ng/ml) + FasFc (50 µg/ml) and dexamethasone (DEX) (0.5 µM) (n=4 each). Bar graphs represent the mean; error bars represent SEM. Statistical analyses were performed by two-tailed Mann-Whitney tests; *p<0.05; n.s., not significant.

Alternatively, Tcon and Treg cells, sorted from lymph nodes of Foxp3-hCD2 reporter mice, were incubated in the absence or presence of CD95L. After 16 hours in culture, the cells were harvested, stained with the active caspase 3/7 fluorogenic substrate and analyzed by confocal microscopy. Like the flow cytometric results, Treg cells displayed higher caspase 3/7 activity indicating higher susceptibility to CD95L compared to Tcon cells (Figure 38).

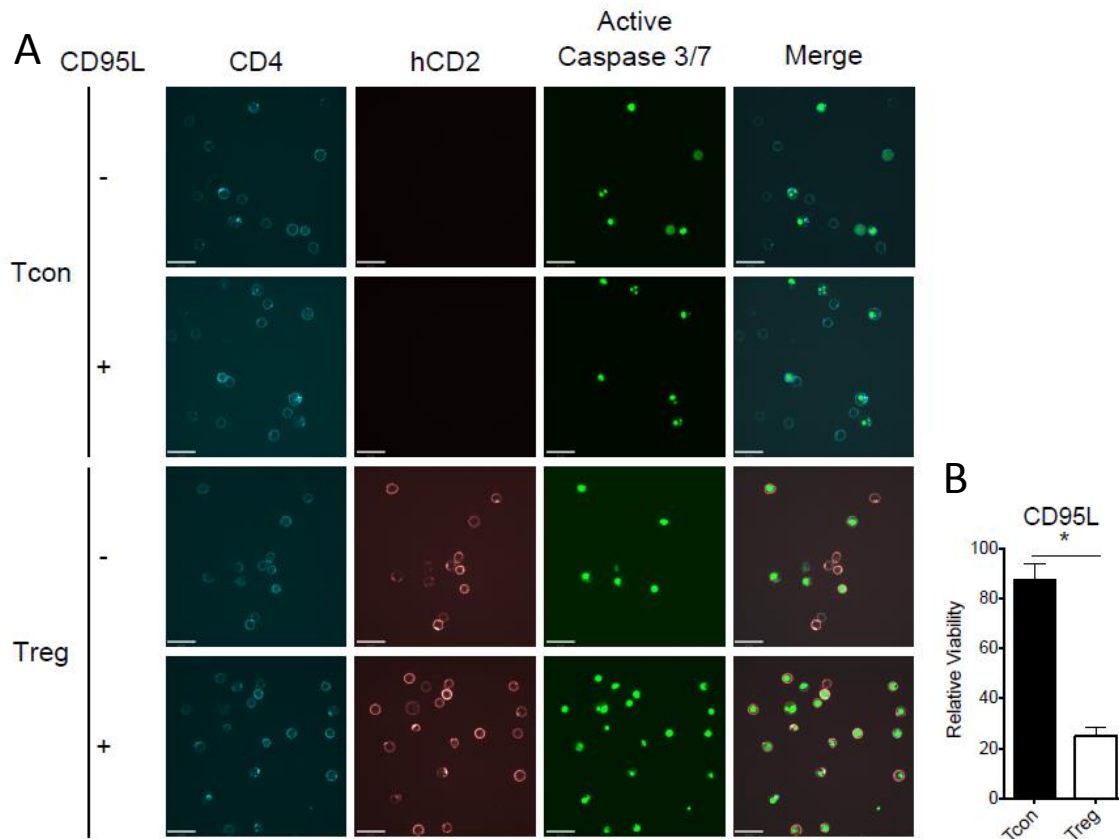


Figure 38. Treg showed higher CD95-mediated apoptosis than Tcon cells

(A) Representative confocal images and (B) summary viability graph. Active-caspase-3/7 staining was performed in sorted Tcon and Treg cells purified from Foxp3-hCD2 reporter mice and cultured in the absence and presence of CD95L for 16 hours (n=4 each). Scale bars= 19 μm. Bar graphs represent the mean; error bars represent SEM. Statistical analyses were performed by two-tailed Mann-Whitney tests; *p<0.05.

5.5 Tcon and Treg cells show identical death receptor profile expression

Extrinsic apoptosis is initiated by the stimulation of death receptors located on the cell surface⁸⁷. In the previous results, Treg cells showed high susceptibility to cell death upon CD95L stimulation and this fact might be due to higher input generated by an augmented CD95 receptor expression. To evaluate the death receptor profile of Tcon and Treg cells, *ex vivo* cell suspensions from lymph nodes were stained with antibodies against the death receptors CD95, DR5 and TNFR1. Flow cytometric analysis comparing Tcon and Treg cell receptor expression showed similar profiles, with CD95 receptor being strongly expressed in both cell types, whereas DR5 and TNFR1 expression was very low in both cases (Figure 39). These results indicate that the

expression of CD95 receptor is not responsible for the higher CD95L susceptibility of Treg cells compared to Tcon cells.

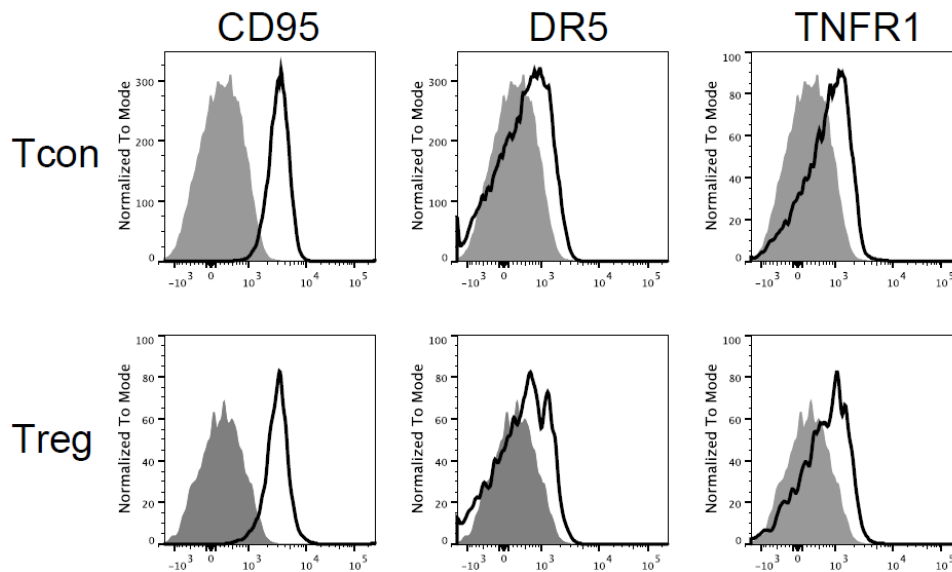


Figure 39. CD95 receptor is highly expressed in Tcon and Treg cells.

Surface expression of the death receptors CD95, DR5, and TNFR1 on Tcon and Treg cells purified from Foxp3-hCD2 reporter mice determined by flow cytometry. Grey area represents the isotype antibody controls.

5.6 Neither anti-CD95L nor QVD could protect the Treg cells of *Cflar*^{ΔFoxp3} mice *in vivo*

Because Treg cells highly expressed the CD95 receptor (Figure 39) and they displayed high sensitivity towards CD95L stimulation (Figures 36, 37 and 38), the CD95 system might mediate the cell death of cFLIP-deficient Treg cells in *Cflar*^{ΔFoxp3} mice. Anti-CD95L was injected into *Cflar*^{ΔFoxp3} mice and control mice in order to block the CD95-mediated pathway and to avoid the death signal in Treg cells. The mice were injected at day 7, 9 and 11 after birth and sacrificed at day 12. Two different anti-CD95L antibodies (Clones: MFL-3 and 3C82) were used in independent experiments. In both cases, the analyses showed comparable levels of Treg cells in the periphery of treated and untreated *Cflar*^{ΔFoxp3} mice, whereas the Treg cell frequencies were remarkable higher in treated control animals (Figure 41). Thus, the CD95L antibody treatment did not have any effect on the animals.

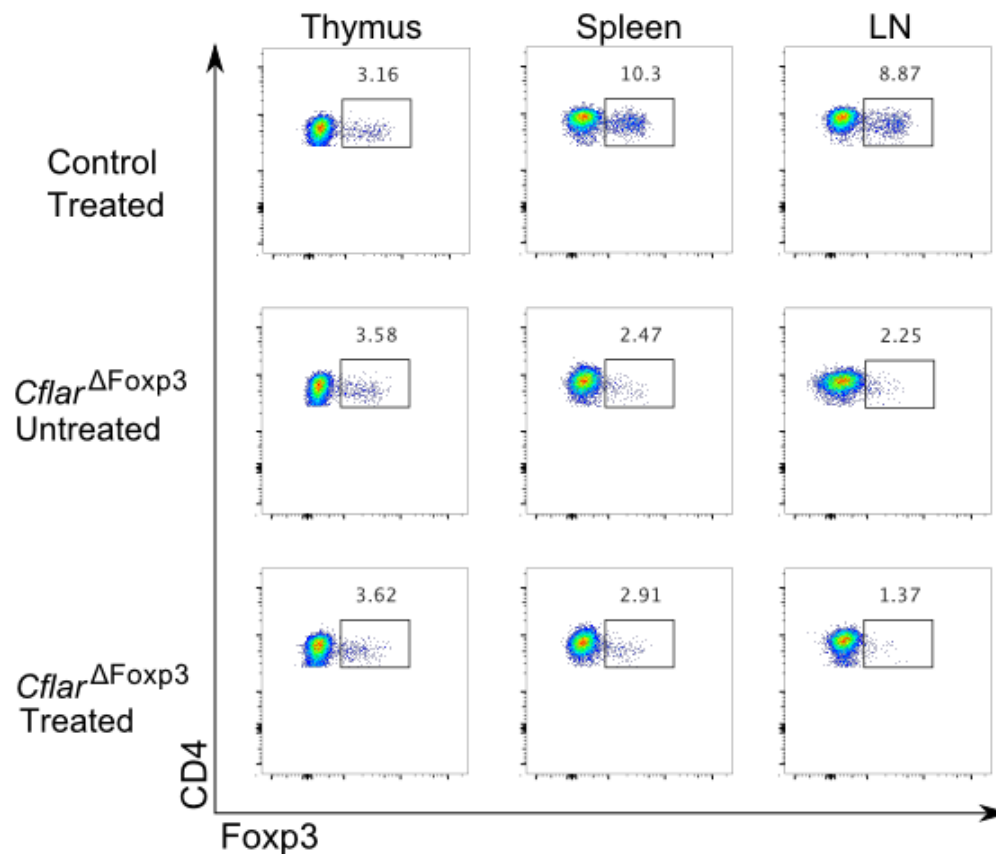


Figure 41. Treg cells frequencies are remarkably lower after anti-CD95L treatment in *Cflar*^{ΔFoxp3} mice.

Flow cytometric dot plots, showing CD4⁺Foxp3⁺ frequencies, from thymus, spleen and lymph nodes (LN) of anti-CD95L (MFL-3)-treated control, untreated *Cflar*^{ΔFoxp3} and anti-CD95L (MFL3) treated-*Cflar*^{ΔFoxp3} mice.

Since the absence of Treg cells in *Cflar*^{ΔFoxp3} mice might be caused by apoptosis, these mice were treated with the pan-caspase inhibitor QVD in order to inhibit this cell death mechanism. *Cflar*^{ΔFoxp3} mice and controls were treated with QVD at day 8, 9 and 10 after birth and sacrificed at day 11. Again, the levels of Treg cells in the periphery, analyzed by flow cytometry were very low in *Cflar*^{ΔFoxp3} mice whereas the controls displayed normal frequencies (Figure 42). The frequencies of Treg cells in the thymus were comparable in both cases (Figure 42).

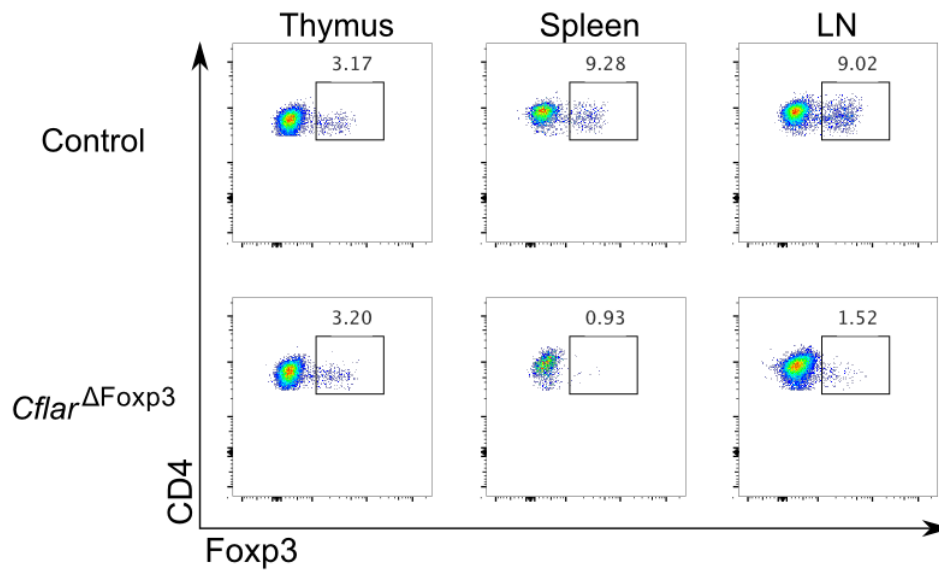


Figure 42. Treg cells are barely detectable in the periphery of *Cflar*^{ΔFoxp3} after QVD treatment.

Flow cytometric dot plots, showing CD4⁺Foxp3⁺ frequencies, from thymus, spleen and lymph nodes (LN) of *Cflar*^{ΔFoxp3} mice and controls after QVD treatment. Representative plots from 2 independent experiments are shown.

5.7 cFLIP_L protects Treg cells from CD95-mediated cell death *in vitro*

Considering that the CD95 receptor, i.e the input, was identical in Tcon and Treg cells but both cell types showed different susceptibility to CD95L stimulation, there had to be a differential mechanism that explains this different behavior. Since cFLIP is an important apoptotic inhibitor of the death receptor-mediated apoptosis⁹⁷, it represented a potential regulator for the Treg susceptibility. To study the impact of cFLIP on CD95-mediated apoptosis, Tcon and Treg cells from thymus of *Cflar*^{ΔFoxp3} and control mice were cultured in the presence of CD95L, TRAIL and TNF α . Tcon viability was slightly affected by CD95L, whereas TRAIL and TNF α stimulation did not have any influence. Thymic Tcon cells from *Cflar*^{ΔFoxp3} mice exhibited a slight reduction in viability compared to thymic Tcon cells from controls. Dexamethasone killed efficiently all cells (Figure 43A). These differences might be produced by an augmented sensitivity in Tcon cells from *Cflar*^{ΔFoxp3} mice due to their enhanced activation status as a result of the cytokine storm produced in these mice. Importantly, notable differences were found between the viability of cFLIP-deficient and -proficient Treg cells upon CD95L stimulation (Figure 43B), indicating that cFLIP might increase the sensitivity threshold to CD95L-mediated cell death of Treg cells.

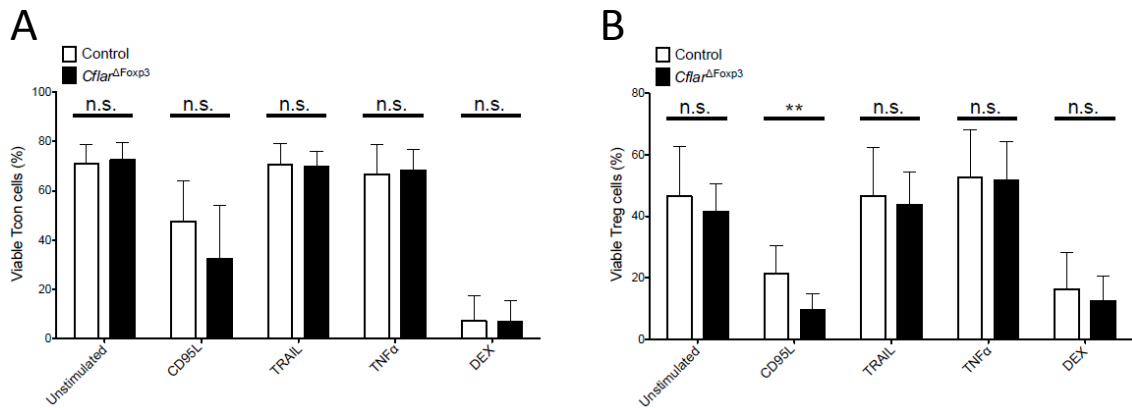


Figure 43. cFLIP-deficient Treg cells are less resistant than cFLIP-proficient Treg cells to CD95-mediated cell death.

Statistical summary of Tcon (A) and Treg (B) viability assessed by flow cytometric analysis of AnnexinV/7AAD staining (control n=18, *Cflar*^{ΔFoxp3} n=8). Cell populations were isolated from *Cflar*^{ΔFoxp3} and control mice by FACS sorting and cultivated for 16 hours in the absence and presence of CD95L (5 ng/ml), TRAIL (20 ng/ml), TNF α (20 ng/ml) and dexamethasone (DEX) (0.5 μ M). (Control n=18, *Cflar*^{ΔFoxp3} n=8). Bar graphs represent the mean; error bars represent SEM. Statistical analyses were performed by two-tailed Mann-Whitney tests; **p<0.01; n.s., not significant.

So far, it was demonstrated that cFLIP protects Treg cells from CD95L-mediated apoptosis, but it was not clear why the proficient Treg cells manifested increased susceptibility to this particular cell death compared to Tcon cells. To clarify this point, the gene expression of the different cFLIP isoforms was examined in both cell types. mRNA levels of total cFLIP were comparable in Treg and Tcon cells, whereas the genetic expression of the long isoform cFLIP_L was significant lower in Treg cells than in Tcon cells, in contrast to the short isoform cFLIP_R (Figure 44). The low cFLIP_L genetic expression explains the increased susceptibility to CD95L-mediated apoptosis in Treg cells.

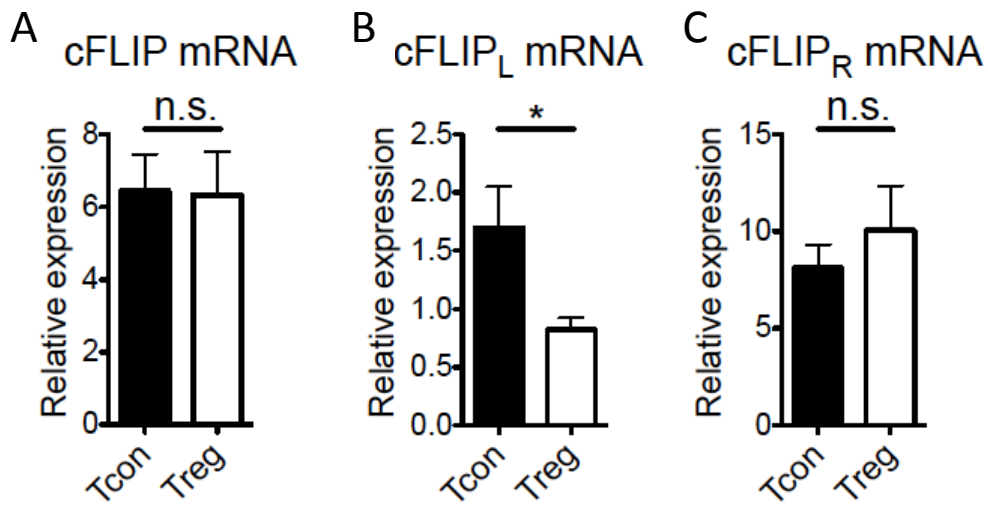


Figure 44. Treg cells manifest lower cFLIP_L genetic expression than Tcon cells.

Expression of c-FLIP (A) and its isoforms c-FLIP_L (B) and c-FLIP_R (C) in Tcon and Treg cells purified from Foxp3-hCD2 reporter mice by FACS sorting and analyzed by qPCR (n= 17 each). Bar graphs represent the mean; error bars represent SEM. Statistical analyses were performed by two-tailed Mann-Whitney tests; *p<0.05; n.s., not significant.

Even though both Tcon and Treg cell types get the same death input due to the identical death receptor expression, Treg cells manifested lower viability. This might be explained by the lower gene expression of cFLIP_L, the long isoform of the apoptotic modulator, in Treg cells compared to Tcon cells.

6. Discussion

6.1. Treg cells show an elevated apoptosis rate under steady-state conditions

Treg cell function has been described as a mechanism to counterbalance the activity of the effector arm of the immune system. They have an essential role in the control of auto-reactive cells, particularly in blocking the activation of T cells that recognize self-antigens, preventing the rise of autoimmune disorders. Since their discovery by Sakaguchi in 1995¹⁶³, Treg cells have been deeply investigated due to their relevance in immune homeostasis. Originally, early studies described Treg cells as an anergic subpopulation of CD4⁺ T cells expressing the alpha chain of the IL-2 receptor (CD25) that are able to prevent autoimmune activity caused by other cells of the immune system^{196,197}. However, further investigations demonstrated that Treg cells manifest a relative high proliferation rate in steady-state conditions^{198–201,221}. One of the most recent *in vivo* studies showed that 50 percent of the Treg cells proliferated after 10 days in homeostatic conditions using 5-bromo-2'-deoxyuridine (BrdU) labeling in mice¹⁹⁹. They also demonstrated the high dynamics of these cells by depleting part of the Treg niche and tracking the rapid filling and the expression of Ki67 protein, which is typically upregulated during active phases of the cell cycle and absent in resting cells¹⁹⁹. The high proliferation of the Treg cells might be related to their affinity to self-antigens. During development in the thymus, selected Treg cells have increased TCR affinity to self-antigens compared to positive selected conventional T cells^{166–168}. This fact means that the Treg cells get continuous TCR stimulation, which would promote their proliferation. Due to the high proliferation of the Treg cells, a counterbalance mechanism is needed in order to maintain the population size and the immune homeostasis. Programmed cell death, and more specifically apoptosis, is proposed as the compensatory process that would dampen the elevated proliferation of Treg cells. Nonetheless, there are no studies showing clearly a high apoptosis rate in regulatory T cell so far. Recently, some studies described how the intrinsic pathway of apoptosis regulates Treg cell death. Initially, reduced expression of the pro-apoptotic protein BIM was reported in aged Treg cells, suggesting its role in the accumulation of these cells in aged mice²⁰⁸. Completing these findings, Tai and colleagues linked the expression of a pro-apoptotic protein signature, including BIM, with the function of the transcription factor Foxp3, which is essential for the Treg suppression capacity and, to date, the most reliable marker used to detect Treg cells. The pro-apoptotic role of Foxp3 is prevented

by common gamma chain-dependent cytokine signals during Treg development¹⁹⁸. However, that study was focused mainly on the thymic development of Treg cells and it did not clarify how the Treg homeostasis is regulated after emigration from the thymus to the periphery. Few months later, Pierson and colleagues published a study, by which the role of the intrinsic pathway of apoptosis in Treg homeostasis was shown. In this study, the authors demonstrated that the cytokine IL-2 regulates the expression of the anti-apoptotic protein MCL-1, which is able to repress the BIM-dependent mitochondrial permeabilization and, in consequence, the initiation of the intrinsic pathway¹⁹⁹. Taken all together, these studies give a reasonable explanation of the mechanism that regulates the Treg population size and the immune homeostasis, giving a prominent role to the intrinsic pathway of apoptosis regulated by the cytokine IL-2. Nevertheless, none of them showed a proof that peripheral Treg cells undergo cell death in order to balance their elevated proliferation under steady-state conditions and they assumed that the Treg cells manifest a raised apoptosis rate.

Consistent with these assumptions, evidences of the elevated apoptosis rate in Treg cells compared to Tcon cells are demonstrated in this thesis by means of *ex vivo* analysis. In all the lymphoid organs analyzed, Treg cells had a higher cell death rate than Tcon cells using different techniques to detect apoptosis, including mitochondrial membrane depolarization (Figure 13), phosphatidylserine exposure on the outer leaflet of the plasma membrane (Figure 14) and activation of effector caspases (Figure 15). These data would support the idea that Treg cells are a very dynamic population during homeostatic conditions, which proliferate continuously, presumably due to constant TCR stimulation. The elevated proliferation rate needs a counterbalance mechanism in order to keep the homeostasis. Since apoptosis is a tight regulated process, it represents a suitable mechanism to equilibrate the size of the Treg cell population⁸⁷. The pan-caspase inhibitor QVD was able to improve the viability of the Treg cells *in vitro*, corroborating the role of apoptosis in Treg cell death (Figure 16). Supporting this idea, IL-2 stimulation, which can inhibit apoptosis in Treg cells¹⁹⁸, increased their viability of the cultures.

T cell activation, triggered by the TCR, can promote either cell proliferation or apoptosis. CD28 co-stimulation increases the expression of the anti-apoptotic protein BCL-XL²¹⁶, whereas in the absence of CD28-induced signal transduction, TCR stimulation promotes apoptosis through the BH3-only protein BIM^{143,222}. Moreover,

TCR stimulation can also trigger, through the CD95 system, activation-induced cell death in T cells^{223–225}. In the case of Treg cells, the induction of cell death via TCR stimulation was partially abolished by QVD as well as IL-2 (Figure 17), demonstrating the contribution of apoptosis in Treg cell death.

6.2. Treg cells behave like TCR-activated Tcon cells

Based on the previous experiment, neither QVD nor IL-2 did show any effect on the viability of unstimulated T con cells. Since naïve Tcon cells do not express the high affinity IL-2 receptor, their unresponsiveness upon IL-2 stimulation was expected. However, the insignificant influence of QVD on Tcell viability manifests that Tcon cell death was minimally mediated by apoptosis in the cell cultures (Figure 18). Interestingly, anti-CD3-stimulated Tcon cells behaved similar to Treg cells to QVD treatment. In this case, the viability of the Tcon cells improved by QVD treatment, indicating that the TCR-mediated cell death was occurring by apoptosis. Taken together, these results demonstrate that apoptosis takes place in Treg cells and activated Tcon cells, but not in resting Tcon cells. Remarkably, only IL-2 was not sufficient to improve the viability of anti-CD3-stimulated Tcon cells (Figure 19), while this cytokine improved the viability of Treg cells in the absence and presence of anti-CD3 (Figures 16 and 17). Thus, in terms of apoptosis activity, Treg cells are comparable to TCR-stimulated Tcon cells. In fact, TCRs from Treg cells have a higher affinity to self-antigens compared to Tcon cells¹⁶⁰ and therefore, the Treg cells are constantly exposed to TCR stimulation in the organism. Combined stimulation with TCR, CD28 and IL-2 promotes the proliferation and represses the apoptosis in Tcon cells²¹⁶. This fact correlates with the results from the Tcon and Treg cell cultures stimulated in parallel with PMA, ionomycin and IL-2, which did not show active caspase 3 (Figure 20). Conversely, unstimulated Treg cells showed active caspase 3, in contrast to unstimulated Tcon cells (Figure 20). In addition, Treg cells display markers which are expressed in Tcon cells only upon activation, such as CD25, GITR, CD154, CTLA-4 and OX40²²⁶. These results support the idea that Treg cells behave like TCR-stimulated T cells, which undergo apoptosis unless they get CD28 and IL-2 stimulation.

6.3. X chromosome inactivation produces Treg chimeras in females

Despite several studies related to the regulation of Treg cell death with the intrinsic pathway of apoptosis, the contribution of the extrinsic pathway was neglected. The regulation of the Treg cell apoptosis by the extrinsic pathway, through the TRAIL system, was negated in a report where the authors showed that the Treg cells were resistant to TRAIL-mediated apoptosis²²⁷. Peculiarly, Treg cells proliferated in contact to bone marrow derived-dendritic cells expressing TRAIL, whereas Tcon cells underwent apoptosis upon the same stimulation. Although both cells types expressed the TRAIL receptor DR5, the presence of the decoy receptor mDc-TRAILR1 in Treg cells would protect the Treg cells but not the Tcon cells from the death input signaling.

In order to assess the role of the extrinsic pathway of apoptosis in Treg cell homeostasis, the death receptor inhibitor cFLIP was deleted in Treg cells in mice, using the Cre-loxP recombination system. In this case, the expression of recombinase Cre was under the control of Foxp3 promotor and *Cflar*, the gene encoding cFLIP, was flanked by loxP sites floxed. This results in the Cre-mediated deletion of *Cflar* when Foxp3 is expressed. Heterozygous animals for both alleles, and hemizygous males in the case of Foxp3^{Cre/Y}, were crossed in order to achieve the deletion of *Cflar* in Treg cells. Multiple combinations of genotypes were generated, including *Cflar*^{ΔFoxp3} mice, which developed numerous abnormalities compared to the rest of the resulting genotypes (Figure 21). Remarkably, *Cflar*^{fl/fl} - Foxp3^{Cre/wt} females, despite containing both *Cflar* alleles floxed and one Cre-expressing chromosome, did not show any abnormality and were included in the group of control mice. This phenomenon is due to the fact that Cre expression is under the control of the Foxp3 promoter, which is located in the X chromosome. In females, one X chromosome is randomly inactivated during the embryogenesis²²⁸. As a consequence, a part of the Treg-precursor cells in the bone marrow had the Cre-containing X chromosome inactivated and another part of Treg-precursor cells had the Cre-containing X chromosome activated. Silencing of one of the X chromosomes produced a chimeric mouse, which results in the generation of two different populations, Cre-expressing Treg cells and Cre-deficient Treg cells, within the same animal. In these mice, Cre-proficient Treg cells die, Cre-deficient Treg cells develop normally and fill the niche by, presumably, homeostatic proliferation, being comparable to *Cflar*^{fl/fl} - Foxp3^{wt/wt} genotype. Moreover, the YFP, i.e. Cre, expression within the Treg compartment of *Cflar*^{fl/fl} - Foxp3^{Cre/wt} females was undetectable (Figure 24),

corroborating the idea that only Cre-deficient Foxp3 positive cells remain in the Treg population. This would explain that although both *Cflar* alleles were floxed, they persisted in the genome due to the Cre deficiency.

Furthermore, theoretically, the Treg compartment of *Cflar*^{wt/wt}-Foxp3^{Cre/wt} females, due to the random X chromosome inactivation, would be equally distributed between Cre-expressing, i.e. YFP positive cells, and non-expressing, i.e. YFP negative cells. In these mice, Treg cells are fully cFLIP-proficient and both cell types should respond identically to cell death. However, the analysis revealed that the percentage of Cre-expressing Treg was lower than the expected 50%. This might be due to a contamination of activated Tcon cells, which express CD25 and were gated in the identification of the Treg compartment or might be due to a possible YFP instability affecting its detection by the cytometer. Alternatively, *Cflar*^{fl/wt}-Foxp3^{Cre/wt} females had about 9% of YFP-expressing Treg cells, indicating a gene-doses effect between the 30% of YFP-expressing Treg cells in *Cflar*^{wt/wt}-Foxp3^{Cre/wt} females and the totally loss of YFP-expressing Treg cells in *Cflar*^{fl/fl}-Foxp3^{Cre/wt} females (Figure 24).

Immunodysregulation polyendocrinopathy enteropathy X-linked (IPEX) syndrome is an autoimmune disease caused by the dysfunction of Foxp3, which is an essential transcription factor for Treg function¹⁷⁰. Remarkably, all the cases of IPEX syndrome have been reported on males, being carrier females completely healthy²²⁹. X chromosome inactivation and the proliferation capacity of Treg cells to refill the niche would explain why carrier females do not develop any symptom. Like in the Foxp3^{Cre/wt} mice, Treg compartment would consist in 2 different subpopulations since the Foxp3 gene is located at the X chromosome. Due to random X chromosome silencing, one population would express the WT allele and the other population would express the mutated/inactive allele. As a consequence, the Foxp3-mutated Treg cells would not develop and all the Treg cells in the organism would express the WT allele. This situation is comparable to the absence of YFP positive Treg cells in *Cflar*^{fl/fl}-Foxp3^{Cre/wt} female mice. Considering this, females are Treg chimeras, having one portion of the Treg population expressing the paternal allele and the other portion the maternal allele, even when both Foxp3 alleles are functional.

6.4. Lack of cFLIP in murine Treg cells results in the disappearance of the Treg cells in the periphery but not in the thymus

The deletion of *Cflar* in Treg cells of *Cflar*^{ΔFoxp3} mice had a notable impact in the Treg cell population. Treg cells were barely detectable in the periphery of these mice (Figures 22 and 23). Paradoxically, Treg cells were produced continuously in the thymus (Figures 22 and 23) in spite of the serious alterations suffered in this organ, such as reduction of size and loss of double positive thymocytes (Figures 23 and 26). The integrity of Treg cell development was not affected because the deletion of *Cflar* occurred in the last developmental step, when Foxp3 is expressed. On the other hand, it was not demonstrated that the deletion of *Cflar* caused directly the death of the cell. This deletion might cause an increase of cell death sensitivity mediated by further stimuli. Another possibility is that cFLIP is intrinsically necessary for Treg survival, and its lack is sufficient to cause cell death. If this is the case, the presence of Treg cells in the thymus might be due to a delay in the deletion of *Cflar* by Cre or/and due to a remaining cFLIP protein previously expressed in the cell. Alternatively, the presence of Treg cells in the thymus, but not in the periphery, might be due to the fact that the death ligand encounter occurs in the periphery, but not in the thymus. Taken together, these findings might explain why the Treg cells are barely detectable in the periphery of *Cflar*^{ΔFoxp3} mice, which are able to produce thymic Treg cells but incapable to maintain them in the periphery. The lack of Treg cells in peripheral organs of *Cflar*^{ΔFoxp3} mice triggers a systemic autoimmune disease due to the absence of a control capable to counterbalance auto-reactive cells.

6.5. Absence of Treg cells in *Cflar*^{ΔFoxp3} mice originates an autoimmune disorder comparable to *scurfy* phenotype

Cflar^{ΔFoxp3} mice developed similar symptomatology to *scurfy* phenotype¹⁷⁴, characterized by a fatal autoimmune disease producing stunting, scaly and ruffled skin, reddened eyes, splenomegaly, lymph nodes enlargement, and death within the first weeks of life (Figures 25 and 26). The absence of suppressive cells produced hyper-activation of the immune system because of the rise of auto-reactive cells and the massive cytokine production. The development of fatal autoimmunity is another proof

of the importance of the Treg cells in immune homeostasis, despite the fact that they represent only about 5-10 % of the CD4⁺ T cell compartment.

Together with the rise of inflammatory cytokines (Figure 33), which has also been reported in *scurfy* mice^{230,231}, the CD4⁺ and CD8⁺ T cells were highly activated in spleen and lymph nodes of *Cflar*^{ΔFoxp3} mice (Figure 29). In all cases, the T cells of *Cflar*^{ΔFoxp3} mice shifted from a naïve to an activated status. In the pLN of control mice, the naïve CD8⁺ T cell population also decreased (Figure 32) but they did not shift to an activated status (Figure 32). Instead, they became central-memory T cells (CD62L⁺, CD44⁺) in the lymph nodes. This effect did not occur in the CD4⁺ T cells of control mice because the central-memory T cells are more prominent in CD8⁺ T cells. The hyper-activation of the immune system in *Cflar*^{ΔFoxp3} mice produced the accumulation of CD4⁺ and CD8⁺ T cells in the spleen (Figure 27). The frequencies of these cells were comparable in pLN of *Cflar*^{ΔFoxp3} mice and control mice. However, the absolute cell number was slightly lower in *Cflar*^{ΔFoxp3} mice (Figure 27), although the lymph nodes were substantially larger than in the control mice (Figure 26). Moreover, the small size and augmented granularity of a considerable group of lymphocytes of *Cflar*^{ΔFoxp3} mice, together with a remarkable low viability (Figure 28) indicated that lymphocytes of *Cflar*^{ΔFoxp3} mice died and accumulated massively in the lymph nodes. This would explain why the frequencies of T cells, which were calculated excluding the death cells, were similar in *Cflar*^{ΔFoxp3} mice and controls whereas the absolute T cell number was lower in the enlarged lymph nodes of *Cflar*^{ΔFoxp3} mice (Figure 27).

6.6. Blocking CD95L or pan-caspase inhibitor treatment is not sufficient to rescue the *scurfy*-like phenotype on *Cflar*^{ΔFoxp3}

Rescue or decreasing symptoms of the autoimmunity in *scurfy* mice by T cell transfer or bone marrow transplant has been reported²³². cFLIP deficiency in Treg cells caused an outcome that was similar to the one in *scurfy* mice (Figures 23, 25 and 26). Since cFLIP is an inhibitor of the death receptor-mediated pathway⁹⁷ and the expression of CD95 in Treg cells was higher compared to other death receptors (Figure 39), the vulnerability of the Treg cells in *Cflar*^{ΔFoxp3} mice might be explained by a lack of protection triggered by the CD95 system. Thereby, anti-CD95L was injected into the *Cflar*^{ΔFoxp3} mice in order

to inhibit the CD95 input in the Treg cells. These experiments were performed using independently two monoclonal anti-CD95L antibodies obtained from different clones. Nevertheless, both anti-CD95L antibodies did not have any impact on the development of the autoimmunity on *Cflar*^{ΔFoxp3} mice (Figure 41). This might suggest that the absence of Treg cells in the periphery of *Cflar*^{ΔFoxp3} mice is not related to increased CD95-mediated apoptosis. Besides the role of cFLIP as anti-apoptotic inhibitor, cFLIP activity has been related to the activation of the NF-κB and ERK pathways^{126,233}. Moreover, Zhang and colleagues showed that cFLIP is essential for T lymphocyte proliferation in a NF-κB-independent manner²³³. Therefore, the disappearance of Treg cells in the periphery of *Cflar*^{ΔFoxp3} mice might be produced by a proliferation defect in the Treg cells. Supporting this idea, pan-caspase inhibitor treatment did not ameliorate the reduction of Treg cells in *Cflar*^{ΔFoxp3} mice, suggesting indirectly that cFLIP is involved in the proliferation of the Treg cells (Figure 42). However, the apoptosis of Treg cells in *Cflar*^{ΔFoxp3} mice cannot be totally excluded by the anti-CD95L and QVD *in vivo* treatments. On the one hand, necroptosis might get activated as a back-up cell death mechanism when apoptosis is inhibited by QVD. On the other hand, the effect of the two treatments might be masked by the high dynamics of the Treg cells. This would produce a very limited rescue effect over the time due to insufficient anti-CD95L or QVD availability. Alternatively, flanking the CD95 gene sequence by loxP sites, i.e. deleting CD95 genetically, would help to determine whether the absence of Treg cells in *Cflar*^{ΔFoxp3} mice is mediated by the CD95 system.

6.7. cFLIP-deficient Treg cells manifest higher susceptibility to CD95L *in vitro* stimulation

In contrast to the results from the anti-CD95 *in vivo* treatment (Figure 41), suggesting that CD95L is not involved in Treg apoptosis, *in vitro* experiments showed that cFLIP confers resistance to CD95-mediated apoptosis. Treg cells from *Cflar*^{ΔFoxp3} mice were more susceptible to cell death than Treg cells from control mice upon CD95L stimulation *in vitro* (Figure 43). That indicates that cFLIP has anti-apoptotic function in Treg cells. Indeed, this thesis corroborates previous findings²²⁰, showing that Treg cells were highly sensitive to CD95-induced apoptosis compared to Tcon cells (Figures 36, 37 and 38). Despite Treg and Tcon cells manifesting comparable CD95 receptor

expression (Figure 39), the reduced expression of cFLIP_L in Treg cells (Figure 44) might explain the differences in terms of resistance to CD95-mediated apoptosis.

6.8. Concluding remarks

Immune homeostasis needs to be tightly regulated for maintaining the capacities of the immune system to protect the organism against multiple threats as well as for being able to tolerate their own structures. Due to their suppressive capacity, Treg cells are a vital cellular mechanism to block autoreactive cells, and avoid autoimmune development. Therefore, the behavior of the Treg population is crucial to keep immune homeostasis. This thesis demonstrated that Treg cells are a dynamic population with an elevated apoptosis rate compared to conventional T cells. Furthermore, the findings approach Treg cells to the status of activated cells.

Moreover, the role of cFLIP in Treg cells was investigated in order to better understand the behavior of Treg cell homeostasis and progress in the knowledge of their regulation. The deficiency of cFLIP resulted in a *scurfy*-like phenotype in mice, demonstrating the vital role of these proteins in Treg cells. The autoimmunity developed in these mice is presumably produced by the absence of Treg cells. The lack of Treg cells in the periphery of *Cflar*^{ΔFoxp3} mice might be due to proliferation defect or enhanced apoptosis. The low gene expression of cFLIP_L compared to Tcon cells might explain the enhanced vulnerability of Treg cells to CD95 *in vitro* stimulation. However, the exact cause for the Treg absence in *Cflar*^{ΔFoxp3} mice remains still not completely resolved and needs further investigations.

Due to their suppressive activity, the modulation of the Treg population might be beneficial in pathogenic conditions. For instance, reducing the Treg compartment in a tumor environment might enhance the immune response against the cancer cells. Alternatively, boosting the Treg population might increase the tolerance to self-antigens in autoimmune diseases. Hence, cFLIP represents a potential target to modulate Treg homeostasis in order to regulate the immune response against cancer and autoimmune diseases.

7. Abbreviations

7AAD	7-aminoactinomycin D
A1A	BCL-2-related protein A1A
AICD	Activation-induced cell death
AIRE	Autoimmune regulator
Ala	Alanine
APAF-1	Apoptotic protease activating factor 1
Asp	Aspartic acid
ATP	Adenosine triphosphate
AxV	Annexin V
BAD	BCL-2 antagonist of cell death
BAK	BCL-2-antagonist/killer-1
BAX	BCL-2-associated X protein
BCA	Bicinchoninic acid
BCL	B-cell lymphoma
BCL-2	B-cell lymphoma-2
BCL-W	B-cell lymphoma-2-like-2
BCL-XL	B-cell lymphoma-extra-large protein
BH	BCL-2 homology
BID	BH3-interacting domain death agonist
BIK	BCL-2-interacting killer
BIM	BCL-2-like-11
BMF	Bcl-2-modifying factor
BOK	BCL-2-antagonist/killer-1
BrdU	5-bromo-2'-deoxyuridine
cAMP	Cyclic adenosine monophosphate
CARD	Caspase recruitment domain
CD	Cluster of differentiation
CD95L	CD95 ligand
cFLIP	Cellular FLIP
cFLIP _L	Cellular FLIP long
cFLIP _R	Cellular FLIP Raji
cFLIP _S	Cellular FLIP short

CTL	Cytotoxic T lymphocytes
CTLA-4	Cytotoxic T-lymphocyte-associated protein 4
Cys	Cysteine
DAMP	Damage-associated molecular patterns
DC	Dendritic cell
DD	Death domain
DED	Death effector domain
DEX	Dexamethasone
DIABLO	Direct IAP binding protein with low pI
DISC	Death-inducing signaling complex
DNA	Deoxyribonucleic acid
DP	Double positive
DR	Death receptor
EDTA	Ethylenediaminetetraacetic acid
ER	Endoplasmic reticulum
FACS	Fluorescence-activated cell sorting
FADD	Fas-Associated Death Domain
FLICE	FADD-like IL-1 β -converting enzyme
FLIP	FLICE-inhibitory protein
Foxp3	Forkhead box protein 3
FPLC	Fast protein liquid chromatography
GFP	Green fluorescent protein
GITR	Glucocorticoid-induced TNFR family related gene
Gln	Glutamine
Gly	Glycine
GTP	Guanosine triphosphate
H&E	Hematoxinilin and eosin
hCD2	Human CD2
His	Histidine
HRK	Harakiri
IAP	Inhibitor of apoptosis proteins
IDO	Indoleamine 2,3-dioxygenase
IFN γ	Interferon gamma

Ig	Immunoglobulin
IKK	Inhibitor of κ B kinase
IL-2	Interleukin 2
IL-4	Interleukin 4
IL-5	Interleukin 5
IL-6	Interleukin 6
IL-10	Interleukin 10
IL-12	Interleukin 12
IL-35	Interleukin 35
IPEX	Idiopathic polyendocrinopathy X-linked
LN	Lymph nodes
MCL-1	Myeloid cell leukaemia 1
MHC	Major histocompatibility complex
mLN	Mesenteric lymph nodes
MMP	Mitochondrial membrane potential
mTOR	Mammalian target of rapamycin
Mut	Mutant
NF- κ B	Nuclear factor κ B
NK	Natural Killer
OMM	Outer mitochondrial membrane
PAMP	Pathogen associated molecular patterns
PBS	Phosphate buffered saline
PCR	Polymerase chain reaction
PI3K-I	Phosphatidylinositol 3-kinase-I
pLN	Peripheral lymph nodes
PMA	Phorbol 12-myristate 13-acetate
PS	Phosphatidylserine
PUMA	BCL-2 binding component-3
PVDF	Polyvinylidene difluoride
qRT-PCR	Quantitative real-time polymerase chain reaction
QVD	Q-VD-OPh
RAG2	Recombination activating gene 2
RIP-1	Receptor-interacting protein 1

ROS	Reactive oxygen species
RT	Room temperature
SDS-PAGE	Sodium dodecyl sulfate-polyacrylamide gel electrophoresis
SEM	Standard error of mean
SMAC	Second mitochondria-derived activator of caspases
SNP	Single nucleotide polymorphism
tBID	Truncated BID
TBS	Tris-buffered saline
Tcon	Conventional T
TCR	T cell receptor
TEC	Thymic epithelial cells
TGF- β	Transforming growth factor beta
Th	T helper
TMRE	Tetramethylrhodamine ethyl ester
TNF	Tumor-necrosis factor
TNFR1	TNF receptor 1
TRADD	TNFR1-associated death domain protein
TRAF	TNFR-associated factor
TRAIL	TNF-related apoptosis-inducing ligand
TRAILR	TNF-related apoptosis-inducing ligand receptor
Treg	Regulatory T
UBC	Ubiquitin-conjugating enzyme E2D 2A
WT	Wild type
XIAP	X-linked inhibitor of apoptosis protein
YFP	Yellow fluorescent protein

8. References

1. Ellis, R. E., Yuan, J. Y. & Horvitz, H. R. Mechanisms and functions of cell death. *Annu. Rev. Cell Biol.* **7**, 663–698 (1991).
2. Metcalf, D., Lindeman, G. J. & Nicola, N. A. Analysis of hematopoiesis in max 41 transgenic mice that exhibit sustained elevations of blood granulocytes and monocytes. *Blood* **85**, 2364–2370 (1995).
3. Daley, S. R., Hu, D. Y. & Goodnow, C. C. Helios marks strongly autoreactive CD4+ T cells in two major waves of thymic deletion distinguished by induction of PD-1 or NF- κ B. *J. Exp. Med.* **210**, 269–85 (2013).
4. Stritesky, G. L. *et al.* Murine thymic selection quantified using a unique method to capture deleted T cells. *Proc. Natl. Acad. Sci. U. S. A.* **110**, 4679–84 (2013).
5. Barber, G. N. Host defense, viruses and apoptosis. *Cell Death Differ.* **8**, 113–126 (2001).
6. Weinstein, G. D., McCullough, J. L. & Ross, P. Cell proliferation in normal epidermis. *J. Invest. Dermatol.* **82**, 623–628 (1984).
7. Barkla, D. H. & Gibson, P. R. The fate of epithelial cells in the human large intestine. *Pathology* **31**, 230–238 (1999).
8. Kroemer, G. *et al.* Classification of Cell Death 2009. *Cell Death Differ.* **16**, 3–11 (2009).
9. Berghe, T. Vanden *et al.* Necroptosis, necrosis and secondary necrosis converge on similar cellular disintegration features. *Cell Death Differ.* **17**, 922–930 (2010).
10. Krysko, D. V., Vanden Berghe, T., D’Herde, K. & Vandenabeele, P. Apoptosis and necrosis: Detection, discrimination and phagocytosis. *Methods* **44**, 205–221 (2008).
11. Garg, A. D. *et al.* Immunogenic cell death, DAMPs and anticancer therapeutics: An emerging amalgamation. *Biochim. Biophys. Acta - Rev. Cancer* **1805**, 53–71 (2010).
12. Kerr, J. F. R., Willie, A. H. & Currie, A. R. Apoptosis: A basic biological phenomenon with wide-ranging implications in tissue kinetics. *Br. J. Cancer* (1972).
13. Taylor, R. C., Cullen, S. P. & Martin, S. J. Apoptosis: controlled demolition at the cellular level. *Nat. Rev. Mol. Cell Biol.* **9**, 231–41 (2008).
14. Lauber, K. *et al.* Apoptotic cells induce migration of phagocytes via caspase-3-mediated release of a lipid attraction signal. *Cell* **113**, 717–730 (2003).

15. Fadok, V. A. *et al.* Exposure of phosphatidylserine on the surface of apoptotic lymphocytes triggers specific recognition and removal by macrophages. *J. Immunol.* **148**, 2207–2216 (1992).
16. Martin, S. J. *et al.* Early redistribution of plasma membrane phosphatidylserine is a general feature of apoptosis regardless of the initiating stimulus: inhibition by overexpression of Bcl-2 and Abl. *J. Exp. Med.* **182**, 1545–1556 (1995).
17. Voll, R. E. *et al.* Immunosuppressive effects of apoptotic cells. *Nature* **390**, 350–351 (1997).
18. Fadok, V. a. *et al.* Macrophages that have ingested apoptotic cells in vitro inhibit proinflammatory cytokine production through autocrine/paracrine mechanisms involving TGF- β , PGE₂, and PAF. *J. Clin. Invest.* **101**, 890–898 (1998).
19. Levine, B. & Klionsky, D. J. Development by Self-Digestion Molecular Mechanisms and Biological Functions of Autophagy. *Dev. Cell* **6**, 463–477 (2004).
20. Yang, Y.-P., Liang, Z.-Q., Gu, Z.-L. & Qin, Z.-H. Molecular mechanism and regulation of autophagy. *Acta Pharmacol. Sin.* **26**, 1421–1434 (2005).
21. Levine, B. Eating oneself and uninvited guests: Autophagy-related pathways in cellular defense. *Cell* **120**, 159–162 (2005).
22. Baehrecke, E. H. Autophagy: dual roles in life and death? *Nat. Rev. Mol. Cell Biol.* **6**, 505–510 (2005).
23. Levine, B. & Yuan, J. Autophagy in cell death: An innocent convict? *J. Clin. Invest.* **115**, 2679–2688 (2005).
24. Galluzzi, L. *et al.* To die or not to die: that is the autophagic question. *Curr. Mol. Med.* **8**, 78–91 (2008).
25. Boya, P. *et al.* Inhibition of macroautophagy triggers apoptosis. *Mol. Cell. Biol.* **25**, 1025–1040 (2005).
26. González-Polo, R.-A. *et al.* The apoptosis/autophagy paradox: autophagic vacuolization before apoptotic death. *J. Cell Sci.* **118**, 3091–3102 (2005).
27. Tasdemir, E. *et al.* Methods for assessing autophagy and autophagic cell death. *Methods Mol. Biol.* **445**, 29–76 (2008).
28. Clarke, P. G. Developmental cell death: morphological diversity and multiple mechanisms. *Anat. Embryol. (Berl)*. **181**, 195–213 (1990).
29. Mills, K. R., Reginato, M., Debnath, J., Queenan, B. & Brugge, J. S. Tumor necrosis factor-related apoptosis-inducing ligand (TRAIL) is required for induction of autophagy during lumen formation in vitro. *Proc. Natl. Acad. Sci. U. S. A.* **101**, 3438–3443 (2004).

30. Thorburn, J. *et al.* Selective inactivation of a Fas-associated death domain protein (FADD)-dependent apoptosis and autophagy pathway in immortal epithelial cells. *Mol. Biol. Cell* **16**, 1189–1199 (2005).
31. Prins, J. *et al.* Tumour necrosis factor induced autophagy and mitochondrial morphological abnormalities are mediated by TNFR-I and/or TNFR-II and do not invariably lead to cell death. *Biochem. Soc. Trans.* **26**, S314 (1998).
32. Pyo, J. O. *et al.* Essential roles of Atg5 and FADD in autophagic cell death: Dissection of autophagic cell death into vacuole formation and cell death. *J. Biol. Chem.* **280**, 20722–20729 (2005).
33. Lum, J. J., DeBerardinis, R. J. & Thompson, C. B. Autophagy in metazoans: cell survival in the land of plenty. *Nat. Rev. Mol. Cell Biol.* **6**, 439–448 (2005).
34. Meijer, A. J. & Codogno, P. Regulation and role of autophagy in mammalian cells. *Int. J. Biochem. Cell Biol.* **36**, 2445–2462 (2004).
35. Candi, E., Schmidt, R. & Melino, G. The cornified envelope: a model of cell death in the skin. *Nat. Rev. Mol. Cell Biol.* **6**, 328–340 (2005).
36. Lippens, S., Denecker, G., Ovaere, P., Vandenabeele, P. & Declercq, W. Death penalty for keratinocytes: apoptosis versus cornification. *Cell Death Differ.* **12 Suppl 2**, 1497–1508 (2005).
37. Festjens, N., Vanden Berghe, T. & Vandenabeele, P. Necrosis, a well-orchestrated form of cell demise: Signalling cascades, important mediators and concomitant immune response. *Biochim. Biophys. Acta - Bioenerg.* **1757**, 1371–1387 (2006).
38. Holler, N. *et al.* Fas triggers an alternative, caspase-8-independent cell death pathway using the kinase RIP as effector molecule. *Nat. Immunol.* **1**, 489–495 (2000).
39. Aravind, L., Dixit, V. M. & Koonin, E. V. Apoptotic molecular machinery: vastly increased complexity in vertebrates revealed by genome comparisons. *Science* **291**, 1279–1284 (2001).
40. Rao, L., Perez, D. & White, E. Lamin proteolysis facilitates nuclear events during apoptosis. *J. Cell Biol.* **135**, 1441–1455 (1996).
41. Wyllie, A. H. Glucocorticoid-induced thymocyte apoptosis is associated with endogenous endonuclease activation. *Nature* **284**, 555–556 (1980).
42. Communal, C. *et al.* Functional consequences of caspase activation in cardiac myocytes. *Proc. Natl. Acad. Sci. U. S. A.* **99**, 6252–6256 (2002).
43. Thiede, B., Treumann, A., Kretschmer, A., Söhlke, J. & Rudel, T. Shotgun proteome analysis of protein cleavage in apoptotic cells. *Proteomics* **5**, 2123–2130 (2005).

44. Browne, K. A., Johnstone, R. W., Jans, D. A. & Trapani, J. A. Filamin (280-kDa actin-binding protein) is a caspase substrate and is also cleaved directly by the cytotoxic T lymphocyte protease granzyme B during apoptosis. *J. Biol. Chem.* **275**, 39262–39266 (2000).
45. Adrain, C., Duriez, P. J., Brumatti, G., Delivani, P. & Martin, S. J. The cytotoxic lymphocyte protease, Granzyme B, targets the cytoskeleton and perturbs microtubule polymerization dynamics. *J. Biol. Chem.* **281**, 8118–8125 (2006).
46. Canu, N. *et al.* Tau cleavage and dephosphorylation in cerebellar granule neurons undergoing apoptosis. *J. Neurosci.* **18**, 7061–7074 (1998).
47. Morishima, N. Changes in nuclear morphology during apoptosis correlate with vimentin cleavage by different caspases located either upstream or downstream of Bcl-2 action. *Genes to Cells* **4**, 401–414 (1999).
48. Ku, N. O., Liao, J. & Omary, M. B. Apoptosis generates stable fragments of human type I keratins. *J. Biol. Chem.* **272**, 33197–33203 (1997).
49. Cotter, T. G., Lennon, S. V., Glynn, J. M. & Green, D. R. Microfilament-disrupting agents prevent the formation of apoptotic bodies in tumor cells undergoing apoptosis. *Cancer Res.* **52**, 997–1005 (1992).
50. Frank, S. *et al.* The Role of Dynamin-Related Protein 1, a Mediator of Mitochondrial Fission, in Apoptosis. *Dev. Cell* **1**, 515–525 (2001).
51. Chiu, R., Novikov, L., Mukherjee, S. & Shields, D. A caspase cleavage fragment of p115 induces fragmentation of the Golgi apparatus and apoptosis. *J. Cell Biol.* **159**, 637–648 (2002).
52. Letai, A. *et al.* Distinct BH3 domains either sensitize or activate mitochondrial apoptosis, serving as prototype cancer therapeutics. *Cancer Cell* **2**, 183–192 (2002).
53. Kuwana, T. *et al.* BH3 domains of BH3-only proteins differentially regulate Bax-mediated mitochondrial membrane permeabilization both directly and indirectly. *Mol. Cell* **17**, 525–535 (2005).
54. Lane, J. D., Allan, V. J. & Woodman, P. G. Active relocation of chromatin and endoplasmic reticulum into blebs in late apoptotic cells. *J. Cell Sci.* **118**, 4059–4071 (2005).
55. Lüthi, A. U. & Martin, S. J. The CASBAH: a searchable database of caspase substrates. *Cell Death Differ.* **14**, 641–650 (2007).
56. Arur, S. *et al.* Annexin I is an endogenous ligand that mediates apoptotic cell engulfment. *Dev. Cell* **4**, 587–598 (2003).

57. Moffatt, O. D., Devitt, A., Bell, E. D., Simmons, D. L. & Gregory, C. D. Macrophage recognition of ICAM-3 on apoptotic leukocytes. *J. Immunol.* **162**, 6800–6810 (1999).
58. Creagh, E. M., Conroy, H. & Martin, S. J. Caspase-activation pathways in apoptosis and immunity. *Immunol. Rev.* **193**, 10–21 (2003).
59. Nicholson, D. W. Caspase structure, proteolytic substrates, and function during apoptotic cell death. *Cell Death Differ.* **6**, 1028–1042 (1999).
60. Cohen, G. M. Caspases: the executioners of apoptosis. *Biochem. J.* **326** (Pt 1, 1–16 (1997).
61. Fuentes-Prior, P. & Salvesen, G. S. The protein structures that shape caspase activity, specificity, activation and inhibition. *Biochem. J.* **384**, 201–232 (2004).
62. Nuñez, G., Benedict, M. a, Hu, Y. & Inohara, N. Caspases: the proteases of the apoptotic pathway. *Oncogene* **17**, 3237–3245 (1998).
63. Kroemer, G., Galluzzi, L. & Brenner, C. Mitochondrial Membrane Permeabilization in Cell Death. *Physiol. Reveiw* 99–163 (2007). doi:10.1152/physrev.00013.2006.
64. Youle, R. J. & Strasser, A. The BCL-2 protein family: opposing activities that mediate cell death. *Nat. Rev. Mol. Cell Biol.* **9**, 47–59 (2008).
65. Cuconati, A., Mukherjee, C., Perez, D. & White, E. DNA damage response and MCL-1 destruction initiate apoptosis in adenovirus-infected cells. *Genes Dev.* **17**, 2922–2932 (2003).
66. Willis, S. N. *et al.* Proapoptotic Bak is sequestered by Mcl-1 and Bcl-xL, but not Bcl-2, until displaced by BH3-only proteins. *Genes Dev.* **19**, 1294–1305 (2005).
67. Hsu, Y. T., Wolter, K. G. & Youle, R. J. Cytosol-to-membrane redistribution of Bax and Bcl-X(L) during apoptosis. *Proc. Natl. Acad. Sci. U. S. A.* **94**, 3668–3672 (1997).
68. Echeverry, N. *et al.* Intracellular localization of the BCL-2 family member BOK and functional implications. *Cell Death Differ.* **20**, 785–99 (2013).
69. Tartaglia, L. A., Ayres, T. M., Wong, G. H. W. & Goeddel, D. V. A novel domain within the 55 kd TNF receptor signals cell death. *Cell* **74**, 845–853 (1993).
70. Lavrik, I., Golks, A. & Krammer, P. H. Death receptor signaling. *J. Cell Sci.* **118**, 265–267 (2005).
71. Ashkenazi, A. & Dixit, V. M. Death receptors: signaling and modulation. *Science* **281**, 1305–1308 (1998).

72. Ashkenazi, A. Targeting death and decoy receptors of the tumour-necrosis factor superfamily. *Nat. Rev. Cancer* **2**, 420–30 (2002).
73. Nijhawan, D. *et al.* Elimination of Mcl-1 is required for the initiation of apoptosis following ultraviolet irradiation. *Genes Dev.* **17**, 1475–1486 (2003).
74. Lindsten, T. *et al.* The combined functions of proapoptotic Bcl-2 family members Bak and Bax are essential for normal development of multiple tissues. *Mol. Cell* **6**, 1389–1399 (2000).
75. Knudson, C. M., Tung, K. S., Tourtellotte, W. G., Brown, G. A. & Korsmeyer, S. J. Bax-deficient mice with lymphoid hyperplasia and male germ cell death. *Science* **270**, 96–99 (1995).
76. Mason, K. D. *et al.* Programmed Anuclear Cell Death Delimits Platelet Life Span. *Cell* **128**, 1173–1186 (2007).
77. Hamel, P., Corvest, V., Giegé, P. & Bonnard, G. Biochemical requirements for the maturation of mitochondrial c-type cytochromes. *Biochim. Biophys. Acta - Mol. Cell Res.* **1793**, 125–138 (2009).
78. Benedict, M. A., Hu, Y., Inohara, N. & Nu, G. Expression and Functional Analysis of Apaf-1 Isoforms. **275**, 8461–8468 (2000).
79. Zou, H., Li, Y., Liu, X. & Wang, X. An APAf-1-cytochrome C multimeric complex is a functional apoptosome that activates procaspase-9. *J. Biol. Chem.* **274**, 11549–11556 (1999).
80. Deveraux, Q. L. & Reed, J. C. IAP family proteins - Suppressors of apoptosis. *Genes Dev.* **13**, 239–252 (1999).
81. Verhagen, a M. *et al.* Identification of DIABLO, a mammalian protein that promotes apoptosis by binding to and antagonizing IAP proteins. *Cell* **102**, 43–53 (2000).
82. Du, C., Fang, M., Li, Y., Li, L. & Wang, X. Smac, a mitochondrial protein that promotes cytochrome c-dependent caspase activation by eliminating IAP inhibition. *Cell* **102**, 33–42 (2000).
83. Vaux, D. L. & Silke, J. Mammalian mitochondrial IAP binding proteins. *Biochem. Biophys. Res. Commun.* **304**, 499–504 (2003).
84. Peter, M. E. & Krammer, P. H. The CD95(APO-1/Fas) DISC and beyond. *Cell Death Differ.* **10**, 26–35 (2003).
85. Sprick, M. R. *et al.* Caspase-10 is recruited to and activated at the native TRAIL and CD95 death-inducing signalling complexes in a FADD-dependent manner but can not functionally substitute caspase-8. *EMBO J.* **21**, 4520–4530 (2002).

86. Micheau, O. & Tschopp, J. Induction of TNF receptor I-mediated apoptosis via two sequential signaling complexes. *Cell* **114**, 181–190 (2003).
87. Krammer, P. H., Arnold, R. & Lavrik, I. N. Life and death in peripheral T cells. *Nat. Rev. Immunol.* **7**, 532–542 (2007).
88. Scaffidi, C. *et al.* Two CD95 (APO-1/Fas) signaling pathways. *EMBO J.* **17**, 1675–1687 (1998).
89. Korsmeyer, S. J. *et al.* Pro-apoptotic cascade activates BID, which oligomerizes BAK or BAX into pores that result in the release of cytochrome c. *Cell Death Differ.* **7**, 1166–73 (2000).
90. Martin, S. J. *et al.* The cytotoxic cell protease granzyme B initiates apoptosis in a cell-free system by proteolytic processing and activation of the ICE/CED-3 family protease, CPP32, via a novel two-step mechanism. *EMBO J.* **15**, 2407–2416 (1996).
91. Medema, J. P. *et al.* Cleavage of FLICE (caspase-8) by granzyme B during cytotoxic T lymphocyte-induced apoptosis. *Eur. J. Immunol.* **27**, 3492–3498 (1997).
92. Atkinson, E. A. *et al.* Cytotoxic T lymphocyte-assisted suicide: Caspase 3 activation is primarily the result of the direct action of granzyme B. *J. Biol. Chem.* **273**, 21261–21266 (1998).
93. Barry, M. *et al.* Granzyme B short-circuits the need for caspase 8 activity during granule-mediated cytotoxic T-lymphocyte killing by directly cleaving Bid. *Mol. Cell. Biol.* **20**, 3781–3794 (2000).
94. Heibein, J. A. *et al.* Granzyme B-mediated cytochrome c release is regulated by the Bcl-2 family members bid and Bax. *J. Exp. Med.* **192**, 1391–1402 (2000).
95. Thome, M. *et al.* Viral FLICE-inhibitory proteins (FLIPs) prevent apoptosis induced by death receptors. *Nature* **386**, 517–521 (1997).
96. Hu, S., Vincenz, C., Buller, M. & Dixit, V. M. A novel family of viral death effector domain-containing molecules that inhibit both CD-95- and tumor necrosis factor receptor-1-induced apoptosis. *J. Biol. Chem.* **272**, 9621–9624 (1997).
97. Irmeler, M. *et al.* Inhibition of death receptor signals by cellular FLIP. *Nature* **388**, 190–195 (1997).
98. Shu, H. B., Halpin, D. R. & Goeddel, D. V. Casper is a FADD- and caspase-related inducer of apoptosis. *Immunity* **6**, 751–763 (1997).
99. Srinivasula, S. M. *et al.* FLAME-1, a novel FADD-like anti-apoptotic molecule that regulates Fas/TNFR1-induced apoptosis. *J. Biol. Chem.* **272**, 18542–18545 (1997).

100. Inohara, N., Koseki, T., Hu, Y., Chen, S. & Núñez, G. CLARP, a death effector domain-containing protein interacts with caspase-8 and regulates apoptosis. *Proc. Natl. Acad. Sci. U. S. A.* **94**, 10717–10722 (1997).
101. Goltsev, Y. V. *et al.* CASH, a novel caspase homologue with death effector domains. *J. Biol. Chem.* **272**, 19641–19644 (1997).
102. Han, D. K. *et al.* MRIT, a novel death-effector domain-containing protein, interacts with caspases and BclXL and initiates cell death. *Proc. Natl. Acad. Sci. U. S. A.* **94**, 11333–11338 (1997).
103. Hu, S., Vincenz, C., Ni, J., Gentz, R. & Dixit, V. M. I-FLICE, a novel inhibitor of tumor necrosis factor receptor-1- and CD-95-induced apoptosis. *J. Biol. Chem.* **272**, 17255–17257 (1997).
104. Rasper, D. M. *et al.* Cell death attenuation by ‘Usurpin’, a mammalian DED-caspase homologue that precludes caspase-8 recruitment and activation by the CD-95 (Fas, APO-1) receptor complex. *Cell Death Differ.* **5**, 271–288 (1998).
105. Chang, D. W. *et al.* C-FLIPL is a dual function regulator for caspase-8 activation and CD95-mediated apoptosis. *EMBO J.* **21**, 3704–3714 (2002).
106. Krueger, a, Schmitz, I., Baumann, S., Krammer, P. H. & Kirchhoff, S. Cellular FLICE-inhibitory protein splice variants inhibit different steps of caspase-8 activation at the CD95 death-inducing signaling complex. *J. Biol. Chem.* **276**, 20633–40 (2001).
107. Scaffidi, C., Schmitz, I., Krammer, P. H. & Peter, M. E. The role of c-FLIP in modulation of CD95-induced apoptosis. *J. Biol. Chem.* **274**, 1541–8 (1999).
108. Kataoka, T. & Tschopp, J. N-terminal fragment of c-FLIP (L) processed by caspase 8 specifically interacts with TRAF2 and induces activation of the NF- κ B signaling pathway. *Mol. Cell. Biol.* **24**, 2627–2636 (2004).
109. Matsuda, I. *et al.* The c-terminal domain of the long form of cellular fliceinhibitory protein (c-FLIPL) inhibits the interaction of the caspase 8 prodomain with the receptor-interacting protein 1 (RIP1) death domain and regulates caspase 8-dependent nuclear factor κ B (NF- κ B). *J. Biol. Chem.* **289**, 3876–3887 (2014).
110. Golks, A., Brenner, D., Fritsch, C., Krammer, P. H. & Lavrik, I. N. c-FLIPR, a new regulator of death receptor-induced apoptosis. *J. Biol. Chem.* **280**, 14507–13 (2005).
111. Tschopp, J., Irmeler, M. & Thome, M. Inhibition of Fas death signals by FLIPs. *Curr. Opin. Immunol.* **10**, 552–558 (1998).
112. Poukkula, M. *et al.* Rapid turnover of c-FLIPshort is determined by its unique C-terminal tail. *J. Biol. Chem.* **280**, 27345–27355 (2005).

113. Ueffing, N. *et al.* A single nucleotide polymorphism determines protein isoform production of the human c-FLIP protein. *Blood* **114**, 572–9 (2009).
114. Kataoka, T. & Tschopp, J. N-terminal fragment of c-FLIP(L) processed by caspase 8 specifically interacts with TRAF2 and induces activation of the NF-kappaB signaling pathway. *Mol. Cell. Biol.* **24**, 2627–2636 (2004).
115. Dohrman, A. *et al.* Cellular FLIP (long form) regulates CD8+ T cell activation through caspase-8-dependent NF-kappa B activation. *J. Immunol.* **174**, 5270–5278 (2005).
116. Davidson, S. M., Stephanou, A. & Latchman, D. S. FLIP protects cardiomyocytes from apoptosis induced by simulated ischemia/reoxygenation, as demonstrated by short hairpin-induced (shRNA) silencing of FLIP mRNA. *J. Mol. Cell. Cardiol.* **35**, 1359–1364 (2003).
117. Marconi, A. *et al.* FLICE/caspase-8 activation triggers anoikis induced by beta1-integrin blockade in human keratinocytes. *J. Cell Sci.* **117**, 5815–5823 (2004).
118. Desbarats, J. *et al.* Fas engagement induces neurite growth through ERK activation and p35 upregulation. *Nat. Cell Biol.* **5**, 118–125 (2003).
119. Bouchet, D. *et al.* Differential sensitivity of endothelial cells of various species to apoptosis induced by gene transfer of Fas ligand: role of FLIP levels. *Mol. Med.* **8**, 612–623 (2002).
120. Kim, H., Whartenby, K. A., Georgantas, R. W., Wingard, J. & Civin, C. I. Human CD34+ hematopoietic stem/progenitor cells express high levels of FLIP and are resistant to Fas-mediated apoptosis. *Stem Cells* **20**, 174–182 (2002).
121. Rescigno, M. *et al.* Fas engagement induces the maturation of dendritic cells (DCs), the release of interleukin (IL)-1beta, and the production of interferon gamma in the absence of IL-12 during DC-T cell cognate interaction: a new role for Fas ligand in inflammatory responses. *J. Exp. Med.* **192**, 1661–1668 (2000).
122. Kiener, P. A. *et al.* Differential induction of apoptosis by Fas-Fas ligand interactions in human monocytes and macrophages. *J. Exp. Med.* **185**, 1511–1516 (1997).
123. Budd, R. C., Yeh, W.-C. & Tschopp, J. cFLIP regulation of lymphocyte activation and development. *Nat. Rev. Immunol.* **6**, 196–204 (2006).
124. Ashany, D., Savir, A., Bhardwaj, N. & Elkouss, K. B. Dendritic cells are resistant to apoptosis through the Fas (CD95/APO-1) pathway. *J. Immunol.* **163**, 5303–5311 (1999).
125. Willems, F. *et al.* Expression of c-FLIP(L) and resistance to CD95-mediated apoptosis of monocyte-derived dendritic cells: inhibition by bisindolylmaleimide. *Blood* **95**, 3478–3482 (2000).

126. Kataoka, T. *et al.* The caspase-8 inhibitor FLIP promotes activation of NF-kappaB and Erk signaling pathways. *Curr. Biol.* **10**, 640–648 (2000).
127. Hennino, A., Berard, M., Casamayor-Pallejà, M., Krammer, P. H. & Defrance, T. Regulation of the Fas death pathway by FLICE-inhibitory protein in primary human B cells. *J. Immunol.* **165**, 3023–3030 (2000).
128. Wang, J. *et al.* Inhibition of Fas-mediated apoptosis by the B cell antigen receptor through c-FLIP. *Eur. J. Immunol.* **30**, 155–163 (2000).
129. Hennino, A., Bérard, M., Krammer, P. H. & Defrance, T. FLICE-inhibitory protein is a key regulator of germinal center B cell apoptosis. *J. Exp. Med.* **193**, 447–458 (2001).
130. Micheau, O., Lens, S., Gaide, O., Alevizopoulos, K. & Tschopp, J. NF-kappaB signals induce the expression of c-FLIP. *Mol. Cell. Biol.* **21**, 5299–5305 (2001).
131. Zhang, J. *et al.* IL-4 potentiates activated T cell apoptosis via an IL-2-dependent mechanism. *J. Immunol.* **170**, 3495–3503 (2003).
132. Lee, S. W., Park, Y., Yoo, J. K., Choi, S. Y. & Sung, Y. C. Inhibition of TCR-induced CD8 T cell death by IL-12: regulation of Fas ligand and cellular FLIP expression and caspase activation by IL-12. *J. Immunol.* **170**, 2456–2460 (2003).
133. Misra, R. S. *et al.* Effector CD4+ T cells generate intermediate caspase activity and cleavage of caspase-8 substrates. *J. Immunol.* **174**, 3999–4009 (2005).
134. Yeh, W. C. *et al.* Requirement for Casper (c-FLIP) in regulation of death receptor-induced apoptosis and embryonic development. *Immunity* **12**, 633–642 (2000).
135. Chau, H. *et al.* Cellular FLICE-inhibitory protein is required for T cell survival and cycling. *J. Exp. Med.* **202**, 405–13 (2005).
136. Zhang, N. & He, Y.-W. An essential role for c-FLIP in the efficient development of mature T lymphocytes. *J. Exp. Med.* **202**, 395–404 (2005).
137. Diefenbach, A. & Raulat, D. H. The innate immune response to tumors and its role in the induction of T-cell immunity. *Immunol. Rev.* **188**, 9–21 (2002).
138. Biron, C. A., Nguyen, K. B., Pien, G. C., Cousens, L. P. & Salazar-Mather, T. P. Natural killer cells in antiviral defense: function and regulation by innate cytokines. *Annu. Rev. Immunol.* **17**, 189–220 (1999).
139. Klas, C., Debatin, K. M., Jonker, R. R. & Krammer, P. H. Activation interferes with the APO-1 pathway in mature human T cells. *Int. Immunol.* **5**, 625–630 (1993).

140. Peter, M. E. *et al.* Resistance of cultured peripheral T cells towards activation-induced cell death involves a lack of recruitment of FLICE (MACH/caspase 8) to the CD95 death-inducing signaling complex. *Eur. J. Immunol.* **27**, 1207–1212 (1997).
141. Schmitz, I. *et al.* Resistance of short term activated T cells to CD95-mediated apoptosis correlates with de novo protein synthesis of c-FLIPshort. *J. Immunol.* **172**, 2194–2200 (2004).
142. Fas, S. C. *et al.* In vitro generated human memory-like T cells are CD95 type II cells and resistant towards CD95-mediated apoptosis. *Eur. J. Immunol.* **36**, 2894–2903 (2006).
143. Bouillet, P. *et al.* Proapoptotic Bcl-2 relative Bim required for certain apoptotic responses, leukocyte homeostasis, and to preclude autoimmunity. *Science* **286**, 1735–1738 (1999).
144. Weant, A. E. *et al.* Apoptosis Regulators Bim and Fas Function Concurrently to Control Autoimmunity and CD8⁺ T Cell Contraction. *Immunity* **28**, 218–230 (2008).
145. Dziarski, R. & Gupta, D. Mammalian PGRPs: Novel antibacterial proteins. *Cell. Microbiol.* **8**, 1059–1069 (2006).
146. Boller, T. & Felix, G. A renaissance of elicitors: perception of microbe-associated molecular patterns and danger signals by pattern-recognition receptors. *Annu. Rev. Plant Biol.* **60**, 379–406 (2009).
147. Raulet, D. H. & Vance, R. E. Self-tolerance of natural killer cells. *Nat. Rev. Immunol.* **6**, 520–31 (2006).
148. Roche, P. a & Furuta, K. The ins and outs of MHC class II-mediated antigen processing and presentation. *Nat. Rev. Immunol.* 1–14 (2015).
149. Oltz, E. M. Regulation of antigen receptor gene assembly in lymphocytes. *Immunol. Res.* **23**, 121–133 (2001).
150. Farber, D. L., Yudanin, N. A. & Restifo, N. P. Human memory T cells: generation, compartmentalization and homeostasis. *Nat. Rev. Immunol.* **14**, 24–35 (2014).
151. Dogan, I. *et al.* Multiple layers of B cell memory with different effector functions. *Nat. Immunol.* **10**, 1292–1299 (2009).
152. Nemazee, D. Receptor editing in lymphocyte development and central tolerance. *Nat. Rev. Immunol.* **6**, 728–740 (2006).
153. Manjarrez-Orduño, N., Quách, T. D. & Sanz, I. B cells and immunological tolerance. *J. Invest. Dermatol.* **129**, 278–288 (2009).

154. Shlomchik, M. J. Sites and Stages of Autoreactive B Cell Activation and Regulation. *Immunity* **28**, 18–28 (2008).
155. Wardemann, H. *et al.* Predominant autoantibody production by early human B cell precursors. *Science* **301**, 1374–1377 (2003).
156. Goodnow, C. C., Sprent, J., Fazekas de St Groth, B. & Vinuesa, C. G. Cellular and genetic mechanisms of self tolerance and autoimmunity. *Nature* **435**, 590–597 (2005).
157. Spits, H. Development of alphabeta T cells in the human thymus. *Nat. Rev. Immunol.* **2**, 760–772 (2002).
158. Davis, M. M. & Bjorkman, P. J. T-cell antigen receptor genes and T-cell recognition. *Nature* **334**, 395–402 (1988).
159. Shortman, K. Cellular aspects of early T-cell development. *Curr. Opin. Immunol.* **4**, 140–146 (1992).
160. Klein, L., Kyewski, B., Allen, P. M. & Hogquist, K. a. Positive and negative selection of the T cell repertoire: what thymocytes see (and don't see). *Nat. Rev. Immunol.* **14**, 377–91 (2014).
161. Fujio, K., Okamura, T. & Yamamoto, K. The family of IL-10-secreting CD4+ T cells. *Adv. Immunol.* **105**, 99–130 (2010).
162. Sakaguchi, S. *et al.* Foxp3+CD25+CD4+ natural regulatory T cells in dominant self-tolerance and autoimmune disease. *Immunol. Rev.* **212**, 8–27 (2006).
163. Sakaguchi, S., Sakaguchi, N., Asano, M., Itoh, M. & Masaaki, T. Immunologic Self-Tolerance Maintained by Activated T Cells Expressing Il-2 Receptor α -Chains (CD25). *J. Immunol.* **155**, 1151–1164 (1995).
164. Maloy, K. J. & Powrie, F. Regulatory T cells in the control of immune pathology. *Nat. Immunol.* **2**, 816–822 (2001).
165. Wong, J. *et al.* Adaptation of TCR repertoires to self-peptides in regulatory and nonregulatory CD4+ T cells. *J. Immunol.* **178**, 7032–7041 (2007).
166. Hsieh, C. S. *et al.* Recognition of the peripheral self by naturally arising CD25+ CD4+ T cell receptors. *Immunity* **21**, 267–277 (2004).
167. Hsieh, C.-S., Lee, H.-M. & Lio, C.-W. J. Selection of regulatory T cells in the thymus. *Nat. Rev. Immunol.* **12**, 157–167 (2012).
168. Chen, W. *et al.* Conversion of peripheral CD4+CD25- naive T cells to CD4+CD25+ regulatory T cells by TGF-beta induction of transcription factor Foxp3. *J. Exp. Med.* **198**, 1875–1886 (2003).

169. Sakaguchi, S. *et al.* Immunologic tolerance maintained by CD25+ CD4+ regulatory T cells: their common role in controlling autoimmunity, tumor immunity, and transplantation tolerance. *Immunol. Rev.* **182**, 18–32 (2001).
170. Bennett, C. L. *et al.* The immune dysregulation, polyendocrinopathy, enteropathy, X-linked syndrome (IPEX) is caused by mutations of FOXP3. *Nat. Genet.* **27**, 20–21 (2001).
171. Russell, W. L., Russell, L. B. & Gower, J. S. Exceptional inheritance of a sex-linked gene in the mouse explained on the basis that the X/O sex-chromosome constitution is female. *Proc. Natl. Acad. Sci. U. S. A.* **45**, 554–560 (1959).
172. Godfrey, V. L., Wilkinson, J. E. & Russell, L. B. X-linked lymphoreticular disease in the scurfy (sf) mutant mouse. *Am. J. Pathol.* **138**, 1379–1387 (1991).
173. Lahl, K. *et al.* Selective depletion of Foxp3+ regulatory T cells induces a scurfy-like disease. *J. Exp. Med.* **204**, 57–63 (2007).
174. Ramsdell, F. & Ziegler, S. F. FOXP3 and scurfy: how it all began. *Nat. Rev. Immunol.* **14**, 343–9 (2014).
175. Asseman, C., Mauze, S., Leach, M. W., Coffman, R. L. & Powrie, F. An essential role for interleukin 10 in the function of regulatory T cells that inhibit intestinal inflammation. *J. Exp. Med.* **190**, 995–1004 (1999).
176. Collison, L. W. *et al.* The inhibitory cytokine IL-35 contributes to regulatory T-cell function. *Nature* **450**, 566–569 (2007).
177. Nakamura, K., Kitani, A. & Strober, W. Cell contact-dependent immunosuppression by CD4(+)CD25(+) regulatory T cells is mediated by cell surface-bound transforming growth factor beta. *J. Exp. Med.* **194**, 629–644 (2001).
178. Joetham, A. *et al.* Naturally occurring lung CD4(+)CD25(+) T cell regulation of airway allergic responses depends on IL-10 induction of TGF-beta. *J. Immunol.* **178**, 1433–1442 (2007).
179. Gondek, D. C., Lu, L.-F., Quezada, S. A., Sakaguchi, S. & Noelle, R. J. Cutting edge: contact-mediated suppression by CD4+CD25+ regulatory cells involves a granzyme B-dependent, perforin-independent mechanism. *J. Immunol.* **174**, 1783–1786 (2005).
180. Zhao, D.-M., Thornton, A. M., DiPaolo, R. J. & Shevach, E. M. Activated CD4+CD25+ T cells selectively kill B lymphocytes. *Blood* **107**, 3925–3932 (2006).
181. Thornton, A. M. & Shevach, E. M. CD4+CD25+ immunoregulatory T cells suppress polyclonal T cell activation in vitro by inhibiting interleukin 2 production. *J. Exp. Med.* **188**, 287–296 (1998).

182. De la Rosa, M., Rutz, S., Dorninger, H. & Scheffold, A. Interleukin-2 is essential for CD4+CD25+ regulatory T cell function. *Eur. J. Immunol.* **34**, 2480–2488 (2004).
183. Deaglio, S. *et al.* Adenosine generation catalyzed by CD39 and CD73 expressed on regulatory T cells mediates immune suppression. *J. Exp. Med.* **204**, 1257–1265 (2007).
184. Zarek, P. E. *et al.* A2A receptor signaling promotes peripheral tolerance by inducing T-cell anergy and the generation of adaptive regulatory T cells. *Blood* **111**, 251–259 (2008).
185. Oukka, M. Interplay between pathogenic Th17 and regulatory T cells. *Ann. Rheum. Dis.* **66 Suppl 3**, iii87–i90 (2007).
186. Bopp, T. *et al.* Cyclic adenosine monophosphate is a key component of regulatory T cell-mediated suppression. *J. Exp. Med.* **204**, 1303–1310 (2007).
187. Tadokoro, C. E. *et al.* Regulatory T cells inhibit stable contacts between CD4+ T cells and dendritic cells in vivo. *J. Exp. Med.* **203**, 505–511 (2006).
188. Huang, C. T. *et al.* Role of LAG-3 in regulatory T cells. *Immunity* **21**, 503–513 (2004).
189. Read, S., Malmström, V. & Powrie, F. Cytotoxic T lymphocyte-associated antigen 4 plays an essential role in the function of CD25(+)CD4(+) regulatory cells that control intestinal inflammation. *J. Exp. Med.* **192**, 295–302 (2000).
190. Oderup, C., Cederbom, L., Makowska, A., Cilio, C. M. & Ivars, F. Cytotoxic T lymphocyte antigen-4-dependent down-modulation of costimulatory molecules on dendritic cells in CD4+ CD25+ regulatory T-cell-mediated suppression. *Immunology* **118**, 240–249 (2006).
191. Fallarino, F. *et al.* Modulation of tryptophan catabolism by regulatory T cells. *Nat. Immunol.* **4**, 1206–1212 (2003).
192. Kuniyasu, Y. *et al.* Naturally anergic and suppressive CD25(+)CD4(+) T cells as a functionally and phenotypically distinct immunoregulatory T cell subpopulation. *Int. Immunol.* **12**, 1145–1155 (2000).
193. Itoh, M. *et al.* Thymus and autoimmunity: production of CD25+CD4+ naturally anergic and suppressive T cells as a key function of the thymus in maintaining immunologic self-tolerance. *J. Immunol.* **162**, 5317–5326 (1999).
194. Fisson, S. *et al.* Continuous activation of autoreactive CD4+ CD25+ regulatory T cells in the steady state. *J. Exp. Med.* **198**, 737–746 (2003).
195. Klein, L., Khazaie, K. & von Boehmer, H. In vivo dynamics of antigen-specific regulatory T cells not predicted from behavior in vitro. *Proc. Natl. Acad. Sci. U. S. A.* **100**, 8886–8891 (2003).

196. Walker, L. S. K., Chodos, A., Eggena, M., Dooks, H. & Abbas, A. K. Antigen-dependent proliferation of CD4⁺ CD25⁺ regulatory T cells in vivo. *J. Exp. Med.* **198**, 249–258 (2003).
197. Vukmanovic-Stejic, M. *et al.* Human CD4⁺ CD25^{hi} Foxp3⁺ regulatory T cells are derived by rapid turnover of memory populations in vivo. *J. Clin. Invest.* **116**, 2423–2433 (2006).
198. Tai, X. *et al.* Foxp3 transcription factor is proapoptotic and lethal to developing regulatory T cells unless counterbalanced by cytokine survival signals. *Immunity* **38**, 1116–28 (2013).
199. Pierson, W. *et al.* Antiapoptotic Mcl-1 is critical for the survival and niche-filling capacity of Foxp3⁺ regulatory T cells. *Nat. Immunol.* **14**, 959–65 (2013).
200. Liston, A. & Gray, D. H. D. Homeostatic control of regulatory T cell diversity. *Nat. Rev. Immunol.* **14**, 154–65 (2014).
201. Xu, D. *et al.* Circulating and liver resident CD4⁺CD25⁺ regulatory T cells actively influence the antiviral immune response and disease progression in patients with hepatitis B. *J. Immunol.* **177**, 739–747 (2006).
202. Roychoudhuri, R., Eil, R. L. & Restifo, N. P. The interplay of effector and regulatory T cells in cancer. *Curr. Opin. Immunol.* **33**, 101–111 (2015).
203. Shimizu, J., Yamazaki, S. & Sakaguchi, S. Induction of tumor immunity by removing CD25⁺CD4⁺ T cells: a common basis between tumor immunity and autoimmunity. *J. Immunol.* **163**, 5211–5218 (1999).
204. Josefowicz, S. Z. *et al.* Extrathymically generated regulatory T cells control mucosal TH2 inflammation. *Nature* **482**, 395–399 (2012).
205. Komatsu, N. *et al.* Heterogeneity of natural Foxp3⁺ T cells: a committed regulatory T-cell lineage and an uncommitted minor population retaining plasticity. *Proc. Natl. Acad. Sci. U. S. A.* **106**, 1903–1908 (2009).
206. Fontenot, J. D. *et al.* Regulatory T cell lineage specification by the forkhead transcription factor Foxp3. *Immunity* **22**, 329–341 (2005).
207. Rubtsov, Y. P. *et al.* Regulatory T cell-derived interleukin-10 limits inflammation at environmental interfaces. *Immunity* **28**, 546–58 (2008).
208. Chougnet, C. *et al.* A major role for Bim in regulatory T cell homeostasis. *J. Immunol.* **186**, 156–63 (2011).
209. Wang, X. *et al.* Preferential control of induced regulatory T cell homeostasis via a Bim/Bcl-2 axis. *Cell Death Dis.* **3**, e270 (2012).

210. Ricci, J. E. *et al.* Disruption of mitochondrial function during apoptosis is mediated by caspase cleavage of the p75 subunit of complex I of the electron transport chain. *Cell* **117**, 773–786 (2004).
211. Sena, L., Li, S., Jairaman, A. & Prakriya, M. Mitochondria are required for antigen-specific T cell activation through reactive oxygen species signaling. *Immunity* **38**, 225–236 (2013).
212. Caserta, T. M., Smith, A. N., Gultice, A. D., Reedy, M. A. & Brown, T. L. Q-VD-OPh, a broad spectrum caspase inhibitor with potent antiapoptotic properties. *Apoptosis* **8**, 345–352 (2003).
213. Cohen, J. J. & Duke, R. C. Glucocorticoid activation of a calcium-dependent endonuclease in thymocyte nuclei leads to cell death. *J. Immunol.* **132**, 38–42 (1984).
214. Bansal, N., Houle, A. & Melnykovich, G. Apoptosis: mode of cell death induced in T cell leukemia lines by dexamethasone and other agents. *FASEB J.* **5**, 211–216 (1991).
215. Hildeman, D. a. *et al.* Activated T cell death in vivo mediated by proapoptotic Bcl-2 family member Bim. *Immunity* **16**, 759–767 (2002).
216. Boise, L. H. *et al.* CD28 costimulation can promote T cell survival by enhancing the expression of Bcl-XL. *Immunity* **3**, 87–98 (1995).
217. Noel, P. J., Boise, L. H., Green, J. M. & Thompson, C. B. CD28 costimulation prevents cell death during primary T cell activation. *J. Immunol.* **157**, 636–642 (1996).
218. Kerstan, A. & Hünig, T. Cutting edge: distinct TCR- and CD28-derived signals regulate CD95L, Bcl-xL, and the survival of primary T cells. *J. Immunol.* **172**, 1341–1345 (2004).
219. Sauer, B. & Henderson, N. Site-specific DNA recombination in mammalian cells by the Cre recombinase of bacteriophage P1. *Proc. Natl. Acad. Sci. U. S. A.* **85**, 5166–5170 (1988).
220. Fritzsching, B. *et al.* In contrast to effector T cells, CD4+CD25+FoxP3+ regulatory T cells are highly susceptible to CD95 ligand- but not to TCR-mediated cell death. *J. Immunol.* **175**, 32–6 (2005).
221. Milanez-Almeida, P., Meyer-Hermann, M., Toker, A., Khailaie, S. & Huehn, J. Foxp3 + regulatory T-cell homeostasis quantitatively differs in murine peripheral lymph nodes and spleen. *Eur. J. Immunol.* **45**, 153–166 (2015).
222. Bouillet, P. *et al.* BH3-only Bcl-2 family member Bim is required for apoptosis of autoreactive thymocytes. *Nature* **415**, 922–926 (2002).

223. Dhein, J., Walczak, H., Bäumler, C., Debatin, K. M. & Krammer, P. H. Autocrine T-cell suicide mediated by APO-1/(Fas/CD95). *Nature* **373**, 438–441 (1995).
224. Brunner, T. *et al.* Cell-autonomous Fas (CD95)/Fas-ligand interaction mediates activation-induced apoptosis in T-cell hybridomas. *Nature* **373**, 441–444 (1995).
225. Ju, S. T. *et al.* Fas(CD95)/FasL interactions required for programmed cell death after T-cell activation. *Nature* **373**, 444–448 (1995).
226. Vu, M. D. *et al.* OX40 costimulation turns off Foxp3 + Tregs. *Blood* **110**, 2501–2510 (2007).
227. Ikeda, T. *et al.* Dual effects of TRAIL in suppression of autoimmunity: the inhibition of Th1 cells and the promotion of regulatory T cells. *J. Immunol.* **185**, 5259–5267 (2010).
228. Deng, X., Berletch, J. B., Nguyen, D. K. & Disteché, C. M. X chromosome regulation: diverse patterns in development, tissues and disease. *Nat. Rev. Genet.* **15**, 367–378 (2014).
229. Wildin, R. S., Smyk-Pearson, S. & Filipovich, A. H. Clinical and molecular features of the immunodysregulation, polyendocrinopathy, enteropathy, X linked (IPEX) syndrome. *J. Med. Genet.* **39**, 537–545 (2002).
230. Kanangat, S. *et al.* Disease in the scurfy (sf) mouse is associated with overexpression of cytokine genes. *Eur. J. Immunol.* **26**, 161–165 (1996).
231. Clark, L. B. *et al.* Cellular and molecular characterization of the scurfy mouse mutant. *J. Immunol.* **162**, 2546–2554 (1999).
232. Smyk-Pearson, S. K., Bakke, a. C., Held, P. K. & Wildin, R. S. Rescue of the autoimmune scurfy mouse by partial bone marrow transplantation or by injection with T-enriched splenocytes. *Clin. Exp. Immunol.* **133**, 193–199 (2003).
233. Zhang, N., Hopkins, K. & He, Y.-W. The long isoform of cellular FLIP is essential for T lymphocyte proliferation through an NF-kappaB-independent pathway. *J. Immunol.* **180**, 5506–5511 (2008).
234. Huehn, J., Polansky, J. K. & Hamann, A. Epigenetic control of FOXP3 expression: the key to a stable regulatory T-cell lineage? *Nat. Rev. Immunol.* **9**, 83–89 (2009).
235. Vignali, D. a a, Collison, L. W. & Workman, C. J. How regulatory T cells work. *Nat. Rev. Immunol.* **8**, 523–532 (2008).

9. Acknowledgements

I want to express my gratitude to my supervisor Prof. Dr. Ingo Schmitz for giving me the opportunity to work in his group and to develop this project, for being always willing to advice and help me and for contributing immensely to my scientific development.

Thanks to my colleagues Frida, Ralf, Tanja, Michaela, Yvonne, Sabrina, Dominique, Christian, Alisha, Tobias, Svenja, Neda, Konstantinos, Lisa and Daniela for their help and wonderful working atmosphere. I particularly want to acknowledge Marc for his assistance, patience and support. I feel very lucky to share these years with him in the lab.

I am profoundly grateful to my parents and sister for having always their support.

My biggest acknowledgment goes to Andrea for her encouragement and love.

10. Declaration of originality

Carlos Plaza Sirvent
Henschelstr. 14
38126 Braunschweig

Erklärung

Hiermit erkläre ich, dass ich die von mir eingereichte Dissertation zu dem Thema

The role of cFLIP in regulatory T cell homeostasis

selbständig verfasst, nicht schon als Dissertation verwendet habe und die benutzten Hilfsmittel und Quellen vollständig angegeben wurden.

Weiterhin erkläre ich, dass ich weder diese noch eine andere Arbeit zur Erlangung des akademischen Grades doctor rerum naturalium (Dr. rer. nat.) an anderen Einrichtungen eingereicht habe.

Magdeburg, 23.06.2015

Carlos Plaza Sirvent

11. Curriculum vitae

First name: Carlos
Family name: Plaza Sirvent
Date of birth: October 31, 1982
Place of birth: Elche, Alicante (Spain)

Education

- 2011-2015 **PhD Student**
Otto-von-Guericke-Universität Magdeburg and HZI Graduate School
Systems-oriented immunology and inflammation research group
Prof. Dr. Ingo Schmitz
Helmholtz Center for Infection Research (HZI), Braunschweig and
Institut für Molekulare und Klinische Immunologie
Otto-von-Guericke-Universität, Magdeburg (Germany)
- 2009-2011 **Master of Biotechnology and Biomedicine (2 years – 120 ECTS)**
Master Project: “Immunomodulatory mechanisms in endometriosis”
University of Alicante (Spain)
- 2001-2007 **Graduate (*Licenciado*, long cycle degree of 5 years) in Biology**
Main subject: Biomedicine
University of Alicante (Spain)
- 1996-2000 ***Bachillerato & C.O.U.***
I.E.S. Cap de l’Horta (Alicante, Spain)

Work experience

- 2011-2015 **Research Assistant (PhD Student)**
Systems-oriented immunology and inflammation research group
Prof. Dr. Ingo Schmitz
Helmholtz Center for Infection Research (HZI), Braunschweig and
Institut für Molekulare und Klinische Immunologie, Otto-von-Guericke-Universität,
Magdeburg (Germany).
- May 2010 – Jul 2011 **Clinical Research Assistant**
Fundación para el Fomento de la Investigación Sanitaria y Biomédica de la Comunidad
Valenciana (Foundation for Promoting Research in the fields of Health and
Biomedicine of the Valencian Community)
- Oct 2006 – Feb 2007 **Laboratory Technician - Internship**
University Hospital Alicante
Laboratory techniques (Immunochemistry, Nephelometry, Immunoassays, Cytometry,
Molecular Biology, Histocompatibility).

Publications

Annemann M, Wang Z, **Plaza-Sirvent C**, Glaubien R, Schuster M, Ewald F, Kühl A, Clayton LK, Siegmund B, Lochner M, Schmitz I. $\text{I}\kappa\text{B}_{\text{NS}}$ regulates TH17 differentiation during gut inflammation and infection. *J Immunol*. 2015 Mar.

Ewald F, Annemann M, Pils MC, **Plaza-Sirvent C**, Neff F, Erck C, Reinhold D, Schmitz I. Constitutive expression of murine c-FLIP_R causes autoimmunity in aged mice. *Cell Death Dis*. 2014 Apr 10.

Schuster M, Annemann M, **Plaza-Sirvent C**, Schmitz I. Atypical $\text{I}\kappa\text{B}$ proteins - nuclear modulators of NF- κB signaling. *Cell Commun Signal*. 2013 Apr 11.

Schuster M, Glaubien R, **Plaza-Sirvent C**, Schreiber L, Annemann M, Floess S, Kühl AA, Clayton LK, Sparwasser T, Schulze-Osthoff K, Pfeffer K, Huehn J, Siegmund B, Schmitz I. $\text{I}\kappa\text{B}(\text{NS})$ protein mediates regulatory T cell development via induction of the Foxp3 transcription factor. *Immunity*. 2012 Dec.

Gil-Guillén V, Orozco-Beltrán D, Carratala Munuera CV, **Plaza-Sirvent C**, Lorca-Amorrich P, López-Pineda A, Vela-Troncoso MP, Soler JJ, Yarza-Cañellas M, Fernández A, Rosado-Bretón L, Olivares-Bautista C, Muñoz-Fernández A; FUMEPOC Study Research Team. FUMEPOC: early detection of chronic obstructive pulmonary disease in smokers. *BMC Public Health*. 2011 May 31.

Gil-Guillen V, Carratala-Munuera C, Ortega JC, Orozco-Beltran D, Ribera JM, Expósito AP, Cánovas PM, Mora EP, Azofra EM, Giménez AF, Lopez-Pineda A, Lorca-Amorrich P, **Plaza-Sirvent C**, Sola EB, Salas-Rico R, Fernandez-Garcia A. Protective factors in patients aged over 65 with stroke treated by physiotherapy, showing cognitive impairment, in the Valencia Community. Protection study in older people (EPACV). *BMC Neurol*. 2012 Oct 5.